Phosphorylation of Skeletal Muscle Pyruvate Dehydrogenase Phosphatase in Response to Insulin Stimulation

Jonathan Robert Choptiany, B.Kin.

Submitted in partial fulfillment of the requirements for the degree
Master of Science in Applied Health Sciences
(Kinesiology)

Under the supervision of Sandra Peters, Ph.D.

Faculty of Applied Health Sciences
Brock University
St. Catharines, Ontario, Canada

Master of Science (2013)

Title: Phosphorylation of Skeletal Muscle Pyruvate Dehydrogenase Phosphatase in Response to Insulin Stimulation

Author: Jonathan R. Choptiany

Supervisor: Dr. Sandra J. Peters

Supervisory Committee: Dr. Paul J. LeBlanc

Dr. Michael J. Plyley

Dr. Brendon Gurd (External Examiner)

Number of Pages: 176

ABSTRACT

Pyruvate dehydrogenase phosphatase (PDP) regulates carbohydrate oxidation through the pyruvate dehydrogenase (PDH) complex. PDP activates PDH, enabling increased carbohydrate flux towards oxidative energy production. In culture myoblasts, both PDP1 and PDP2 undergo covalent activation in response to insulin–stimulation by protein kinase C delta (PKCδ). Our objective was to examine the effect of insulin on PDP phosphorylation and PDH activation in skeletal muscle. Intact rat extensor digitorum longus muscles were incubated (oxygenated at 25°C, 1g of tension) for 30min in basal or insulin–stimulated (10 mU/mL) media. PDH activity increased 58% following stimulation, (p=0.057, n=11). Serine phosphorylation of PDP1 (p=0.047) and PDP2 (p=0.006) increased by 29% and 48%, respectively (n=8), and mitochondrial PKCδ protein content was enriched by 45% in response to stimulation (p=0.0009, n=8). These data suggest that the insulin–stimulated increase in PDH activity in whole tissue is mediated through mitochondrial migration of PKCδ and subsequent PDP phosphorylation.

ACKNOWLEDGEMENTS

To Dr. LeBlanc & Dr. Plyley: a sincere thank you for everything that you have contributed to this thesis. Your expertise and time are valuable commodities, thank you for providing both to me. I am very fortunate to have worked alongside such professionals.

To my lab mates: it has been a pleasure to work alongside you over the course of this project. You have all provided fantastic support while watching me pull my hair out on a daily basis in the lab. Thank you for being great friends. I can only hope that I have been as supportive to you, as you have to me.

To Sandy: I could not have asked for a better mentor. I will never be able to thank you enough for the opportunity to complete this work, and for your patience throughout its completion. This degree represents a significant period of growth in my life. Thank you for supporting me at every step.

TABLE OF CONTENTS

LIST OF FIGURES

LIST OF TABLES

LIST OF ABBREVIATIONS

AMPK	adenosine monophosphate–activated protein kinase
APS	ammonium persulfate
AST	aspartate transaminase
ATP	adenosine triphosphate
BSA	bovine serum albumin
Ca^{2+}	calcium ion
cm	centimetre
CHO	carbohydrates
CoA	coenzyme A
CoxIV	cytochrome *c* oxidase subunit 4
CS	citrate synthase
CS_{TS}	citrate synthase total mitochondrial suspension
CS_{WH}	citrate synthase whole homogenate
$CuSO_4$	copper sulfate
DCA	dichloroacetic acid
ddH_2O	double–distilled water
DTNB	5,5'–dithiobis[2–nitrobenzoic acid]
DTT	dithiothreitol
EDL	extensor digitorum longus muscle
EDTA	ethylenediaminetetraacetic acid
EGTA	ethylene glycol tetraacetic acid
E1	pyruvate dehydrogenase

E1α	pyruvate dehydrogenase alpha–subunit
E2	dihydrolipoyl transacetylase
E3	dihydrolipoyl dehydrogenase
E3BP	E3 binding protein
$FADH_2$	reduced flavin adenine dinucleotide
g	acceleration due to gravity
g	gram
HCl	hydrochloric acid
HEPES	N–(2–hydroxyethyl)–piperazineethanesulfonic acid
K–acetate	potassium acetate
KCl	potassium chloride
kDa	kilodalton
kg	kilogram
K–glut	potassium glutamate
$KHCO_3$	potassium bicarbonate
KH_2PO_4	potassium dihydrogen phosphate
KOH	potassium hydroxide
L	litre
M	molar concentration
mAb	monoclonal antibody
mg	milligram
Mg^{2+}	magnesium ion
$MgCl_2$	magnesium chloride

$MgSO_4$	magnesium sulfate
mL	millilitre
mM	millimolar concentration
mm	millimetre
mRNA	messenger ribonucleic acid
mU	milliunit
NaCl	sodium chloride
NAD^+	nicotinamide adenine dinucleotide
NADH	reduced nicotinamide adenine dinucleotide
NaF	sodium fluoride
NaOH	sodium hydroxide
Na_2EDTA	disodium ethylenediaminetetraacetic acid
Na_2HPO_4	disodium hydrogen phosphate
NEM	N–ethylmaleimide
nM	nanomolar concentration
nm	nanometre
pAb	polyclonal antibody
PBS	phosphate–buffered saline
PCA	perchloric acid
PDH	pyruvate dehydrogenase complex
PDH*a*	pyruvate dehydrogenase complex (active form)
PDK	pyruvate dehydrogenase kinase
PDP	pyruvate dehydrogenase phosphatase

PDPr	pyruvate dehydrogenase phosphatase regulatory subunit
PDP1	pyruvate dehydrogenase phosphatase isoform 1
PDP2	pyruvate dehydrogenase phosphatase isoform 2
PKCδ	protein kinase C delta isoform
PVDF	polyvinylidene fluoride membrane
rpm	revolutions per minute
SDS	sodium dodecyl sulfate
SEM	standard error of the mean
TA	tibialis anterior muscle
TBST	tris–buffered saline with Tween
TCA	tricarboxylic acid cycle
TEMED	tetramethylethylenediamine
TPP	thiamine pyrophosphate
Tris HCl	Tris hydrochloride
v/v	volume–to–volume ratio
w/v	weight–to–volume ratio
α–KG	alpha ketoglutaric acid
µg	microgram
µL	microlitre
µM	micromolar concentration
1°Ab	primary antibody
2°Ab	secondary antibody
^{14}C–Asp	radiolabeled aspartic acid

° C	degrees in Celsius

CHAPTER 1:

INTRODUCTION

Pyruvate dehydrogenase (PDH) is a tightly regulated mitochondrial multi–enzyme complex that plays an important role in skeletal muscle metabolism. The relative balance of energy expended to accomplish any physical task depends upon the fuel partitioning of three major sources: carbohydrates (CHO), fat and protein. Every physical task involves unique energy requirements, and all require energy that is primarily recruited from one of these sources. For example, activities of maximal intensity predominantly utilize CHO stores, whereas exercise characterized by light and moderate intensities relies more heavily on fat stores (Howlett et al., 1998). The amount of energy we utilize from each energy source is known as fuel partitioning, which is determined by complex metabolic demands (as reviewed by Harris, Bowker–Kinley, Huang, & Wu, 2002). As the largest organ in the human body, skeletal muscle tissue is one site of focal importance with respect to CHO and fat oxidation (Proctor, O'Brien, Atkinson, & Nair, 1999). The PDH complex regulates the relative contribution of carbohydrate stores towards energy provision. Consequently, regulation of the PDH complex in skeletal muscle has major implications towards glucose disposal as well as whole body glucose homeostasis. PDH regulation is accomplished by the overall activities of two phosphatases (PDP1 & PDP2; PDH upregulation via dephosphorylation) and four kinases (PDK 1–4; PDH down regulation via phosphorylation). PDP and PDK contents and activities are subject to adaptation in response to metabolic perturbation. This thesis serves to investigate the effects of insulin stimulation upon the covalent activation of both PDP isoforms, and by extension PDH activation, in intact rat extensor digitorum longus skeletal muscle tissue.

LITERATURE REVIEW

Pyruvate Dehydrogenase: The Background

The role of the pyruvate dehydrogenase (PDH) complex is to determine and regulate overall whole–body carbohydrate oxidation. This enzyme complex is the link between glycolysis and the tricarboxylic acid (TCA) cycle in every cell containing mitochondria (Harris et al., 2002). Furthermore, PDH is responsible for appropriating the rate of oxidative phosphorylation and subsequent ATP production from carbohydrate derived carbon sources (Putman et al., 1993). Whether one is participating in high–intensity exercise or simply thinking, carbohydrate–derived energy is being used at different rates. The role of the active pyruvate dehydrogenase complex (PDH*a*) is to assist in meeting such varied metabolic demands, amongst cooperative energy production pathways (e. g. beta oxidation). PDH controls the flux of carbohydrate–derived acetyl–CoA into the TCA cycle, thereby determining the rate of activity for the complex towards oxidative metabolism (Howlett et al., 1998, Putman et al., 1993). Pathways do exist for glucose to be metabolized non–oxidatively, such as gluconeogenesis or lactate production (Chokkalingam et al., 2007), but metabolism involving the PDH complex specifically leads to oxidative CHO utilization (Howlett et al., 1998, Putman et al., 1993). Although acetyl–CoA production stems from multiple pathways, the PDH complex produces acetyl–CoA from pyruvate, which is a metabolic intermediate made from glucose stores through glycolysis (Putman et al., 1993).

The stoichiometry of the basic pyruvate dehydrogenase reaction can be summarized as follows:

$$\textit{Pyruvate} + NAD^+ + \textit{CoA} \rightarrow\rightarrow \textit{PDH} \rightarrow\rightarrow \textit{Acetyl–CoA} + \textit{NADH} + CO_2$$

This reaction illustrates the irreversible oxidative decarboxylation of pyruvate to form acetyl–CoA (Smolle & Lindsay, 2006; Spriet & Heigenhauser, 2002). Occurring in the mitochondria, three–carbon pyruvate molecules are catabolized into two–carbon acetyl–CoA molecules, including the release of the reducing equivalent nicotinamide adenine dinucleotide (NADH), and the production of carbon dioxide (Smolle & Lindsay, 2006; Spriet & Heigenhauser, 2002). From a chemistry standpoint, decarboxylation is significant because once a carbon is removed and released as gaseous carbon dioxide, it cannot be re–fixed to its predecessor. As a result, the three–carbon intermediate derived from glucose cannot be replaced. Furthermore, this alteration to the structure of pyruvate represents a noteworthy physiological commitment, as these two–carbon compounds are now fully committed towards oxidation. Such carbohydrate sources are now unavailable to be integrated other metabolic processes that require three–carbon molecules, such as gluconeogenesis (Spriet & Heigenhauser, 2002).

The basic PDH reaction features a set of three individual reactions that take place within the mitochondrial matrix, as the PDH complex is believed to be located in close proximity to the cristae of the inner mitochondrial membrane (Margineantu, R. Brown, G. Brown, Marcus, & Capaldi, 2002; Schnaitman & Greenawalt, 1968). Each of the three reactions involves different subunits within the complex. The first reaction is a key irreversible step through a non–equilibrium, rate limiting enzyme (Smolle & Lindsay, 2006; Spriet & Heigenhauser, 2002). Due to the nature of this enzyme classification, there is no metabolic pathway to reproduce glucose from acetyl–CoA stores, echoing previous statements regarding commitment to oxidation. The PDH complex functions uni–directionally and literally traps its products within the inner membrane of the

mitochondria (Spriet & Heigenhauser, 2002; Smolle & Lindsay, 2006). On the contrary, downstream reactions within the PDH complex (reactions 2 and 3) involve near–equilibrium enzymes, which process substrates according to the law of mass action. In these instances, directionality is dependent upon an accumulation of substrate on either side of the reaction. To summarize the basic reaction, PDH alters the chemical structure of metabolic intermediates through uni–directional processing in order to commit carbohydrates towards oxidative metabolism.

In order to specifically meet demand for carbohydrate oxidation, the PDH complex is capable of establishing varying levels of activity. Increased PDH complex activity is observed when dietary carbohydrate intake is relatively high (Putman et al., 1993). In contrast, when dietary carbohydrate intake is low (as seen during fasting, starvation, and high–fat diet implementation), PDH activity is decreased (LeBlanc, Harris, & Peters, 2007; Pehleman, Peters, Heigenhauser, & Spriet, 2005). When PDH activity is down–regulated, acetyl–CoA substrate for the TCA cycle is produced through alternate energy production pathways (Harris et al., 2002). Beyond dietary perturbations, conditions do exist in which the body needs to conserve carbohydrates. When necessary, PDH activity will adjust accordingly. As an example, brain and nervous tissues require a constant supply of glucose in order to maintain functioning levels that cannot drop below a certain threshold (Harris et al., 2002). As a result, this scenario makes the conservation of endogenous carbohydrates a physiological priority. In the event that carbohydrate stores are depleted or dietary carbohydrate intake is low, carbohydrate oxidation in peripheral body tissues will be reduced (Harris et al., 2002).

Skeletal muscle is an exemplary tissue where PDH regulation is a high priority. By virtue of its total mass, skeletal muscle is the largest organ as well as the largest site of glucose disposal in the body (Stump, Henriksen, Wei, & Sowers, 2006). When carbohydrate stores and glucose homeostasis require maintenance, skeletal muscle is an example of a tissue that can readily adjust the PDH activity state in order to satisfy metabolic requirements. Scenarios also exist where there is a need to increase carbohydrate oxidation. In situations requiring large increases in energy provision, such as physical activity, intercellular communication will promote increased PDH activity proportional to exercise intensity and energy demand (Howlett et al., 1998).

The PDH complex is situated at a major metabolic junction in the mitochondria, and its continuum of activity is grand in scope. PDH can be rapidly activated in order to support physical activity, and can also be silenced in order to address basic metabolic needs. PDH is present in numerous tissues throughout the body, and therefore possesses great influence over whole body glucose homeostasis. Thus, especially in tissues with metabolic plasticity such as skeletal muscle, tight regulation of the PDH complex is a major metabolic priority.

PDH: Structural & Functional Synergy

The PDH complex is comprised of three distinct enzyme subunits: E1 (consisting of alpha & beta monomers), E2 and E3, which combine for a total weight of 9500 kDa (Harris et al., 2002). The PDH subunits catalyze mutually dependent individual reactions in a coordinated manner (Jilka, Rahmatullah, Kazemi, & Roche, 1986). Furthermore, it appears as if the function of the PDH complex is entirely dependent upon the spatial relationships between these three entities. The focal component underlying the structure

of each PDH complex is a three–dimensional core, which consists of roughly 60 E2 subunit proteins in a pentagonal dodecahedron chemical structure (Hiromasa, Fujisawa, Aso, & Roche, 2004; Smolle & Lindsay, 2006). However, further analysis has generated speculation regarding the distribution of E2 subunits within this core. Studies have reported that the number of E2 subunits may be 48 (Hiromasa *et al*., 2004) or 40 (Brautigam, Wynn, J. Chuang, & D. Chuang, 2009). Stemming from each respective E2 protein within this core are two free–swinging lipoyl arms (jointly known as a "super arm"), which anchor the remaining enzymes within the complex (Harris et al., 2002; Patel & Roche, 1990). Core attachment through the lipoyl arms enables E1 and E3 enzymes to move and fold with dynamic fluidity. This latter characteristic greatly enhances physical interaction and communication within the entire PDH complex (Smolle & Lindsay, 2006). Based upon this fundamental structure, E2 subunits provide the blueprint for which the remaining components of the complex depend upon for stability and reliable activity.

The PDH complex super arm consists of two lipoyl arms, however it is significant to note the presence of three uniform lipoyl domains within the super arm (Harris et al., 2002). All three lipoyl domains are roughly 80 amino acids in length, and are directly responsible for anchoring all bound members of the complex in proper position (Patel & Roche, 1990; Smolle & Lindsay, 2006). For example, all E1 subunits bind to the E2 core at an E1 binding site that is common to all PDH complexes in mitochondria. Subsequently, this binding site is anchored by a lateral lipoyl domain (lipoyl domain A), which is located directly adjacent along one lipoyl arm of the collective super arm (Smolle & Lindsay, 2006). Furthermore, a secondary yet absolutely critical feature of

lipoyl domain A is that it houses binding sites for the primary regulatory proteins (kinases and phosphatases) of the PDH complex (Harris et al., 2002). These regulatory proteins are major players with respect to establishing conformational changes that establish appropriate PDH complex activity levels (a dynamic concept to be discussed later).

A second lipoyl domain (lipoyl domain B) is responsible for double duty, as it anchors both the E1 binding site and lipoyl domain A (Smolle & Lindsay, 2006). Lipoyl domains A and B comprise one of the two free–swinging lipoyl arms (Harris et al., 2002). These three zones are oriented in a linear fashion with respect to the E2 core (as a point of reference), where each domain receives support from its distal counterpart in series.

The final lipoyl domain (lipoyl domain C) exhibits the same general characteristic as domains A and B. Domain C is responsible for anchoring the final member of the PDH complex, the E3 enzyme. However, the structural relationship between E3 subunits and the E2 core involves the presence of a non–catalytic E3 binding protein (E3BP) (Harris et al., 2002; Jilka et al., 1986; Smolle & Lindsay, 2006). E3BP is responsible for the chemical connection between E3 subunits and the E2 core, and typical mammalian PDH complexes contain E3 and E3BP subunits in equal concentrations (Hiromasa et al., 2004). Furthermore, lipoyl domain C is unique in the sense that it is the only domain on the second free–swinging lipoyl arm.

In summary, it is generally believed that the PDH complex super arm consists of two lipoyl arms. One of the two lipoyl arms contains lipoyl domains A and B that serve to anchor the E1 subunit and the PDH regulatory enzymes, and the second arm contains lipoyl domain C, which serves to anchor the E3 subunit, and an E3 binding protein (Harris et al., 2002; Smolle & Lindsay, 2006). This structure clearly defines each

respective member of the PDH complex as organized components of a mapped sequence to facilitate essential interaction and regulation within the complex.

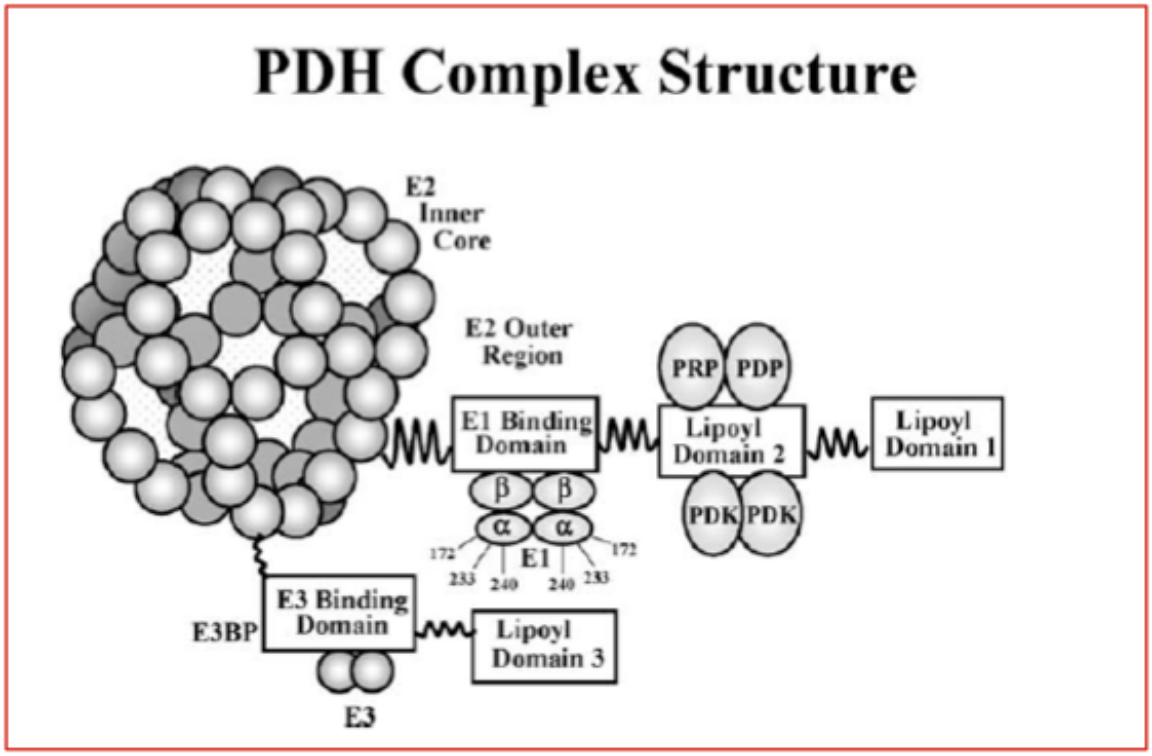

Figure 1. Structure of the mitochondrial PDH complex (Harris et al., 2002).

PDH: Individual Reactions

A defining characteristic of the PDH complex is that proper functioning always relates back to fundamental structure. All binding domains and lipoyl domains are interconnected to neighbouring components within the complex by a series of proline and alanine rich amino acid chains of approximately 30 amino acids in length (Harris et al., 2002; Smolle & Lindsay, 2006). The purpose of these chain links is to render the super arm more flexible, in order to enable lipoyl arm mobility (Smolle & Lindsay, 2006). The functional fluidity of the lipoyl arms is crucial to the overall efficiency and economy of the PDH complex. It is this multilateral action that enhances the proper relay of all

metabolic intermediates produced by individual E1, E2 and E3 reactions (Patel & Roche, 1990; Smolle & Lindsay, 2006).

The E1 enzyme (pyruvate dehydrogenase) is a heterotetramer that is composed of 4 monomer units (2 alpha and 2 beta), with an active site located at the interface of these components (Harris et al., 2002). In the presence of the cofactor thiamine diphosphate, E1 is responsible for the decarboxylation of three–carbon pyruvate molecules, leading to the production of two–carbon acetyl intermediates and carbon dioxide (Gutowski & Lienhard, 1976; Robinson & Chun, 1993; Smolle & Lindsay, 2006). This is the only non–equilibrium reaction within the PDH reactions, which distinguishes this step as the primary regulator of aerobic carbohydrate flux. The E2 enzyme (dihydrolipoyl transacetylase) is responsible for the production and release of acetyl–CoA, coupling the two–carbon intermediates yielded from E1 with available free CoA within the mitochondrial matrix (Smolle & Lindsay, 2006). E2 subunits begin this redox reaction in an oxidized state, and are subsequently reduced by the acetyl group produced in the E1 reaction to generate a stable intermediate. Now oxidized, the acetyl intermediate is reduced through combination with free CoA and released as acetyl–CoA. The E2 reaction is recognized as the source of working substrate for TCA cycle flux, as acetyl–CoA is the primary substrate of oxidative metabolism.

The E2 subunit must be re–oxidized before reacting with another acetyl intermediate, and re–oxidation is accomplished through the last reaction in the PDH complex. The E3 enzyme (dihydrolipoyl dehydrogenase) is the energy–transferring reaction of the PDH complex (Patel & Roche, 1990; Smolle & Lindsay, 2006). This enzyme transfers electrons from flavin adenine dinucleotide ($FADH_2$) to nicotinamide

adenine dinucleotide (NAD^+) in order to produce NADH, which is the reduced form of NAD^+ (Smolle & Lindsay, 2006; Yeaman, 1989). As a consequence, the E2 core is re–oxidized, and one full cycle of the PDH reactions has been completed. All PDH complex subunits are now chemically prepared to accept more substrate. Unlike the first reaction involving E1, reactions two and three in this sequence are near–equilibrium reactions that depend on substrate channeling from upstream subunits within the complex. This observation further solidifies the notion that the E1 subunit catalyzes the rate limiting reaction of the PDH complex.

Although independent, all three reactions depend upon one another and this is illustrated by the manner in which their isolated functions extend to the complex as a whole. The E2 subunit is the central player in the PDH complex from a structural and functional standpoint, as this enzyme forms the core foundation for which E1 and E3 moieties organize and execute their respective physiological functions (Harris et al., 2002).

In order to promote the interaction of E1, E2 and E3 enzymes, the PDH complex relies upon a classic cross–bridging mechanism to couple all active sites (Smolle & Lindsay, 2006). Tight, non–covalent bonds exist between E1 and E2 enzymes, as well as E3 and E3BP subunits. However, the same cannot be said between E2 and E3 enzymes. These structural relationships are of particular significance, because in an instance where E1 is bound to E2, the E3 lipoyl arm is not bound to E2 due to steric hindrance, and vice versa (Smolle & Lindsay, 2006). Consequently, both lipoyl arms (anchoring E1 and E3) are free to shuttle within the complex and execute the necessary cross–bridging activity in order to claim space on available E2 active sites.

It should be noted that E3BPs remain bound to isolated E2 subunits at all times, even when an E3 lipoyl domain is not interacting with and bound to E2 (Jilka et al., 1986). In fact, although a cohesive unit, E2 and E3BP are structurally distinct units (Jilka et al., 1986). Furthermore, through analytical ultracentrifugation of isolated recombinant human PDH components, it has been shown that E3 subunits do not bind to E2 cores lacking E3 binding proteins (Hiromasa et al., 2004). These findings strongly support the notion that E3BP is entirely responsible and available for the chemical connection between the E3 subunit and the E2 core.

This mechanism of activity is precisely what keeps the PDH complex moving at a predetermined rate (Yeaman, 1989). Physical interplay amongst the subunits is a direct application of the amino acid chain linkers, and highlights the importance of possessing free flowing lipoyl arms. Without such a defined structure, a regulatory function of this nature would not be possible. As a result, this synergistic mechanism allows for all metabolic intermediates produced within the complex to be shuttled for further catabolism as substrate for other enzymes within the complex (Smolle & Lindsay, 2006). The degree of chemical communication and networking seen in the PDH complex between glycolysis and oxidative metabolism is what opens the door for such tight regulation and management of carbohydrate stores.

PDH: "Macro" Regulation

The PDH complex is a cooperative unit that functions under strict regulation. Control of the complex is completely dependent upon the metabolic demands that are experienced in given physical situations. Many physiological perturbations exist that promote regulatory signaling towards the complex (e.g., nutritional, physical activity) (as

reviewed by Peters, 2003). As a consequence of these conditions, regulation of the PDH complex is centrally focused around covalent regulation. The phosphorylation state of the complex is the major influence upon PDH activity, and it can be denoted that this method of regulation via phosphorylation and dephosphorylation as a system of coarse, or "macro-level" regulation. Furthermore, covalent regulation reconnects with the concept of fuel partitioning, as the specific activity level of the complex determines the degree to which acetyl–CoA production is driven by carbohydrate or fat metabolism (Harris et al., 2002).

Covalent regulation of the PDH complex is accomplished by a series of four pyruvate dehydrogenase kinase isoforms (PDK1–4) (Bowker–Kinley, Davis, Wu, Harris, & Popov, 1998) and a pair of pyruvate dehydrogenase phosphatase isoforms (PDP1–2) (Huang et al., 1998). The relative activity of PDH regulatory enzymes in skeletal muscle is significant, as this tissue represents the greatest site for glucose disposal in the body (Stump et al., 2006). All regulatory proteins bind to the complex by way of lipoyl domain A, which is directly adjacent to the E1 subunit (Harris et al., 2002). Kinase enzymes bind to the complex as a dimer and attach phosphate molecules specifically to one of three serine residues on the alpha subunits of the E1 enzyme. The presence of tightly bound PDK causes interference in substrate channeling, leading to deactivation of the PDH complex (Harris et al., 2002). Moreover, it is the function of loosely bound phosphatase enzymes to reactivate the complex through dephosphorylation reactions (Smolle & Lindsay, 2006). Although E1 features alpha and beta subunits, it is only the alpha subunit that is a target for covalent modification (Yeaman et al., 1978). The relative activities of

the PDK and PDP enzymes determine the precise activity state of the PDH complex, and subsequent carbohydrate flux through oxidative metabolism (Harris et al., 2002).

Through the mechanism of covalent regulation, it should be understood that PDH complexes are never fully active or inactive at any given time (Harris et al., 2002). In actuality, flux through the complex lies along a sensitive continuum ranging from high to low activity states. Summated PDK and PDP activity levels are reflected in this overall phosphorylation state (Sugden & Holness, 2003). In a relatively high phosphorylation state, PDH activity will be lower, thereby inhibiting carbohydrate oxidation. As a result, fat oxidation will be activated to a greater degree. In a relatively low phosphorylation state, the complex will be more open and active, which will lead to a higher reliance on carbohydrates. Ongoing changes that occur during physical activity or dietary perturbations subsequently effect and alter the phosphorylation state of the complex, leading to fluctuations in PDH activity levels (as reviewed by Peters, 2003).

PDH: "Micro" Regulation

There are numerous physiological scenarios that affect pyruvate dehydrogenase activity by altering the phosphorylation state of the complex. This range of metabolic states may be thought of as the "micro" level of PDH regulation. It is these metabolic states that exert a fine regulatory influence upon the regulatory enzymes controlling the overall phosphorylation state, or "macro" level, of organization. In general, a higher concentration of reaction products (e.g., acetyl–CoA, NADH) will cause increased PDK activity, resulting in decreased PDH complex activity. For example, high–fat feeding studies have demonstrated increased in acetyl–CoA production via beta–oxidation in order to conserve carbohydrate stores. Consequently, PDK activity is increased in order

to down–regulate PDH complex activity (Peters, 2003). Furthermore, a higher concentration of substrate (e.g., pyruvate, coenzyme A, NAD^+) will cause decreased PDK activity, resulting in increased PDH complex activity (Yeaman, 1989). For example, physical activity causes increased glycolytic flux leading to increased pyruvate production, and pyruvate is a potent allosteric inhibitor of PDK activity (Peters, 2003). In the short term, with respect to acute regulation, PDH can be reversibly regulated by the influence of the complex's chemical intermediates. A strong presence of acetyl–CoA or NADH will inhibit PDH flux though increased PDK activity, whereas high levels of free coenzyme A and NAD^+ will antagonize this effect through increased PDP activity (as reviewed by Harris et al., 2002; Sugden & Holness, 2003). Another strong inhibitor of PDH phosphorylation by PDK is pyruvate. As the central working substrate of the PDH reaction, PDK activity is minimal and increased PDH flux will be observed when an abundance of this substrate is recruited for oxidation (Spriet & Heigenhauser, 2002).

In relation to the structure of the PDH complex, PDK and PDP enzymes bind to the E2 core via lipoyl domain A, which is the inner lipoyl domain of the E1 lipoyl arm (Harris et al., 2002). Both regulatory enzymes bind at the same location, and it is the presence of one or the other that activates or inhibits active site coupling amongst the PDH subunits (as reviewed by Harris et al., 2002). There are three serine residues (sites 1, 2 and 3) located in the E1–alpha (E1α) active site that are targeted for phosphorylation. Phosphorylation of these sites occurs in a specific order, where kinases target serine residue 1 first, followed by the 2^{nd} and 3^{rd} sites (Kolobova, Tuganova, Boulatnikov, & Popov, 2001). This tendency may be related to residue location, as sites 1 and 2 are located on the edge of the E1α active site and can be accessed more easily compared to

site 3, which is buried more deeply in the enzyme structure (as reviewed by Maj, Cameron, & Robinson, 2006). On the other hand, dephosphorylation via PDP can occur in random sequence with less specific tendencies (Kolobova et al., 2001). Beyond specific binding patterns, investigation has also revealed that phosphorylation at each serine residue can have varying effects within the complex. Phosphorylation at site 1 is sufficient to fully inactivate the PDH complex. However, phosphorylation of sites 2 and 3 demonstrate additional effects (Kolobova et al., 2001). The major function of site two is to promote PDH inactivation; however, this site also exhibits inhibitory effects toward PDH reactivation via PDP enzymes. The only role of serine residue 3 is to prevent reactivation via PDP (Kolobova et al., 2001). It is important to visualize that the E1 binding domain (location of the E1α serine residues) is proximal to the E2 core relative to lipoyl domain A, which is where the regulatory enzymes PDK and PDP bind. This structural detail demonstrates that PDK and PDP work in a linear fashion that directly affects the interaction between adjacent E1 and E2 subunits of the PDH complex. Based upon this complex structure, we can gain a better understanding of how all PDH subunits interact in such an efficient manner.

All four isoenzymes of skeletal muscle PDK are able to phosphorylate the serine residues of the E1α subunit (Bowker–Kinley et al., 1998). The differing kinase isoenzymes have been distinguished by the numbers 1–4, as each isoform features its own set of unique characteristics. Although all four PDKs are capable of phosphorylating E1α serine residues, their specific roles in reference to PDH activity are still uncertain (as reviewed by Bowker–Kinley et al., 1998). Research has demonstrated varying patterns of allosteric regulation amongst the four PDKs, and this is demonstrated through unique

enzyme kinetics, allosteric activation and inhibition, phosphorylation site specificity, as well as tissue distribution in the body.

In a study completed by Bowker–Kinley et al. (1998), major tissue (heart, brain, spleen, liver, skeletal muscle, kidney, and the testes) distributions of all four PDK isoenzymes were determined through Northern blot analysis of messenger ribonucleic acid (mRNA) concentrations in rats. PDK1 was highly expressed in heart tissue, and was not found in any other major tissue in the body. A similar distribution pattern was noted for PDK3, as this enzyme was dominantly expressed in testes with extremely low and insignificant levels detected in other tissues. PDK4 was abundant in skeletal muscle and heart tissues, and weakly distributed in all other tissues. Lastly, PDK2 was found in every tissue tested, making this isoform the most ubiquitous and abundant.

Pertaining to PDK enzyme kinetics, Kolobova et al. (2001) conducted an *in vitro* study measuring the amount of phosphate incorporated from adenosine triphosphate (ATP) to PDH E1α serine residues in order to determine fundamental rates of activity for all four human recombinant PDK isoenzymes. PDK characteristics were determined by measuring phosphorylation rates through a direct molar relationship (mol/mol) between molecules of phosphate and molecules of the PDH E1 subunit. Through this method, it was determined that PDK1 was the most active isoform with the highest V_{max}, incorporating 3.4 moles of phosphate from ATP per mol of E1. Under the same conditions PDK2, PDK3 and PDK4 reported measurements of 1.6 moles, 2.8 moles and 2.6 moles, respectively (Kolobova et al., 2001). These numbers are of particular significance, as PDK enzymes appear to function according to a phenomenon known as ‘half of the site’ reactivity. Every E1α subunit contains 3 serine residues, each with 2

sites for potential phosphorylation, which provides a total of 6 potential phosphorylation sites (Kolobova et al., 2001; Sugden & Holness, 2003). However, according to 'half of the site' reactivity, it was observed that the maximal number of phosphate molecules that could be incorporated in E1 was 3. Results from this study demonstrate that only PDK1, PDK3 and PDK4 follow this trend. PDK2 appears to be the only isoenzyme deviating from this principle, reporting a lower rate of activity of phosphate incorporation per mole of E1 (Kolobova et al., 2001).

Pyruvate is known to have a strong inhibitory influence on PDK activity. However, each isoform responds differently to this allosteric inhibition, which has revealed more information with regard to specific isoenzyme characteristics (Bowker–Kinley et al., 1998). Synthetic dicholoroacetate (DCA) was tested in order to assess PDK inhibition by pyruvate, as this chemical is known to mimic the effect of pyruvate as a specific inhibitor of PDK activity (Bowker–Kinley et al., 1998). PDK2 responds very strongly to allosteric inhibition by pyruvate, as the addition of 0.2 mM of DCA was required to reduce PDK2 activity by half. PDK1 and PDK4 are less sensitive to inhibition by pyruvate, as they required 1 mM and 0.5 mM of DCA, respectively, in order to reduce activity levels by half. PDK3 was the only isoform that required a much higher concentration of DCA (8 mM) to exert the same influence upon this enzyme (Bowker–Kinley et al., 1998). This finding is significant as it demonstrates the ability of PDK3 to contribute to the regulation of CHO oxidation in the presence of high glycolytic rates and high intracellular pyruvate concentrations.

PDK1 appears to be the most powerful isoenzyme in the PDK family, yet PDK2 is the most ubiquitous in rat tissue (Kolobova et al., 2001). Beyond these leading

characteristics, PDK4 is known to play a significant role specifically within skeletal muscle tissue (Bowker–Kinley et al., 1998). PDK3 appears to be the least understood member of the PDK family in skeletal muscle, primarily due to its extremely low mRNA concentration and protein expression. Another distinctive difference between all kinases is their serine site specificity for phosphorylation. For example, while all four PDKs are capable of phosphorylating serine residues 1 and 2, only PDK1 has demonstrated an ability to phosphorylate site 3 (Kolobova et al., 2001). This observation speaks highly to the potency of PDK1 towards inactivating the complex, as this isoform has shown the ability to incorporate phosphate at a rate 2–fold higher than PDK3 and PDK4, and 3–fold higher relative to PDK2.

Another noteworthy observation refers to the rates at which each serine residue is phosphorylated. Site 1 is the major PDH inactivating site, while sites 2 and 3 contribute less to inactivation and serve to prevent PDH reactivation by PDP (Kolobova et al., 2001). This pattern of activity is reflected in the activity rates of all kinases at each site. At site 1, PDK1 incorporated 2.9 moles of phosphate per mol of E1α, whereas PDK2, PDK3 and PDK4 incorporated an average of 1.5 moles of phosphate at site 1 (Kolobova et al., 2001). Furthermore, site 2 phosphorylation rates decreased to 2.8, 1.0, 1.6 and 1.7 mol/mol for PDK1, PDK2, PDK3 and PDK4 respectively, data that further characterizes PDK1 as the most active PDK isoform within the PDH complex. PDK2, PDK3 and PDK4 demonstrate enhanced site specificity relative to PDK1 through their decreased activity levels at all serine residues, and these trends have been reported previously. As reviewed by Maj et al. (2006), site specificity for site 1 is in the following order: PDK2 > PDK4 > PDK1 > PDK3. For site 2, specificity order is PDK3 > PDK4 > PDK2 > PDK1. Recall that these

are the two sites that all kinases can act upon, and based upon the established unique individual activity levels (with PDK1 exhibiting higher activity than all other PDKs), it is not surprising to notice PDK1 is at the lower end of the specificity spectrum for both phosphorylation sites.

The common ground connecting the two PDP isoenzymes is that they both require magnesium (Mg^{2+}) for activity. However, PDP1 and PDP2 do have a sub–set of individual characteristics. In addition to Mg^{2+}, PDP1 also requires calcium ions (Ca^{2+}). In fact, the only way that PDP1 can bind to the PDH regulatory domain is through a chemical interaction requiring Ca^{2+} (Huang et al., 1998). Furthermore, calcium presence stimulates PDP1 activity as well by increasing the sensitivity of PDP1 to intracellular magnesium, leading to a 10–fold increased rate of activity (Huang et al., 1998). Furthermore, PDP1 is the only phosphatase to feature a regulatory subunit (PDPr). This regulatory molecule functions by blocking the PDP1 active site in order to compete with intracellular magnesium (Yan, Lawson, & Reed, 1996). In the event that an association with magnesium is prevented through competitive inhibition, PDP1 activity is inhibited. Therefore, PDP1 sensitivity towards magnesium is decreased through an inhibitory effect (Yan et al., 1996).

From a tissue distribution perspective, PDP1 is most abundantly expressed in the heart, brain, testes and skeletal muscle, and it is the dominant phosphatase enzyme in calcium–sensitive tissues, such as skeletal muscle and brain (Huang et al., 1998). The primary role of PDP enzymes is to stimulate the oxidation of carbohydrate sources for energy production; therefore, a significant presence of PDP1 in tissues that rely heavily upon CHO oxidation is logical.

PDP2 does not require calcium in order to function, and it is typically targeted in metabolic scenarios involving nutritional or hormonal perturbations (as reviewed by Harris et al., 2002). PDP2 is highly expressed in adipose tissue, but is also expressed in the heart, kidneys and liver (Huang et al., 1998). Based upon the fact that this isoenzyme is not functionally dependent upon calcium ions, and does not feature a distinct regulatory component, we are led to believe that PDP2 is the less regulated isoenzyme of the PDP family. However, PDP2 has been shown to function at a rate of activity 50–fold lower than PDP1, potentially eliminating the need for fine–tuned regulation (as reviewed by Sugden & Holness, 2003). Although PDP2 features simpler enzyme kinetic and regulation, the presence of insulin is known to effect sensitivity towards magnesium, leading to increased enzyme activity (Caruso et al., 2001).

Rationale: Evidence for the Covalent Regulation of PDP

In the past decade, the literature has demonstrated considerable evidence implicating additional regulatory mechanisms of PDP enzymes in skeletal muscle tissue. Pertinent studies focused on these explicitly suggest covalent modification as a regulator of *in vivo* PDP activity. The most recent support for this development exists through experiments that highlight significant discrepancies between maximal PDP enzyme activities and the intramuscular contents of PDP protein. This discrepancy has been observed in human skeletal muscle (Love et al., 2011) and various fiber type compositions (I, IIA & IIX/B) in rat hindlimb skeletal muscle (LeBlanc et al, 2007; LeBlanc et al., 2008). Furthermore, this phenomenon has been reported in response to multiple metabolic perturbations, such as aerobic exercise training (LeBlanc et al., 2008) and nutritional manipulation (LeBlanc et al., 2007).

From an investigatory perspective, these results have been documented within longitudinal (LeBlanc et al., 2007; LeBlanc et al., 2008) and cross–sectional study designs (Love et al., 2011). This consistency between experimental designs is significant, providing an integrated analysis that promotes the understanding of stable regulatory adaptations amongst the basal kinetics of PDP enzymes. The consistent documentation of this finding across methodologies has provided convincing validity towards this development. However, further investigation at the whole–tissue and cellular levels is required in order to identify the mechanisms underlying covalent modification of PDP.

Expression of both PDP isoforms (PDP1 & PDP2) is capable of being up– (LeBlanc et al., 2008) and down–regulated (LeBlanc et al., 2007), depending on metabolic perturbation. This plasticity is consistent with other catalytic subunits and proteins within the PDH complex (LeBlanc, Peters, Tunstall, Cameron–Smith, & Heigenhauser, 2004b; Maury et al., 1995). One study from LeBlanc et al. (2007) examined the regulatory potential of PDP enzymes in rat skeletal muscle in response to 48 hours of starvation. In comparison to fed counterparts, significantly decreased PDP activity levels were observed within all major skeletal muscle fiber types of food–deprived subjects (LeBlanc et al., 2007). Consequently, it was hypothesized that fat oxidation was part of the cellular efforts to conserve carbohydrate intermediates, which is a widely accepted response to nutritional states such as starvation and carbohydrate restriction (Sugden, Howard, Munday, & Holness, 1993). Furthermore, the change observed in PDP activity was reflected in a decreased flux through active PDH complexes in food–deprived rats (LeBlanc et al., 2007). It should also be noted that PDP activity measures are performed on mitochondrial extracts and are independent of

mitochondrial effectors. Therefore, PDP activity measures reflect stable changes that are a result of a given perturbation. However, when protein content of PDP isoforms was quantified between fed and food–deprived rats using Western blot analysis, no significant differences were reported with respect to PDP1 protein content. These findings suggest that the observed changes in PDP activity were not solely due to changes in PDP1.

PDP1 is the ubiquitous isoform in skeletal muscle tissue (Huang et al., 1998), and its influence may be expected to dissipate in the context of nutritional perturbation. PDP1 activity may indeed be reduced in response to starvation; however, this is not illustrated through measures of whole muscle protein content. PDP2 protein content was significantly reduced in red gastrocnemius muscles of food–deprived rats, but PDP2 protein was entirely undetectable in soleus and white gastrocnemius muscles of all subjects (LeBlanc et al., 2007). A decreased PDP2 content is not surprising based upon this isoform's sensitivity to insulin (Popp, Kiechle, Kotagal, & Jarett, 1980). In nutritional states where carbohydrate intake is dramatically reduced, intracellular signaling mechanisms that activate this isoenzyme may be silenced, effectively removing the driving force behind PDP2 transcription. This finding would have been significantly convincing if mirrored in PDP1, as well as in tissues that do not rely predominantly upon aerobic energy production through the PDH complex. However, the presence of PDP2 in skeletal muscle tissue has been nearly untraceable (Huang et al., 1998). Therefore, it cannot be accepted with confidence that a reduction in PDP activity in skeletal muscle is strictly due to decreased PDP2 isoform content (LeBlanc et al., 2007).

A second study from LeBlanc et al. (2008) subjected lean and obese Zucker rats to 8 weeks of aerobic endurance training. Results demonstrated that 8 weeks of aerobic

training significantly increased PDP activity levels in all major fiber types of obese rats (LeBlanc et al., 2008). This finding was also observed in lean counterparts, but only in select oxidative muscles (soleus, 84% type I; red gastrocnemius, 30–51% type I) (LeBlanc et al., 2007) that rely upon aerobic energy production (LeBlanc et al., 2008). The training response in both subsamples indicates that an increased capacity to activate the PDH complex and oxidize carbohydrates is not limited to the treatment of nutritional challenges. However, as previously described, the protein content of individual PDP isoforms did not mirror patterns observed in enzyme activity. Increased PDP1 protein content reached statistical significance only in highly oxidative soleus muscles (LeBlanc et al., 2008). Significance was reached in red gastrocnemius muscles of obese rats, but was absent in lean counterparts; however, a smaller magnitude in adaptation is to be expected when working with lean subjects. Nonetheless, this detail may speak to a substantial physiological need with obesity and does not rule out the potential presence of PDP covalent regulation. With respect to PDP2 protein content, PDP2 was once again only detected in red gastrocnemius, and no significant differences were observed in response to aerobic endurance training (LeBlanc et al., 2008).

In lieu of the physiological properties of PDP1, a cause and effect relationship between PDP activity and PDP1 expression cannot be made according to this investigation. With respect to PDP2, PDP1 is found in overwhelming quantities in skeletal muscle tissue (Huang et al., 1998), and its activity is almost entirely dependent upon the presence of intracellular calcium ions (Lawson et al., 1993). An enzyme of this nature would be expected to exhibit stable increases in skeletal muscle protein expression in response to an 8–week exercise training program with continuous allosteric activation.

The fact that this adaptation was not observed across all conditions and fiber types in concert with increased enzyme activity lends greater support to the notion that PDP enzymes may in fact be under the influence of an alternate level of regulation. It is reasonable to suggest covalent regulation as one potential alternate, as the phosphorylation of PDP would persist through the mitochondrial extraction procedure.

Based upon the established regulatory adaptability of PDP activity, it is reasonable to suggest that relationships may exist between markers of metabolic fitness and PDP activity. Only one study has attempted to establish such correlations through the use of human skeletal muscle biopsies (Love et al., 2011). This study demonstrated that individuals with increased muscular aerobic capacity possessed a greater capacity for carbohydrate oxidation, as citrate synthase activity was significantly correlated with PDP activity (nmol • minute^{-1} • mg mitochondrial protein^{-1}) (Love et al., 2011). However, PDP1 protein content in whole muscle samples only accounted for 18% of the variance in PDP activity at the whole muscle level (Love et al., 2011). This finding illustrates that in a human sample characterized by significant variability in whole–body and muscular aerobic capacity, PDP1 protein content within whole tissue is not the sole determining factor of PDP activity, suggesting again that there is an alternative long–term regulatory mechanism for PDP activity.

The covalent activation of PDP via phosphorylation has been previously demonstrated, but only in a cell culture model. Through the use of L6 myoblasts, it has been determined that the protein kinase C–delta (PKCδ) isoform undergoes rapid and transient translocation to mitochondria in response to insulin receptor activation (Caruso et al., 2001). Investigation of multiple kinase families, including various isoforms within

these families, showed that selective inhibition of PKCδ eliminates insulin–stimulated activity of the PDH complex. Inhibition of phosphatidylinositol–3–kinase and mitogen–activated protein kinase families, as well as PKC–beta and PKC–epsilon isoforms caused no change in basal activities of the active PDH complex, indicating that these enzymes are uninvolved in the signaling cascade responsible for PDP phosphorylation (Caruso et al., 2001).

PDP and PDK proteins act upon the E1α regulatory subunit of the PDH complex inside the mitochondria (Schnaitman & Greenawalt, 1968), and confirmation of PKCδ translocation to this region of the cell is crucial in establishing a direct physical relationship for this PKC isoform and PDP. Western blot analysis of basal [non–insulin–stimulated] cells has confirmed that PKCδ is primarily detected in the nuclear and cytosolic subcellular fractions (Caruso et al., 2001). However, insulin stimulation led to an increased presence of PKCδ in mitochondrial and plasma membrane fractions of L6 myoblasts with reciprocal decreased content in the nucleus and cytosol. In addition to this subcellular redistribution, PKCδ activity was increased 2–fold within the mitochondria and plasma membrane in response to insulin stimulation (Caruso et al., 2001). Taken together, these data indicate that PKCδ responds directly to insulin–signaling and targets regulatory proteins of the PDH complex downstream.

PDH complex activity levels are dependent upon concomitant changes to the combined regulatory activities of PDK and PDP enzymes (Linn, Pettit, & Reed, 1969). Through the use of a non–specific phosphatase inhibitor (sodium fluoride) and the suppression PKCδ protein expression, insulin activation of PDP activity was inhibited by 95% in L6 myoblasts (Caruso et al., 2001). In comparison to basal controls, insulin

induced no effect on PDK activity whatsoever. The presence of a general kinase inhibitor (dichloroacetic acid) completely blocked PDK activity in both cell lines, and treatment with the same PKCδ antisense oligonucleotide caused no change in PDK activity levels (Caruso et al., 2001). These findings demonstrate that the insulin–stimulated activation and translocation of PKCδ targets only PDP specifically, as opposed to inactivating PDK. Furthermore, analysis of mitochondrial subfractions from L6 myoblasts demonstrated a radiolabeled ^{32}P–phosphorylation of both PDP isoforms in response to PKCδ activation (Caruso et al., 2001). This experiment has established a physical protein–protein interaction in the form of phosphorylation upon PDP isoenzymes by PKCδ in cultured cells. However, there have been no studies to date to examine this regulation in a more physiological model.

Based upon the fact that skeletal muscle is the major target of insulin action (Caruso et al., 2001), this signaling cascade presents a physiologically relevant explanation to current anomalies observed in studies of mammalian skeletal muscle PDP activity. Furthermore, it is must be understood that these L6 myoblasts expressed wild–type human insulin receptors (Caruso et al., 2001). This methodological feature is significant with the respect to the extrapolation of these findings to PDH regulation in human skeletal muscle. However, these results have not yet been confirmed in intact skeletal muscle. More research is required in order to demonstrate these signaling mechanisms at the whole tissue level.

Further support for an alternate intracellular signaling cascade leading to PDP phosphorylation has been suggested in response to AMP–activated protein kinase (AMPK) activation (Smith, Bruce, & Dyck, 2005). AMPK stimulation by 5–amino–4–

imidazolecarbomoxide riboside significantly increased AMPK α2 isoform activity in soleus skeletal muscle strip incubations, promoting increased glucose uptake and fatty acid oxidation towards overall ATP production. Glucose oxidation was increased, potentially as a secondary response to an increase in glucose uptake, as demonstrated by significant increases in PDH*a* activity (Smith et al., 2005). However, increased flux through PDH*a* was observed with concurrent decreases in pyruvate concentrations, which is the primary working substrate for the basic PDH reaction (Smith et al., 2005). Consequently, these findings have generated further speculation that the PDH complex may be a direct downstream target of activated AMPK during times of decreased energy charge in skeletal muscle.

CHAPTER 2:

Statement of the Problem

Mammalian skeletal muscle has demonstrated responsive and adaptable PDP enzyme maximal activity through a variety of metabolic perturbations. However, these measurements of PDP maximal enzyme activity cannot be fully accounted for by changes in PDP skeletal muscle protein content. Sufficient evidence exists to implicate the covalent modification of predominant PDPs in mammalian skeletal muscle. Mirrored results between *in vivo* muscle tissues (human & rat) and cell culture lines confirm the regulatory potential of PDP enzymes. Collectively, these results demonstrate a discrepancy between PDP isoenzyme protein content and total PDP maximal enzyme activity. Therefore, this evidence confirms the need to further advance the understanding of PDP enzyme regulation by studying the phosphorylation state of PDP1 and PDP2 isoenzymes.

Purpose

The purposes of this thesis are: 1) to determine if there are differences in phosphorylation levels in PDP1 and PDP2 isoenzymes between basal and insulin–stimulated conditions at the whole tissue level; and 2) to investigate whether mitochondrial enrichment of PKCδ is correlated with content of phosphorylated PDP1 and PDP2 in intact skeletal muscle.

Hypotheses

1) It is expected that phosphorylation levels of PDP isoforms will be increased in response to insulin stimulation compared to basal conditions.
2) Total PDP and PDH*a* enzyme activity levels are expected to increase in response to insulin stimulation, and are expected to mirror any increases in PDP1 & PDP2 phosphorylation (immunoprecipitation and Western blotting).
3) Due to the fact that PKCδ has been shown to phosphorylate PDP isoforms, it is expected that increased mitochondrial enrichment of PKCδ will be observed in response to insulin stimulation.

CHAPTER 3:

METHODS

Study Design

This study implemented one treatment (insulin stimulation) with 80 match–paired rat extensor digitorum longus muscles from 40 male Long Evans rats. Phosphorylation of both PDP isoforms (PDP1 & PDP2) was determined at two sites: threonine (data not shown) and serine. Following surgical extraction, all muscles were incubated for a 30–minute equilibration period in incubation medium (Medium199; Sigma–Aldrich, Oakville, Ontario, Canada). Muscles underwent incubation for a second 30 minute interval under basal (Medium199 only) or insulin–stimulated (Medium199 and 10 mU/mL Humilin–R) conditions. Following the experimental incubation period, 44 muscles were immediately frozen in liquid nitrogen and stored at –80° C for subsequent biochemical analysis. Frozen tissue was reserved for Western blotting of phospho–Akt protein content and for the determination of PDH*a* activity by radiolabeled ^{14}C–acetyl–CoA accumulation. Furthermore, frozen tissue was reserved for immunoprecipitation and Western blotting procedures in order to verify PDP phosphorylation. The remaining 36 muscles were used fresh for the isolation of subsarcolemmal mitochondria. First, mitochondria were used for the analysis of PDP and CS activities. Analysis of PDP activity was expected to compliment any changes in PDP1 and PDP2 phosphorylation. Second, mitochondria were reserved for the analysis of mitochondrial PKCδ enrichment via Western blotting. PKCδ is believed to be the kinase responsible for phosphorylation of both PDP1 & PDP2 within the mitochondria (Caruso et al., 2001). Tyrosine residues were not investigated as a potential site of PDP phosphorylation, as the PKC family of

kinases targets serine and threonine residues only (Breitkreutz, Braiman–Wiksman, Daum, Denning, & Tennenbaum, 2007).

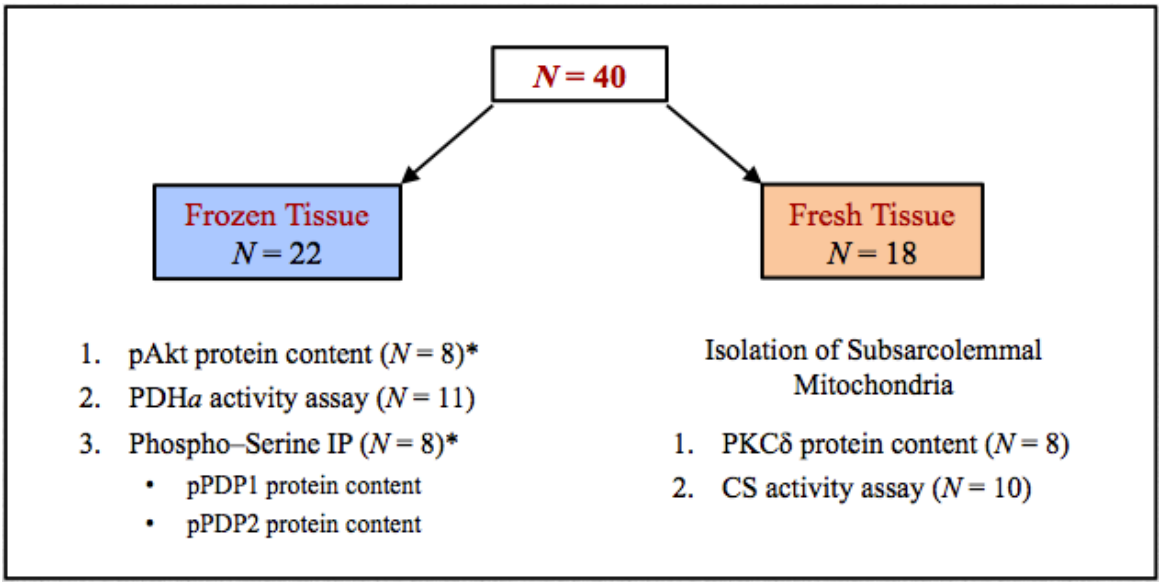

Figure 2. Match–paired EDL tissue allocation by methodological procedure.
*Five of eight match–paired muscles used in both procedures.

Animals

Male (n = 40) Long Evans rats weighing an average of 110 ± 19 grams were obtained from Charles River Laboratories (Saint–Constant, Québec, Canada) at 3 weeks of age. All animals were housed in a controlled environment with a 12:12–h light–dark cycle, and were fed standard rat chow (23% protein, 11% fat, 67% carbohydrate; 5012 Rat Diet, Lab Diet, Aberfoyle, Ontario, Canada) and water *ad libitum*. Animals were acclimatized to their new surroundings for 1 week before experiments commenced. All study protocols were approved by the Brock University Animal Care and Use Committee (ACUC). All procedures were consistent with the ethics of animal experimentation as set out by the Canadian Council on Animal Care (CCAC).

Surgeries

Animals were anaesthetized with an intraperitoneal injection of pentobarbital sodium (Euthanyl; Bimeda, Cambridge, Ontario, Canada) using a 27–gauge needle (60 mg/1 kg body weight). Surgeries did not commence until the palpebral reflex and the toe pinch withdrawal response were absent. Bilateral extensor digitorum longus (EDL) muscles were extracted with defined and pre–sutured tendons intact (Gittings, 2009). At the conclusion of the dissection procedure, animals were euthanized humanely with an overdosed intraperitoneal injection of pentobarbital sodium (120 mg/kg body weight). Animals were monitored post–operatively until the cessation of cardiac activity was observed.

Muscle Incubations

Isolated muscle incubations were performed using a structurally intact skeletal muscle model. Immediately following extraction, longitudinal EDL muscles were placed in a controlled organ bath as quickly as possible (<5 s) in order to maintain tissue viability. Sutured muscles were fully submerged in a petri dish containing pre–warmed (25° C) and oxygenated (95% O_2–5% CO_2) Medium199 in preparation for the incubation apparatus. The petri dish was used in order to minimize tissue degradation variability between individual muscles, ensuring that all muscles were rapidly introduced to *in vitro* oxygenated conditions (Bonen, Clark, & Henriksen, 1994). Once distal sutures were hooked and secured in the petri dish, the muscles were inserted into a 15 mL incubation reservoir (Radnoti LLC, Monrovia, California, U.S.A.) containing pre–warmed and oxygenated Medium199. Proximal sutures were then suspended on force displacement transducer hooks (Grass Technologies, West Warwick, Rhode Island, U.S.A.). With both

sutures properly fixed within the incubation apparatus, the force transducer was adjusted to maintain 1 g of resting tension throughout the incubation period. Resting tension was applied in order to recreate an *in vivo* resting workload upon EDL muscles (Cermak, LeBlanc, Peters, Vandenboom, & Roy, 2009). All EDL muscles underwent an equilibration period (30 minutes) in order to return to baseline conditions after the rigors of surgical stress. For study of basal control muscles, equilibration incubations were maintained for a second 30–minute interval. For the incubation of contralateral insulin–stimulated experimental muscles, Medium199 contained 10 mU/mL of human insulin (Humilin–R, Eli Lilly, Toronto, Ontario, Canada) (Collier, Bruce, Smith, Lopaschuk, & Dyck, 2006; Pehleman et al., 2005; Smith et al., 2007; Stefanyk et al., 2011). Experimental muscles were also incubated for an additional 30–minute interval. At the end of the incubation period, muscles were either immediately freeze–clamped in liquid nitrogen and stored at –80° C or processed fresh for the isolation of subsarcolemmal mitochondrial.

Previous research has illustrated that incubation conditions must be controlled properly to ensure that adequate diffusion of substrates and gases is permitted. Furthermore, conditions must be critically designed in order to maintain tissue viability and the biochemical integrity of metabolic pathways (Bonen et al., 1994). Young rats were obtained for all experiments in order to examine incubated EDL muscles of appropriate size and thickness. This selection was made with an aim to prevent oxygenation and diffusion limitations to all EDL muscle fibers. Rat EDL muscles were chosen over mouse EDL muscles as the most scientifically appropriate, as the mouse has a significantly higher metabolic rate than the rat (Bonen et al., 1994). This difference in

animal model is significant, as the use of the mouse model could lead to a greater consumption of oxygen by peripheral muscle fibers, therefore limiting oxygen supply to deeper fibers and producing anoxic conditions (Bonen et al., 1994). An incubation medium temperature of 25° C was selected in order to further promote the oxygenation of internal muscle fibers. All EDL muscles under study did not exceed a thickness of 2 mm (Cermak et al., 2009; Bonen et al., 1994), which is an appropriate diameter to ensure complete oxygenation of all fibers in an *in vitro* incubation medium warmed to 25° C (Hill, 1972). With respect to rats at 4 weeks of age and an average weight of 110.21 ± 19.85 grams, the critical muscle thickness for adequate oxygenation of EDL muscles *in vitro* at 25° C is 1.94 mm (Segal & Faulkner, 1985).

Mitochondrial Isolation

Intact subsarcolemmal mitochondria were isolated as originally described by Makinen and Lee (1968) and adjusted by Jackman and Willis (1996). Mitochondria were extracted from fresh extensor digitorum longus muscles following resting and insulin–stimulated incubations. Using an inverted petri dish placed on ice, fresh muscles were finely cut by hand using mincing scissors as quickly as possible. Approximately 5–15 mg of minced muscle was immediately frozen in liquid nitrogen and stored at –80° C for allocation to the citrate synthase activity assay (discussed later in the citrate synthase activity assay).

The remaining minced muscle was weighed and immediately placed in 500 μL of solution 1 (100 mM KCl, 40 mM Tris HCl, 10 mM Tris base, 5 mM $MgSO_4$, 5 mM Na_2EDTA, 1 mM ATP, 200 μM 7,8–dihydroxycoumarin (kinase inhibitor), and 1 PhosSTOP tablet/10 mL (phosphatase inhibitor: Roche Applied Science, Laval, Québec,

Canada), pH 7.4). Muscles were further minced in solution 1 and transferred into a glass homogenizing potter and topped up with additional solution 1 in order to produce a 20–fold dilute sample. All muscles were homogenized as gently as possible until an opaque homogenate was produced. Rigorous homogenization was avoided in order to maintain as many intact mitochondria as possible. Homogenates were then transferred to culture tubes in preparation for differential centrifugation.

Samples were first centrifuged at 700 x *g* for 10 minutes at 4° C in order to remove large cellular debris. Supernatants containing mitochondria were retained and transferred to clean eppendorf tubes. Supernatants were then centrifuged at 14,000 rpm for 10 minutes at 4° C in order to pellet mitochondria. Supernatants from this second spin were discarded. Mitochondria were resuspended in 10 volumes of solution 2 (100 mM KCl, 40 mM Tris HCl, 5 mM Tris base, 1 mM $MgSO_4$, 100 μM Na_2EDTA, 250 μM ATP, 1% BSA, (w/v) 200 μM 7,8–dihydroxycoumarin, and 1 PhosSTOP tablet/10 mL, pH 7.4) in order to bind and remove all free fatty acids present in solution. Samples were then centrifuged at 7,000 rpm for 10 minutes at 4° C to recollect the mitochondria after washing. As a final washing step, mitochondria were resuspended in 10 volumes of solution 3 (100 mM KCl, 40 mM Tris HCl, 5 mM Tris base, 1 mM $MgSO_4$, 100 μM Na_2EDTA, 250 μM ATP, 200 μM 7,8–dihydroxycoumarin, and 1 PhosSTOP tablet, pH 7.4) and once again centrifuged at 7,000 rpm for 10 minutes at 4° C. Following all washing steps, mitochondria were resuspended in a sucrose and mannitol buffer (220 mM sucrose, 70 mM mannitol, 10 mM Tris HCl, 100 μM Na_2EDTA, 200 μM 7,8–dihydroxycoumarin, and 1 PhosSTOP tablet/10 mL, pH 7.4) at a 1:1 w/v ratio (1 mg wet tissue weight/1 μL). A 5 μL aliquot of the mitochondrial suspension was added to 95 μL

of sucrose and mannitol to produce a mitochondrial total suspension (CS_{TS}) for mitochondrial recovery analysis (discussed later in the citrate synthase activity assay). The remaining volumes of all mitochondrial extracts were reserved for use in the PDP activity assay. All products of the mitochondrial isolation procedure (whole tissue sections, mitochondrial extracts, and mitochondrial total suspensions) were stored at –80° C for future citrate synthase and PDP experiments.

Immunoprecipitation

A piece of frozen EDL tissue (~20 mg) was homogenized on ice in 25 volumes of lysis buffer containing 50 mM Tris base (pH 7.4), 150 mM NaCl, 1 mM EGTA, 200 µM 7,8–dihydroxycoumarin (Sigma–Aldrich, Oakville, Ontario, Canada), protease inhibitor cocktail (Roche Applied Science, Laval, Québec, Canada), and phosphatase inhibitor cocktail (Roche Applied Science, Laval, Québec, Canada). Each prepared homogenate was aliquoted into two portions, each containing 500 µg of protein. Volumes of whole homogenate containing 500 µg of protein were calculated according to protein determinations obtained through Bradford assay analysis. A 500 µL aliquot of lysis buffer was also prepared as a sample blank. Aliquots were incubated with polyclonal primary antibodies against serine or threonine phosphorylation residues (Millipore, Billerica, Massachusetts, U.S.A.) in order to bind all proteins in the phosphorylated state. Incubations with primary antibodies were carried out overnight at 4° C with gentle agitation (Elion, 2006). Immediately following the first round of incubations, all samples were loaded with 20 µL of protein G–PLUS agarose bead conjugate suspension (Santa Cruz Biotechnology, Dallas, Texas, U.S.A.) for a second overnight incubation at 4° C with gentle agitation (Elion, 2006). Samples were centrifuged at 13,000 rpm for 3

minutes and immunoprecipitated pellets were collected. All supernatants were discarded at this stage. Depending on the nature of the study, supernatants may have needed to be retained for Western blotting in order to ensure that all proteins of interest were cleared from the cell lysate and contained strictly within the immunoprecipitated pellet. Pellets were washed twice with 500 µL of 1x PBS and underwent centrifugation at 13,000 rpm for 1 minute following each wash. Aspirated supernatants from the washing phase were discarded. After the final wash, immunoprecipitated pellets and diluted whole homogenates (1 µg/µL) were resuspended in 2x electrophoresis sample buffer containing 50 nM Tris–HCl (pH 6.8), 2% (w/v) SDS, 10% (v/v) glycerol, 5% (v/v) 2–mercaptoethanol and 0.1% (w/v) bromophenol blue. All samples were solubilized in boiling water for 5 minutes before undergoing Western blot analysis.

Whole homogenates and blanks were included in the Western blot analysis for two significant reasons: 1) as a point of verification, as detection of PDP1 & PDP2 in whole homogenate ensured the proper technical execution of the analysis; and 2) as repeated samples within blots for the normalization of sample comparisons and analyses.

Western Blot Analysis

Standard sodium dodecyl sulfate polyacrylamide gel electrophoresis was performed using 6% stacking and 14% separating gels. Proteins underwent migration for 2 hours at 120 volts in running buffer containing 31 mM Tris–HCl (pH 8.3), 240 mM glycine, and 0.1% (w/v) SDS. Electrophoretically–separated proteins were transferred onto polyvinylidene fluoride (PVDF) membrane (Immobilon–P, Millipore, Billerica, Massachusetts, U.S.A.) for 1 hour at 100 volts. The transfer buffer contained 25 mM Tris–HCl (pH 8.3), 192 mM glycine, 20% (v/v) methanol, and 0.1% (w/v) SDS.

Membranes were incubated in Tris–buffered saline–Tween (TBST) buffer (pH 7.5) containing 20 mM Tris base, 137 mM NaCl, 0.1% (v/v) Tween–20, with 5% (w/v) non–fat dry milk for 1 hour in order to block all non–specific binding sites. Membranes were then incubated overnight in 5% milk–TBST containing monoclonal primary antibodies against both PDP isoforms (PDP1 and 2; Kamiya Biomedical, Seattle, Washington, U.S.A.), monoclonal antibody against phospho–Akt (Cell Signaling Technology, Danvers, Massachusetts, U.S.A.), monoclonal primary antibody against PKCδ (Cell Signaling Technology, Danvers, Massachusetts, U.S.A.), or monoclonal primary antibody against CoxIV (Invitrogen Corporation, Grand Island, New York, U.S.A.). Membranes were washed 3 times with TBST, and incubated for 1 hour in 5% milk–TBST containing peroxidase–conjugated goat anti–mouse IgG or goat anti–rabbit secondary antibody (Sigma–Aldrich, Oakville, Ontario, Canada). Membranes underwent a second round of washing with TBST, and immunoprecipitated antibody–antigen complexes were visualized using a Fluorchem 5500 imaging station (Alpha Innotech, San Leandro, California, U.S.A.) after the addition of Luminata Forte chemiluminescent detection substrate (Millipore, Billerica, Massachusetts, U.S.A.). Blots were washed and total protein was stained with Ponceau S (Sigma–Aldrich, Oakville, Ontario, Canada), which was used to normalize sample loading between lanes on each blot.

Table 1. *Protein specific ratios between primary antibodies and 5% blocking solution for Western blot development*.

Protein of Interest	Molecular Weight (kDa)	Primary Antibody	Commercial Dilution	Working Solution
Pyruvate Dehydrogenase Phosphatase Isoform 1	53	Anti–Pyruvate Dehydrogenase Phosphatase 1 mAb (mouse IgG)	1:3000	3 µL 1°Ab in 9 mL blocking solution
Pyruvate Dehydrogenase Phosphatase Isoform 2	53	Anti–Pyruvate Dehydrogenase Phosphatase 2 mAb (mouse IgG)	1:3000	3 µL 1°Ab in 9 mL blocking solution
Phospho–Akt	60	Anti–Phospho–Akt mAb (rabbit IgG)	1:1000	7 µL 1°Ab in 7 mL blocking solution
Protein Kinase C–Delta	78	Anti–Protein Kinase C–Delta mAb (rabbit IgG)	1:1000	7 µL 1°Ab in 7 mL blocking solution
Cytochrome *c* Oxidase Subunit 4	18	Anti–Cytochrome *c* Oxidase Subunit 4 mAb (mouse IgG)	1:1000	7 µL 1°Ab in 7 mL blocking solution
Serine phosphorylated proteins	0–250	Anti–Phosphoserine pAb (rabbit IgG)	1:500	14 µL 1°Ab in 7 mL blocking solution

Table 2. *Antibody specific ratios between secondary antibodies & 5% blocking solution for Western blot development*.

Primary Antibody	Secondary Antibody	Commercial Dilution	Working Solution
Anti–Pyruvate Dehydrogenase Phosphatase 1 mAb	Horseradish Peroxidase Conjugated Goat Anti–Mouse	1:5000	2 µL 2°Ab in 10 mL blocking solution
Anti–Pyruvate Dehydrogenase Phosphatase 2 mAb	Horseradish Peroxidase Conjugated Goat Anti–Mouse	1:5000	2 µL 2°Ab in 10 mL blocking solution
Anti–Phospho–Akt mAb (rabbit IgG)	Horseradish Peroxidase Conjugated Bovine Anti–Rabbit	1:5000	2 µL 2°Ab in 10 mL blocking solution
Anti–Protein Kinase C–Delta pAb (rabbit IgG)	Horseradish Peroxidase Conjugated Bovine Anti–Rabbit	1:5000	2 µL 2°Ab in 10 mL blocking solution
Anti–Cytochrome *c* Oxidase Subunit 4 (IgG)	Horseradish Peroxidase Conjugated Goat Anti–Mouse	1:5000	2 µL 2°Ab in 10 mL blocking solution
Anti–Phosphoserine pAb	Horseradish Peroxidase Conjugated Bovine Anti–Rabbit	1:5000	2 µL 2°Ab in 10 mL blocking solution

Pyruvate Dehydrogenase Assay

Pyruvate dehydrogenase activity (active form; PDH*a*) was measured as previously described (LeBlanc et al., 2008; Putman et al., 1993), based upon the original methods of Constantin–Teodosiu, Cederblad, and Hultman (1991b). Working under liquid nitrogen, a piece of EDL tissue (10–20 mg) was chipped from the frozen whole muscle sample. The muscle fragment was added to a cooled homogenizing potter containing 200 μL of homogenizing buffer (pH 7.8; 200 mM sucrose, 50 mM KCl, 5 mM $MgCl_2$, 5 mM EGTA, 50 mM Tris HCl, 50 mM NaF, 5 mM DCA, and 0.1% (v/v) Triton X–100). Tissue was briefly homogenized by hand on ice to introduce PDK (DCA) and PDP (NaF) inhibitors immediately. Additional buffer was added in order to produce a 30–fold dilution, and samples underwent motor–driven homogenization at 400 rpm on ice until completion.

For each sample, the PDH*a* assay was run in triplicate; duplicate reactions were initiated with pyruvate and one assay blank was run with ddH_2O. In order to determine the PDH*a* reaction rate, each sample was measured at 1, 2, and 3–minute intervals. Therefore, nine sub–samples result from each sample homogenate. In preparation for each sample's assay, nine labeled culture tubes were loaded with 720 μL of PDH*a* reagent mix. The mixed solution was comprised of 75% (v/v) PDH*a* assay buffer (pH 7.8) containing 144.4 mM Tris, 0.72 mM EDTA, and 1.44 mM $MgCl_2$; 8.33% (v/v) 39 mM NAD^+; 8.33% (v/v) 13 mM CoA; and 8.33% (v/v) 13 mM TPP. Using a positive displacement pipette, 30 μL of homogenate was added to each tube. Culture tubes were then placed in a block heater and warmed to 37° C in preparation for optimal reaction conditions.

Assay reactions were initiated by adding 30 µL of 26 mM pyruvate (ddH_2O for blanks). Culture tubes were gently vortexed and immediately returned to the block heater. At this point in time, a stopwatch was started in order to monitor the tracking of reactions. At precisely 1, 2, and 3–minute intervals, 200 µL of active sample was transferred to labeled eppendorfs, which were pre–loaded with 40 µL of 0.5 M PCA in order to halt reactions. After acidifying at room temperature for 5 minutes, samples were neutralized with 10 µL of 1 M $KHCO_3$. Neutralized samples were centrifuged at 10,000 x *g* for 3 minutes at room temperature, and the resulting supernatant was reserved for the determination of acetyl–CoA content.

Acetyl–CoA Assay

In order to determine acetyl–CoA concentrations for each sample, three reactions involving radiolabeled ^{14}C–aspartate were conducted in order to tag endogenous acetyl–CoA concentrations produced via PDH (Cederblad, Carlin, Constantin–Teodosiu, Harper, & Hultman, 1990). In a culture tube, radiolabeled ^{14}C–oxaloacetate was first produced from a radiolabeled ^{14}C–aspartic acid substrate via aspartate transaminase (AST). Via the AST enzyme, radiolabeled ^{14}C–aspartate (amino acid) was deaminated in order to produce ^{14}C–radiolabeled oxaloacetate (ketoacid). The liberated amine group was then transaminated to alpha–ketoglutarate (ketoacid) and glutamate (amino acid) was produced.

^{14}C–aspartate + alpha–ketoglutarate →→ AST →→ ^{14}C–oxaloacetate + glutamate

In separate culture tubes, radiolabeled ^{14}C–oxaloacetate and exogenous citrate synthase (CS) were then introduced to all neutralized PDH*a* samples. Via the CS enzyme, acetyl functional groups (2–carbon) from endogenous acetyl–CoA and ^{14}C–radiolabeled

oxaloacetate (4–carbon) were condensed in order to produce radiolabeled ^{14}C–citrate (6–carbon).

$$^{14}C\text{–}oxaloacetate + acetyl\text{–}CoA + H_2O \rightarrow\rightarrow CS \rightarrow\rightarrow {}^{14}C\text{–}citrate + CoASH$$

This reaction was performed with a great enough concentration of radiolabeled ^{14}C–oxaloacetate in order to ensure that acetyl–CoA was the limiting reactant.

At this point in the assay, all endogenous acetyl–CoA was represented as radiolabeled ^{14}C–citrate. However, samples contained radiolabeled ^{14}C–citrate as well as leftover unreacted radiolabeled ^{14}C–oxaloacetate. This presented a problem, as both compounds are negatively charged anions, and acetyl–CoA content is eventually determined by the quantification of radiolabeled ^{14}C–anions. Therefore, all remaining radiolabeled ^{14}C–oxaloacetate was reaminated via AST in order to reproduce radiolabeled ^{14}C–aspartate, which is a positively charged cation.

$$^{14}C\text{–}oxaloacetate + glutamate \rightarrow\rightarrow AST \rightarrow\rightarrow {}^{14}C\text{–}aspartate + alpha\text{–}ketoglutarate$$

This reaction was performed with a sufficiently high concentration of glutamate in order to ensure that any remaining radiolabeled ^{14}C–oxaloacetate was the limiting reactant.

Using an ion exchange resin, positively charged compounds were separated from all samples. Resin–containing pellets were discarded, which left only radiolabeled ^{14}C–citrate in the supernatant solution. Following this purification, radiolabeled ^{14}C–citrate (reflective of endogenous acetyl–CoA concentrations) was the only radiolabel remaining in each sample. All samples underwent scintillation counting in order to determine their respective radioactivity. Acetyl–CoA concentrations were determined based upon an acetyl–CoA standard curve. PDH*a* activities were then calculated based upon through linear regression based upon each sample's radioactivity.

Citrate Synthase Assay

Citrate synthase activity was determined using samples collected via the mitochondrial isolation procedure in order to calculate mitochondrial recovery. The previously frozen piece of EDL tissue was homogenized on ice in 100 volumes of homogenizing buffer containing 100 mM KH_2PO_4 (pH 7.3) and 0.05% (w/v) BSA. Total mitochondrial suspension samples were retrieved from –80° C, as these samples were prepared in advance. All samples were frozen and thawed three times using liquid nitrogen in order to lyse mitochondrial membranes and release mitochondrial contents into solution. All CS assay reactions (whole homogenates and total mitochondrial suspensions) were performed in 250 µL blackened–sidewall microcuvettes.

Microcuvettes contained the following reagents: 150 µL of 100 mM Tris buffer (pH 8.3); 25 µL of 1 mM dithiobis–2–nitrobenzoic acid (DTNB) (pH 8.3); 40 µL of 3 mM acetyl–CoA; 10 µL of 10% Triton–X; and 10 µL of sample (CS_{WH} or CS_{TS}). Once the microcuvette had been prepared, 15 µL of 10 mM oxaloacetic acid was added in order to initiate the citrate synthase reaction:

$$\textit{Acetyl–CoA + Oxaloacetic acid} \rightarrow\rightarrow \textit{CS} \rightarrow\rightarrow \textit{Citrate + CoASH}$$

Upon the completion of the reaction, all liberated CoASH condensed with DTNB in order to produce DTNB–CoA. This secondary reaction caused a colour shift in the cuvette, with the original clear and translucent sample turning slightly yellow.

Using a spectrophotometer (Biochrom, Cambridge, England), sample absorbance was measured at 412 nm in 30–second intervals for a total of 5 minutes. Absorbance was tracked once the assay reaction was proceeding at maximal steady state (~30 seconds). Any change observed in sample absorbance at a given interval was dependent upon the

concentration of DTNB–CoA present in solution. Maximal citrate synthase activity was calculated on the basis of the molar absorption coefficient of DTNB at a wavelength of 412 nm, and the dilution factor of the sample undergoing analysis (whole homogenate or total suspension). Please refer to Appendix 2 for a detailed summary of the citrate synthase calculations. Once CS activities were determined for all whole homogenates and total mitochondrial suspensions, mitochondrial recovery was calculated based upon the following calculation (Love et al., 2011, Srere, 1969):

$$\% \text{ Mitochondrial recovery} = (CS_{TS} \div CS_{WH}) \bullet 100$$

Pyruvate Dehydrogenase Phosphatase Assay

The PDP assay was performed on mitochondrial extracts. PDP activity was determined using a serine/threonine phosphatase assay system kit (Promega, Madison, Wisconsin, U. S. A.) and a custom synthetic PDH E1α phosphopeptide substrate (New England Peptide, Gardner, Massachusetts, U. S. A.). The assay was performed as previously described (LeBlanc et al., 2008; Love et al., 2011) with one adjustment that will be described later.

In preparation for the assay, mitochondrial suspensions were diluted to a final protein concentration of 2 μg/μL with sucrose and mannitol and a total volume of 50 μL. Samples were frozen and thawed three times using liquid nitrogen in order to lyse mitochondrial membranes in preparation for centrifugation. Samples were centrifuged at 21,400 x *g* for 1 hour at 4° C in order to remove large cellular debris. Supernatants containing PDP protein of interest were retained, while pellets were discarded.

During the course of the 1–hour spin, a phosphate standard curve (0, 0.1, 0.2, 0.5, 1, 2 nM inorganic phosphate) and phosphate–reducing spin columns were prepared. Ten

mL of ddH_2O was passed through each spin column via gravity in order to moisten column filters. Spin columns were then loaded with 10 mL of Sephadex–G25 resin. Once the resin flowthrough drained by gravity, Sephadex beads were equilibrated with 10 mL of column storage buffer containing 10 mM Tris (pH 7.5), 1 mM EDTA, and 0.02% (w/v) sodium azide. Spin columns were centrifuged at 600 x *g* for 5 minutes at 4° C ensuring that all column storage buffer was collected. Mitochondrial supernatants were passed through spin columns via centrifugation at 600 x *g* for 5 minutes at 4° C in order to remove endogenous phosphate within in each sample.

Purified mitochondrial samples (5 µL) were added to a 96–well plate in addition to 11 µL of reaction buffer containing 250 mM imidazole (pH 7.2); 1 mM EGTA; 25 mM $MgCl_2$; 0.1% (v/v) 2–mercaptoethanol; and 0.05% (w/v) BSA, as well as 21 µL of phosphate free water. The well plate was then incubated for 10 minutes at 37° C in order to equilibrate the samples for optimal reaction conditions. Previous studies conducted in our laboratory (LeBlanc et al., 2007; LeBlanc et al., 2008; Love et al., 2011) have implemented a general phosphatase inhibitor at this stage in the assay in order to isolate the function of the metal–dependent serine/threonine protein phosphatase (PPM) family, of which PDP is a member (Barford, 1996; Wera & Hemmings, 1995). However, unlike the preceding studies from our laboratory, an alternative phosphatase inhibitor cocktail (Roche Applied Science, Laval, Québec, Canada) was included in all solutions of the mitochondrial isolation procedure. The reasoning for this substitution is that the previous inhibitor was no longer commercially available for purchase. This alternative cocktail inhibitor targets the non–metal–dependent serine/threonine (PPP) phosphatase family, which is the only other classification of serine/threonine protein phosphatase.

Consequently, the traditional phosphatase inhibitor added during the assay itself was omitted.

The PDP reactions were initiated through the addition of 13 µL of 1.5 mM phosphopeptide substrate. The reaction proceeded for 30 minutes at 37° C, enabling endogenous PDP to dephosphorylate the synthetic PDH E1α phosphopeptide. Reactions were halted through the addition of 50 µL of molybdate dye to each well containing samples or phosphate standards. A 30–minute incubation at room temperature followed to allow for molybdate dye colour development. Standard curve and sample absorbance was measured at 600 nm in a microplate reader.

Tyrosine–Histidine–Glycine–Histidine–**(p)Serine**–Methionine–Serine–Aspartic Acid–Proline–Glycine–Valine–**(p)Serine**–Tyrosine–Arginine

Figure 3. Synthetic PDH E1α phosphopeptide amino acid sequence.

Statistical Analysis

Data are reported as mean ± standard error of the mean (n = 8, n = 10 or n = 11 per group as indicated). To enhance statistical power, one EDL muscle was used for the basal condition, and the second EDL muscle from the same animal was used for the insulin–stimulated condition. Match–paired samples were analyzed for significance using paired samples T–tests. Statistical significance was accepted at $p < 0.05$.

CHAPTER 4:

RESULTS

General Observations

Subject characteristics (n = 40) reveal two divergent subgroups with respect to animal weights (Table 1). In one grouping, similarly lighter weights were reported for those procedures that did not involve mitochondrial isolations (pAkt, PDH*a*, and immunoprecipitation analyses). In the second grouping, heavier weights were reported for the one procedure that required mitochondrial isolation (PKCδ). These similarities are expected, as all EDL tissue samples were collected from male Long Evans rats, aged 28 days. Tissue sampling for the mitochondrial analyses required more time to perform, enabling some subjects within these lots of animals to grow heavier.

Table 3. Rat weights presented by methodological procedure.

Methodological Procedure	Mean Weight (g)
phospho–Akt Western blotting (n = 8)	102 ± 6^{A}
PDH*a* Activity Assay (n = 11)	98 ± 6^{A}
PDP1 & PDP2 Immunoprecipitation (n = 8)	$106 \pm 4^{A,B}$
Mitochondrial PKCδ Western blotting (n = 8)	127 ± 8^{B}

B, significantly different from A.

Phospho–Akt Protein

Western blotting was performed against pAkt, a major target of the insulin–signaling cascade for glucose uptake, in order to verify a tissue response to insulin stimulation. Insulin stimulation of EDL tissue (Fig. 4, A and B) led to a 10–fold increase in pAkt protein content ($p = 0.0002$).

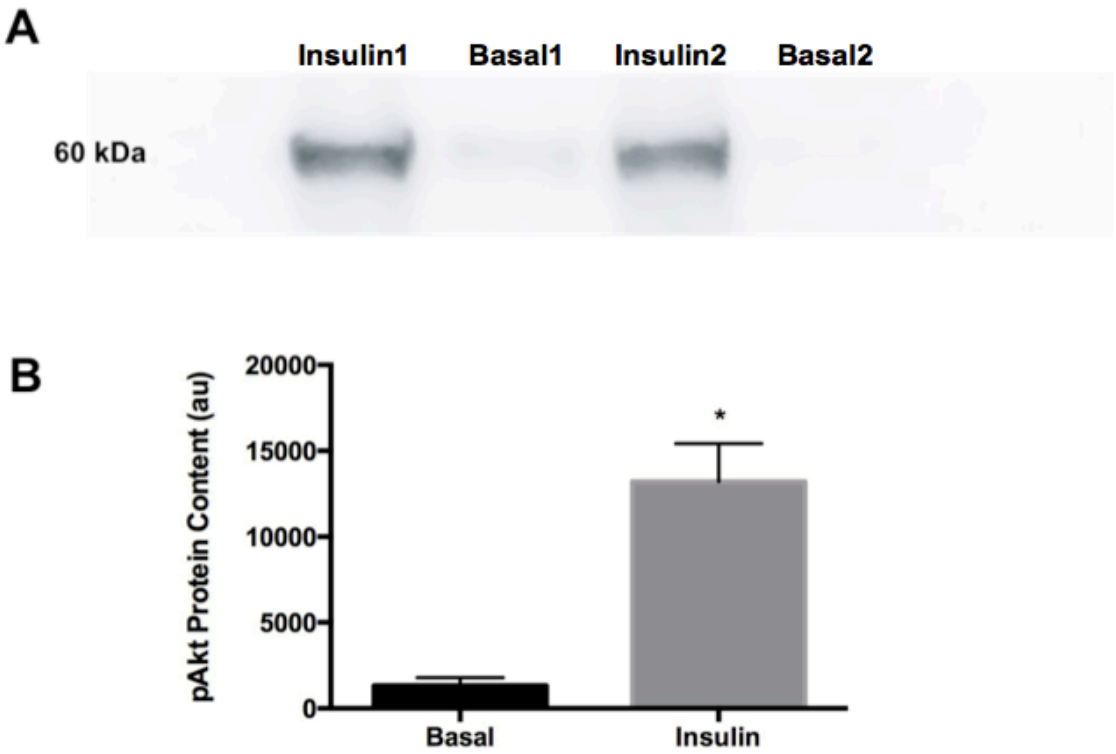

Fig. 4. **A**: representative Western blot of phosphorylated Akt (pAkt, 60 kDa) protein in extensor digitorum longus skeletal muscle tissue incubated in basal and insulin–stimulated (10 mU/mL) media. The four lanes depict two matched–paired subjects. 30 µg of total skeletal muscle whole homogenate was loaded per lane. **B**: paired t–test comparison of pAkt protein content (arbitrary units) obtained from 8 matched–paired subjects. Values are expressed as means ± SEM. *Significant from basal counterpart, $p < 0.05$.

PDHa Activity

Insulin stimulation led to a 58% increase in PDH*a* activity expressed per kilogram of wet weight tissue compared to basal counterparts (Fig. 5), but failed to reach statistical significance ($p = 0.057$).

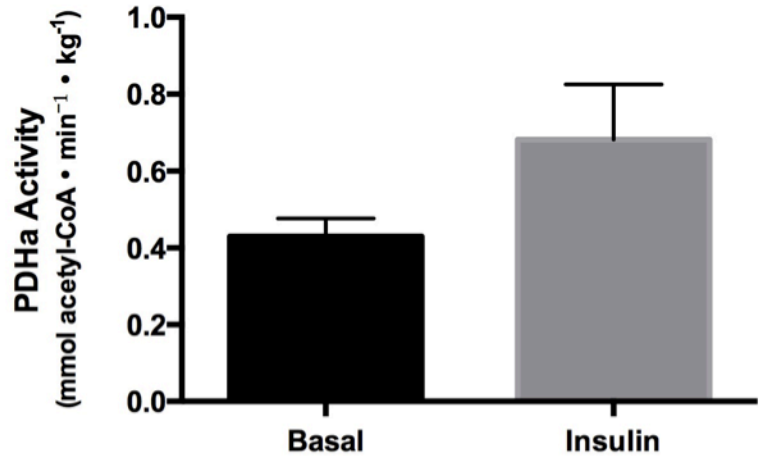

Fig. 5. Paired t–test comparison of PDH*a* activity per kilogram of wet weight tissue in extensor digitorum longus (EDL) skeletal muscle tissue incubated in basal and insulin–stimulated (10 mU/mL) media. Values are expressed as means ± SEM.

Immunoprecipitated Phospho–Serine PDP Protein

Insulin stimulation led to significantly increased immunoprecipitated serine–phosphorylated protein for both PDP isoforms. PDP1 phosphorylation (Fig. 6, A and B) increased by 29% ($p = 0.047$), and PDP2 phosphorylation (Fig. 7, A and B) increased by 48% ($p = 0.006$). Immunoprecipitation was also performed to test for the phosphorylation of threonine residues, which was not found amongst PDP isoforms (data not shown).

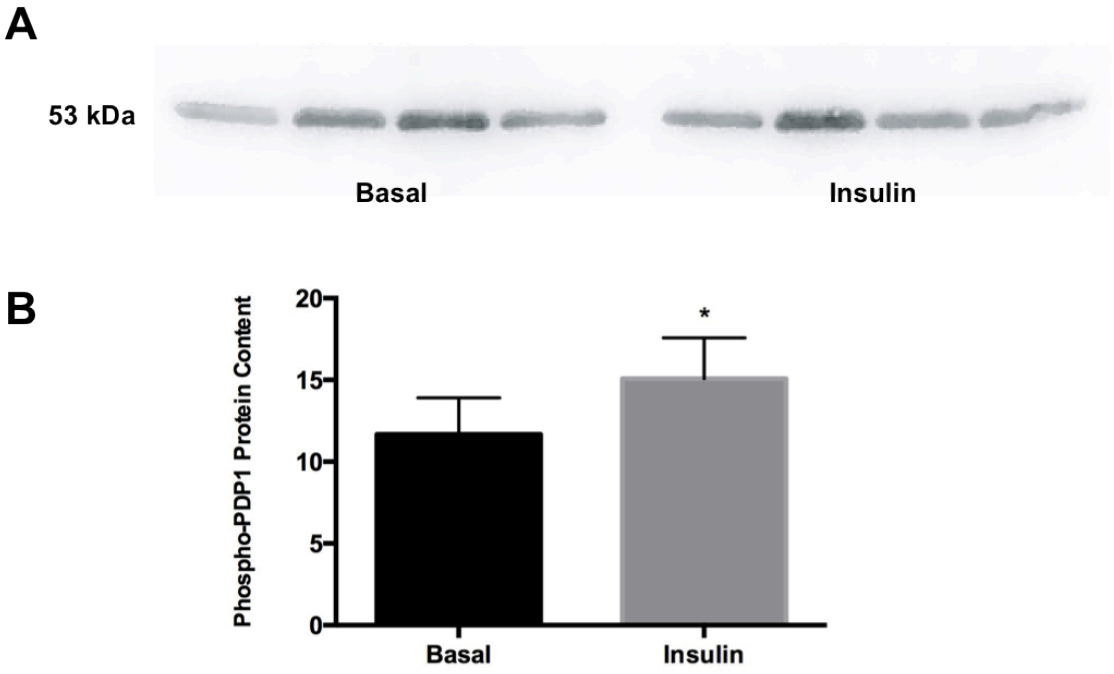

Fig. 6. **A**: representative Western blot of immunoprecipitated serine–phosphorylated pyruvate dehydrogenase phosphatase 1 (pPDP1, 53 kDa) protein in extensor digitorum longus skeletal muscle tissue incubated in basal and insulin–stimulated (10 mU/mL) media. The eight lanes depict four matched–paired subjects. 10 µL of whole homogenate phosphoserine extract was loaded per lane. pPDP1 protein (arbitrary units) was normalized to total protein per lane via Ponceau S stain (arbitrary units). **B**: paired t–test comparison of phospho–PDP1 protein content obtained from eight matched–paired subjects. Values are expressed as means ± SEM. *Significant from basal counterpart, $p < 0.05$.

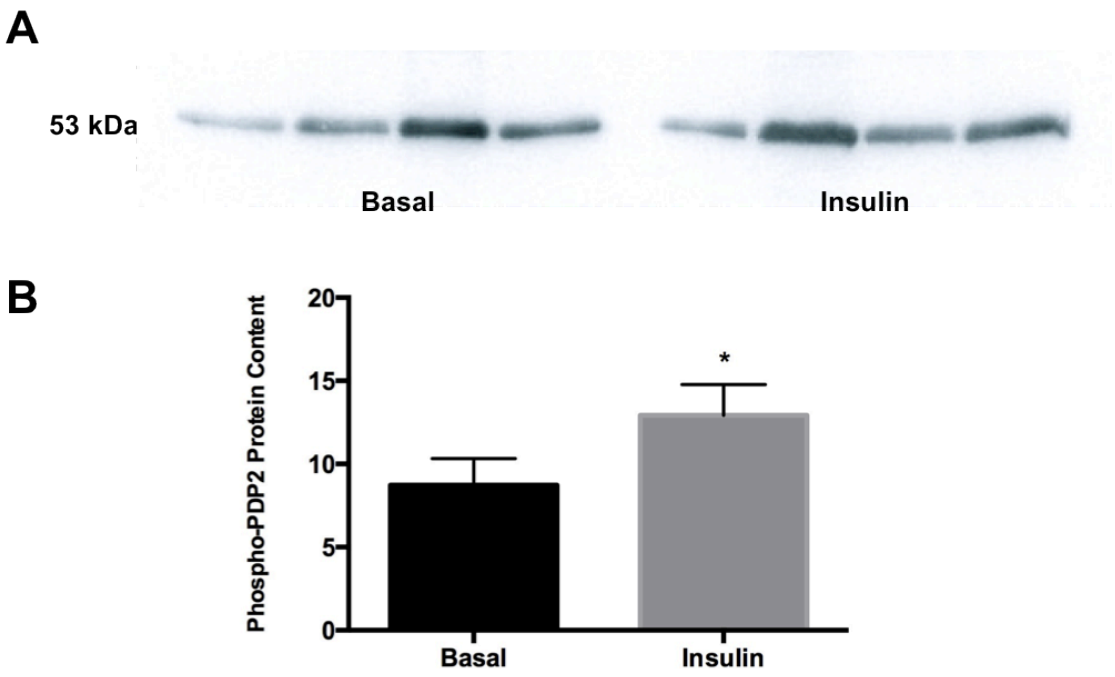

Fig. 7. **A**: representative Western blot of immunoprecipitated serine–phosphorylated pyruvate dehydrogenase phosphatase 2 (pPDP2 kDa) protein in extensor digitorum longus skeletal muscle tissue incubated in basal and insulin–stimulated (10 mU/mL) media. The eight lanes depict four matched–paired subjects. pPDP2 protein (arbitrary units) was normalized to total protein per lane via Ponceau S stain (arbitrary units). **B**: paired t–test comparison of phospho–PDP2 protein content obtained from eight matched–paired subjects. Values are expressed as means ± SEM. *Significant from basal counterpart, $p < 0.05$.

Mitochondrial PKCδ Protein

Mitochondrial subfractions were isolated in order to investigate potential enrichment of PKCδ in response to insulin stimulation. Mitochondrial PKCδ protein content (Fig. 8, A and B) increased by 45% ($p = 0.0009$).

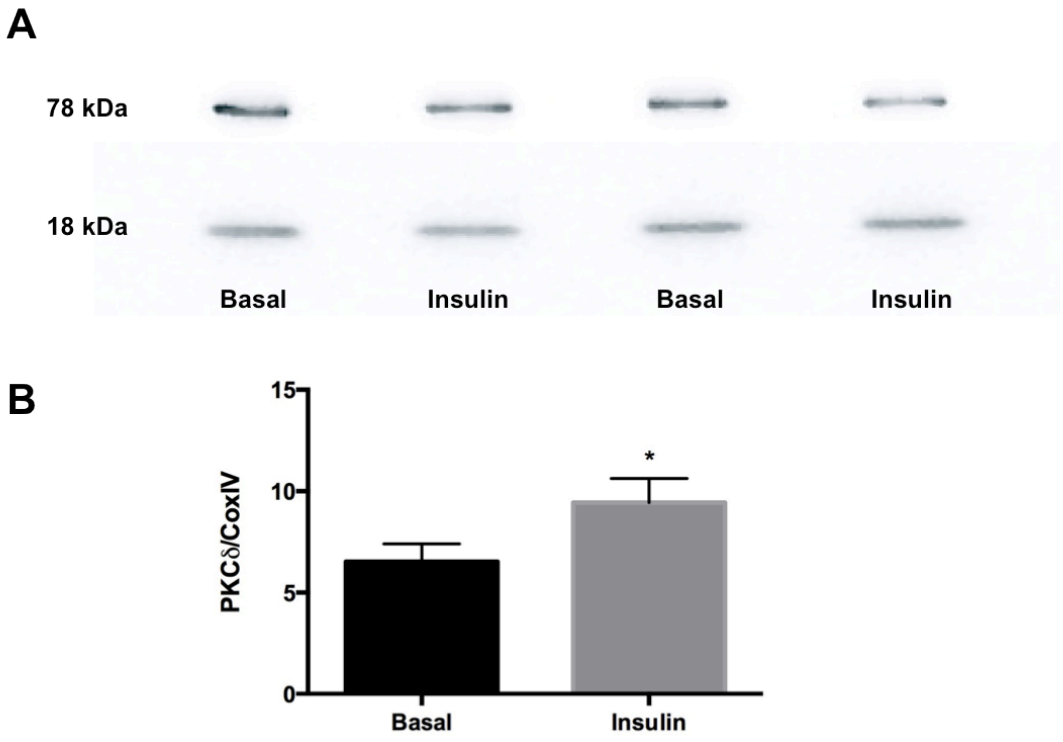

Fig. 8. **A**: representative Western blots of protein kinase C–delta (PKCδ, 78 kDa) and cytochrome *c* oxidase subunit 4 (CoxIV, 18 kDa) protein in mitochondrial subfractions from extensor digitorum longus skeletal muscle tissue incubated in basal and insulin–stimulated (10 mU/mL) media. The four lanes depict two matched–paired subjects. 3 μg of total mitochondrial protein was loaded per lane in both instances. PKCδ protein content (arbitrary units) was normalized to CoxIV protein content (arbitrary units). **B**: paired t–test comparison of mitochondrial PKCδ protein content obtained from eight matched–paired subjects. Values are expressed as means ± SEM. *Significant from basal counterpart, $p < 0.05$.

PDP and CS Activity

Pyruvate dehydrogenase phosphatase activity assay data is not shown. The PDP assay was unable to be completed based upon the preparation of mitochondria collected for the procedure. All four solutions used in the mitochondrial isolation procedure contained a general phosphatase inhibitor cocktail (Roche Applied Science, Laval, Québec, Canada), which appeared to have blocked PDP activity altogether. Additional pilot–testing of mitochondria that were extracted without inhibitors exhibited PDP activity, but those mitochondria extracted for PDP and CS analyses did not have activity. Inhibitors were included in the buffers in attempt to lock the phosphorylation state of each sample following whole tissue incubations, and to prevent cytosolic kinases and phosphatases from adding or removing phosphates during tissue homogenization procedures. Product information for the inhibitors clearly stated that the PPP family of protein phosphatases was targeted for inhibition, and not the PPM family of protein phosphatases (of which PDP is a member). However, specific phosphatase catalytic and regulatory domains respond to different forms of inhibition (Barford, 1996; Wera & Hemmings, 1995). Therefore, mitochondria were prepared under the assumption that the PDP enzymes would be unaffected. At the time of this decision, a great deal of importance was placed upon locking the phosphorylation state of the PDH enzyme complex as well as isolating the function of the PPM phosphatase.

Pilot testing using uninhibited mitochondrial samples yielded successful results in the PDP assay. However, not enough uninhibited samples remained in order to analyze a full data set of basal and insulin–stimulated samples. PDP assay data will be recollected at a later date using uninhibited samples to complete this study.

Citrate synthase activity data, which would have been used to calculate mitochondrial recovery and muscle PDP activity, are reported in Appendix 3.

CHAPTER 5:

DISCUSSION

General Summary

This study is the first that we know of to examine the phosphorylation state of both PDP1 and PDP2 in response to insulin stimulation using intact skeletal muscle tissue. Furthermore, to the best of our knowledge, this is the first study to examine PDH complex activity by way of acetyl–CoA accumulation in response to insulin stimulation. The major findings of the present study are: 1) PDH*a* activity increased by 58% in response to insulin stimulation compared to basal counterparts ($p = 0.057$); 2) insulin stimulation led to increased phosphorylation of both PDP isoforms, with PDP1 and PDP2 increasing by 29% ($p = 0.047$) and 48% ($p = 0.006$), respectively; and 3) mitochondrial protein content of PKCδ was enriched by 45% in response to insulin stimulation ($p = 0.0009$).

PDHa Activity

The present study demonstrated increased PDH complex in the active form in response to insulin stimulation (hypothesis 2). Although failing to reach statistical significance, the increased PDH*a* activity was trending strongly ($p = 0.057$). This finding supports previous research that implicates the PDH complex as a target of secondary messaging as part of the insulin–signaling cascade (Benelli et al., 1994; Caruso et al., 2001; Huang, Wu, Bowker–Kinley, & Harris, 2002; Popp et al., 1980). To the best of the authors' knowledge, this practice for PDH*a* activity measurement at the whole tissue level and in response to insulin stimulation has not been utilized in any previous literature.

One study has established increased PDH*a* activity in response to insulin stimulation, although within vastly different physiological contexts (Caruso et al., 2001).

The work of Caruso et al. (2001) implemented cell culture models, and reported a 2–fold increase in PDH*a* activity (measured via radioactive CO_2 production from labeled pyruvate) in L6 myoblasts. This effect was observed at an insulin concentration of 100 nM. The present study has extended these findings to more complex and less controllable physiological systems, coupled with a supra–physiological insulin stimulation of 10 mU/mL, which corresponds to 71.74 nM (Heinemann, 2010). To contrast these stimulation criteria, plasma insulin concentrations peaked at ~75 μU/mL (~538 pM) in response to a high–carbohydrate meal following a 6 day high–fat diet in healthy subjects (Bigrigg, Heigenhauser, Inglis, LeBlanc, & Peters, 2009). At this point, it can only be speculated that such a potent stimulation was required to elicit this effect in PDH*a* activity, as the only studies to demonstrate these findings have done so outside physiologically relevant ranges. Separate from the work of Caruso et al. (2001), the insulin concentration used in the current study was selected in order to elicit maximal insulin–stimulated glucose transport into the cell, which was based upon research from one lab that performs similar whole tissue incubation experiments (Stefanyk et al., 2011). Further investigation may be required to narrow the physiological range of concentrations that elicit this response.

With respect to the PDH*a* method conducted within our laboratory, no documented precedent could be referenced to contrast the insulin–stimulated PDH*a* activities observed in this study. Two recent studies from our laboratory (LeBlanc et al., 2007; LeBlanc et al., 2008) using an identical procedure reported similar resting PDH*a* activities as those seen in the current study. Basal EDL muscles had resting PDH*a* values ranging from 0.202–0.732 mmol • min^{-1} • kg wet weight tissue (mean of 0.43; $n = 11$).

Other rat hindlimb tissues have demonstrated a similar range: 0.18–0.36 in soleus, 0.64–0.85 in red gastrocnemius, and 0.31–0.41 nmol • min^{-1} • g wet weight tissue in white gastrocnemius (LeBlanc et al., 2007; LeBlanc et al., 2008). Although fiber typing and carbohydrate oxidative potential undoubtedly varies across these muscles, a case can be made for general consistency in PDH*a* activity between resting rat skeletal muscle tissue. Consequently, the current resting PDH*a* values observed in EDL tissue can be accepted with the confidence that methodological procedures were performed successfully. Within this context, it would be expected that insulin stimulation would lead to increased activity levels, and therefore, the observation of a 58% increase in insulin–stimulated PDH*a* activity can be accepted as theoretically sound.

Pertaining to the insulin–stimulated PDH*a* values presented in this study, two physiological mechanisms are to be considered as potential explanations. First, insulin is a hormone that is impermeable to the cell membrane and dependent upon secondary messaging to elicit its effects (Pirola, Johnston, & van Obberghen, 2004). This recognition of hormone classification is of particular importance, as it provides support for any speculation of covalent modification upon PDH regulators. Second, increases in PDH*a* activity may simply be a consequence of increased glucose uptake and substrate provision in response to insulin stimulation. Increased glucose uptake could increase glycolytic flux and cytosolic pyruvate concentrations, which would inhibit PDK and contribute to increased PDH*a* activity. The incubating media used in all experiments (Medium199; Sigma–Aldrich, Ontario, Canada) contained a glucose concentration of 5.5 mmol/L, which is within the normal range of fasting blood glucose levels. Increased

glucose uptake and catabolism could very well lead to an influx of metabolic intermediates that accelerate the basic PDH reaction (Peters, 2003).

Immunoprecipitation and PDP Phosphorylation

Both PDP1 and PDP2 isoforms underwent increased phosphorylation in response to insulin stimulation (hypothesis 1). As with PDH*a* results from the current study, these findings are consistent with previous research in cell culture models (Caruso et al., 2001). Phosphorylation of the PDP1 isoform increased by 29% ($p = 0.047$) and PDP2 phosphorylation increased by 48% ($p = 0.006$). Although these results have reached statistical significance, it is interesting to note that increased phosphorylation occurred to differing extents between both isoforms.

Prior to the commencement of this study, it was hypothesized that phosphorylation of PDP isoforms would increase in response to insulin stimulation. However, this hypothesis did not extend to any differences between isoforms with respect to any magnitude in response. Tissue distributions of PDP isoforms have revealed that PDP1 is highly expressed in rat skeletal muscle tissue, whereas PDP2 is overly expressed in rat liver (Huang et al., 1998). PDP1 is virtually undetectable in liver tissue and the same can be said for PDP2 in skeletal muscle; however, the specific muscle from which this analysis occurred was unspecified. From this perspective, one could argue that analysis of the PDP1 isoform will provide the greatest opportunity to observe a treatment's effect in studies implementing skeletal muscle models. Consequently, the increase in PDP1 phosphorylation observed in the current study may be interpreted as somewhat surprising.

PDP1 activity is largely dependent upon the presence of calcium ions (Huang et al., 1998), and PDP1 protein content is known to increase in response to aerobic training (LeBlanc et al., 2008). However, decreases in PDP2 protein content and activity induced by starvation and diabetes have exhibited recovery in response to treatment with insulin (Huang, Wu, Popov, & Harris, 2003). Therefore, from a regulatory perspective, one could argue that the analysis of the PDP2 isoform will provide the greatest opportunity to observe the effects of insulin stimulation, irrespective of tissue expression. Furthermore, in contrast to the findings from Huang et al. (1998), detection of PDP2 protein in rat EDL skeletal muscle tissue through Western blotting was not problematic. With all such factors taken into consideration, the stronger response observed in PDP2 phosphorylation is quite encouraging and consistent with previous literature from a theoretical perspective.

One limitation of our method to detect PDP phosphorylation is that sample loading between conditions during Western blotting was not based upon quantified protein determination after immunoprecipitation. Consequently, we cannot guarantee that basal and insulin–stimulated match–paired samples were studied under equal representation. Once the immunoprecipitation procedure had taken place, which requires the addition of protein IgG (anti–phosphoserine antibody and agarose beads) to skeletal muscle whole homogenates, we were unable to quantify sample protein content strictly representative of phosphorylated protein content. However, multiple steps were taken to control for this issue. First, protein determinations were quantified for each sample whole homogenate (μg/μL) prior to immunoprecipitation procedures. Second, using this data, sufficient primary antibody (40 μL) was applied in order to clear all serine–phosphorylated proteins within a given quantity of prepared sample homogenate (500 μg).

This calculation is supported by product information from the antibody provider (AB1603, Anti–Phosphoserine Antibody; Billerica, MA, USA) and directed specifically towards the practice of immunoprecipitation techniques. Third, immunoprecipitation optimization procedures were pilot tested, which implemented an increasing gradient of anti–phospho–serine primary antibody (10, 20, 30 and 40 μL) as a method to ensure that all phosphorylated PDP protein was collected. Results from this pilot analysis revealed no change in phospho–PDP1 protein content following immunoprecipitation using 30 and 40 μL of anti–phospho–serine primary antibody. As a result, these measures of control have provided assurance that all serine–phosphorylated proteins were harvested in both basal and insulin–stimulated samples in preparation for Western blotting of phospho–PDP1 and phospho–PDP2.

Prior to electrophoresis, the samples were boiled in order to dissociate all protein–antibody–agarose bead interactions. From this purified suspension, 10 μL from match–paired samples were loaded for comparative Western blotting of phosphorylated PDP isoforms. As previously reported, all supernatants from immunoprecipitation experiments were discarded prior to Western blotting. In hindsight, this is now considered an oversight and limitation to the immunoprecipitation procedure. Western blotting immunoprecipitated supernatants against anti–phospho–serine primary antibody with negative results would have been demonstrated the clearance of all phosphorylated proteins.

A second limitation of our ability to detect PDP phosphorylation pertains to the ordering of antibodies applied towards immunoprecipitation and Western blotting. For all experiments involved in this study, immunoprecipitation was performed with a non–

specific anti–phospho–serine primary antibody. Following immunoprecipitation, Western blotting was performed against PDP1 and PDP2 in order to quantify phosphorylation between basal and insulin–stimulated conditions. PDP is known to interact with other proteins that are serine–phosphorylated, and other protein interactions may potentially exist that have yet to be established. The possibility exists that the phosphorylation data presented in this study may not reflect changes in PDP phosphorylation in direct response to insulin stimulation compared to basal stimulation. In order to overcome this limitation, immunoprecipitation must be performed using anti–PDP1 and anti–PDP2 antibodies, following by Western blotting against serine–phosphorylated PDP within the immunoprecipitated pellet.

Results of the present PDP1 and PDP2 phosphorylation analyses suggest that the covalent modification of PDH regulating proteins underlies changes in PDH*a* activity in response to insulin stimulation. While this finding does not rule out the fact that increased glucose uptake in response to insulin stimulation occurred, these results support previous literature that PDPs are under their own system of regulatory control (Caruso et al., 2001). Furthermore, three recent studies from within this laboratory have all identified discrepancies pertaining to the relationship between PDP activity levels and intramuscular PDP protein content (LeBlanc et al., 2007; LeBlanc et al., 2008; Love et al., 2011). These studies all suggested that an additional level of enzymatic control could account for the inconsistencies within their findings. The immunoprecipitation data from the present study confirmed that PDPs are capable of undergoing covalent modification, and suggest that PDP protein content and functional activity may not always correlate as a result.

Mitochondrial PKCδ Enrichment

Previous research has implicated PKCδ as the kinase responsible for PDP phosphorylation and upregulation (Caruso et al., 2001). Along with our PDP phosphorylation measures in whole tissue, these results suggest that a potential mechanism for PDP phosphorylation occurs in the mitochondria similar to what had previously been observed in cell culture (hypothesis 3). Our methodologies involved primarily subsarcolemmal mitochondrial isolations, which provided an opportunity to verify the mitochondrial enrichment of PKCδ and further substantiate established findings. Through Western blot analysis, it was observed that insulin stimulation led to a 45% increased enrichment of mitochondrial PKCδ ($p = 0.0009$). PKCδ protein content was normalized to mitochondrial CoxIV protein content. CoxIV was selected as a mitochondrial housekeeping protein, as the content of this protein in mitochondria is not believed to change in response to insulin stimulation.

As a mitochondrial matrix–associated enzyme complex, it is not exactly known how PKCδ exerts phosphorylation upon PDP, or how it is able to enter the mitochondria per se. However, evidence does exist that highlights the capability for functional proteins to localize and permeate skeletal muscle mitochondria to facilitate metabolic processes. This has been observed in cytosolic lipid droplet proteins, which have been visualized inside the mitochondrial matrix space using electron microscopy (Bosma et al., 2011). Furthermore, Caruso et al. (2001) observed increased mitochondrial and decreased cytosolic contents of PKCδ in response to insulin stimulation in L6 myoblasts. Therefore, PKCδ may enter the mitochondrial matrix in order to come into physical contact with regulatory subunits of the PDH complex.

Future Directions

Results from the current study can be applied towards further investigation. First, although immunoprecipitation data from this study has suggested that PDP1 and PDP2 are capable of undergoing serine phosphorylation, this methodology should be refined in order to confirm the current findings. In order to clearly demonstrate that PDP isoforms undergo increased phosphorylation in response to insulin stimulation, immunoprecipitation must be performed against PDP1 and PDP2 isoforms in separate experiments. Following immunoprecipitation, Western blotting of harvested PDP pellets against anti–phospho–serine primary antibody may confirm changes in phosphorylation for each PDP isoform respectively. On another note however, limitations of the current phosphorylation data perhaps provide justification for the production of anti–phospho–PDP1 and anti–phospho–PDP2 primary antibodies in order to advance these findings.

Second, it has only been speculated that the covalent modification of PDP isoforms will result in PDP activation, accompanied by increased PDP activity. Methodological issues pertaining to the PDP assay have been established, as previously stated. Additional work is required to overcome these current issues, namely by selecting an ideal phosphatase inhibitor in order to isolate the specific activity of PDH phosphatases. The addition of PDP activity assay data would greatly enhance the existing data of current study, and would allow for more robust conclusions with respect to a potential signaling cascade between insulin stimulation and regulators of the PDH complex.

Third, results from this study can be applied towards further research involving the contractile stimulation of intact skeletal muscle tissue. Physical activity is a major

mechanism leading to increased PDH activity (Howlett et al., 1998), yet the covalent activation of PDP protein has yet to be established in response to this perturbation. Current equipment within the Centre for Bone and Muscle Health can allow for this study to be reproduced using an *in vitro* incubation model with contractile stimulation. Previous research has suggested a potential signaling cascade between AMPK and PDH, irrespective of increased substrate provision to the PDH complex (Smith et al., 2005). However, limitations surrounding immunoprecipitation and PDP activity assay procedures will also have to be addressed in order to investigate this question.

Summary and Perspectives

This study is the first that we know of to examine changes in activity of the PDH complex in response to insulin stimulation using intact skeletal muscle tissue. Furthermore, this study also confirms previous findings conducted in cell culture by Caruso et al. (2001) that 1) with indirect evidence, both PDP1 and PDP2 are subject to covalent regulation at their serine residues, with increased phosphorylation observed in response to insulin stimulation; and 2) PKCδ is enriched in subsarcolemmal mitochondria serving as the potential kinase responsible for the phosphorylation of PDP in response to insulin stimulation. Taken together, this is the first study that we know of to demonstrate these findings at the whole tissue level with greater physiological relevance in comparison to work in cell culture models. Furthermore, these data extend studies previously conducted in our laboratory (LeBlanc et al., 2007; LeBlanc et al., 2008; Love et al., 2011). Each of these studies demonstrated analytical discrepancies between intramuscular PDP protein content and PDP activity. All three studies speculated a novel form of regulation upon PDP isoforms at the whole tissue level, and results of the current

study suggest that covalent modification of PDP may have contributed to previous findings.

It has long been reported that insulin is an activator of the PDH complex, based upon its ability to reverse the effects of PDH activity suppression via increased PDK protein expression in response to diabetic perturbations (Wu et al., 1998; Wu, Inskeep, Bowker–Kinley, Popov, & Harris, 1999). The current study suggests the presence of a signaling cascade between insulin receptor activation and the PDH complex via covalent regulation of PDP. However, without PDP activity data to support the PDP phosphorylation data presented in this study (hypothesis 2), an established sequence of signaling events cannot be confirmed between mitochondrial PKCδ enrichment, covalent activation of PDP, and increased PDH*a* activity.

REFERENCES

1. Antolic, A., Harrison, R., Farlinger, C., Cermak, N. M., Peters, S. J., LeBlanc, P., & Roy, B. D. (2007). Effect of extracellular osmolality on cell volume and resting metabolism in mammalian skeletal muscle. *American Journal of Physiology. Regulatory, Integrative and Comparative Physiology*, *292*, R1994–R2000.
2. Barford, D. (1996). Molecular mechanisms of the protein serine/threonine phosphatases. *Trends in Biochemical Sciences*, *21*, 407–412.
3. Benelli, C., Caron, M., de Gallé, B., Fouque, F., Cherqui, C., & Clot, J. P. (1994). Evidence for a role of protein kinase C in the activation of the pyruvate dehydrogenase complex by insulin in Zajdela hepatoma cells. *Metabolism: Clinical and Experimental*, *43*, 1030–1034.
4. Bigrigg, J. K., Heigenhauser, G. J., Inglis, J. G., LeBlanc, P. J., & Peters. S. J. (2009). Carbohydrate refeeding after a high–fat diet rapidly reverses the adaptive increase in human skeletal muscle PDH kinase activity. *American Journal of Physiology. Regulatory, Integrative and Comparative Physiology*, *297*, R885–R891.
5. Bonen, A., Clark, M. G., & Henriksen, E. J. (1994). Experimental approaches in muscle metabolism: hindlimb perfusion and isolated muscle incubations. *The American Journal of Physiology*, *266*, E1–E16.
6. Bosma, M., Minnaard, R., Sparks, L. M., Schaart, G., Losen, M., de Baets, M. H., … Hesselink, M. K. (2012). The lipid droplet coat protein perilipin 5 also localizes to muscle mitochondria. *Histochemistry and Cell Biology*, *137*, 205–216.

7. Bowker–Kinley, M. M., Davis, W. I., Wu, P., Harris, R. A., & Popov, K. M. (1998). Evidence for existence of tissue–specific regulation of the mammalian pyruvate dehydrogenase complex. *The Biochemical Journal*, *329*, 191–196.
8. Bradford, M. M. (1976). A rapid and sensitive method for the quantification of microgram quantities of protein utilizing the principle of protein–dye binding. *Analytical Biochemistry*, *72*, 248–254.
9. Breitkreutz, D., Braiman–Wiksman, L., Daum, N., Denning, M. F., & Tennenbaum, T. (2007). Protein kinase C family: on the crossroads of cell signaling in skin and tumor epithelium. *Journal of Cancer Research and Clinical Oncology*, *133*, 793–808.
10. Caruso, M., Maitan, M. A., Bifulco, G., Miele, C., Vigliotta, G., Oriente, F., … Beguinot, F. (2001). Activation and mitochondrial translocation of protein kinase Cδ are necessary for insulin stimulation of pyruvate dehydrogenase complex activity in muscle and liver cells. *The Journal of Biological Chemistry*, *276*, 45088–45097.
11. Cederblad, G., Carlin, J. I., Constantin–Teodosiu, D., Harper, P., & Hultman, E. (1990). Radioisotopic assays of CoASH and carnitine and their acetylated forms in human skeletal muscle. *Analytical Biochemistry*, *185*, 274–278.
12. Cermak, N. M., LeBlanc, P. J., Peters, S. J., Vandenboom, R., & Roy, B. D. (2009). Effect of extracellular osmolality on metabolism in contracting mammalian skeletal muscle in vitro. *Applied Physiology, Nutrition, and Metabolism*, *34*, 1055–1064.

13. Chokkalingam, K., Jewell, K., Norton, L., Littlewood, J., van Loon, L. J. C., Mansell, P., … Tsintzas, K. (2007). High–fat/low–carbohydrate diet reduces insulin–stimulated carbohydrate oxidation but stimulates nonoxidative glucose disposal in humans: An important role for skeletal muscle pyruvate dehydrogenase kinase 4. *The Journal of Clinical Endocrinology and Metabolism*, *92*, 284–292.

14. Cohen, J. (1992). A power primer. *Psychological Bulletin*, *112*, 155–159.

15. Collier, C. A., Bruce, C. R., Smith, A. C., Lopaschuk, G., & Dyck, D. J. (2006). Metformin counters the insulin–induced suppression of fatty acid oxidation and stimulation of triacylglycerol storage in rodent skeletal muscle. *American Journal of Physiology. Endocrinology and Metabolism*, *291*, E182–E189.

16. Constantin–Teodosiu, D., Carlin, J. I., Cederblad, G., Harris, R. C., & Hultman, E. (1991a). Acetyl group accumulation and pyruvate dehydrogenase activity in human muscle during incremental exercise. *Acta Physiologica Scandinavica*, *143*, 367–372.

17. Constantin–Teodosiu, D., Cederblad, G., & Hultman, E. (1991b). A sensitive radioisotopic assay of pyruvate dehydrogenase complex in human muscle tissue. *Analytical Biochemistry*, *198*, 347–351.

18. Elion, E. A. (2006). Detection of protein–protein interactions by coprecipitation. *Current Protocols in Neuroscience*, *35*, 5.25.1–5.25.10.

19. Gittings, W. (2009). M.Sc. Thesis. Brock University, Ontario, Canada.

20. Gutowski, J. A., & Lienhard, G. E. (1976). Transition state analogs for thiamin pyrophosphate–dependent enzymes. *The Journal of Biological Chemistry*, *251*, 2863–2866.

21. Harris, R. A., Bowker–Kinley, M. M., Huang, B., & Wu, P. (2002). Regulation of the activity of the pyruvate dehydrogenase complex. *Advances in Enzyme Regulation*, *42*, 249–256.

22. Heinemann, L. (2010). Insulin assay standardization: leading to measures of insulin sensitivity and secretion for practical clinical care: response to Staten et al. *Diabetes Care*, *33*, e83.

23. Hill, D. K. (1972). Resting tension and the form of the twitch of rat skeletal muscle at low temperature. *The Journal of Physiology*, *221*, 161–171.

24. Hiromasa, Y., Fujisawa, T., Aso, Y., & Roche, T. E. (2004). Organization of the cores of the mammalian pyruvate dehydrogenase complex formed by E2 and E2 plus the E3–binding protein and their capacities to bind the E1 and E3 components. *The Journal of Biological Chemistry*, *279*, 6921–6933.

25. Howlett, R. A., Parolin, M. L., Dyck, D. J., Hultman, E., Jones, N. L., Heigenhauser, G. J. F., & Spriet, L. L. (1998). Regulation of skeletal muscle glycogen phosphorylase and PDH at varying exercise power outputs. *The American Journal of Physiology*, *275*, R418–R425.

26. Huang, B., Gudi, R., Wu, P., Harris, R. A., Hamilton, J., & Popov, K. M. (1998). Isoenzymes of pyruvate dehydrogenase phosphatase. DNA–derived amino acid sequences, expression, and regulation. *The Journal of Biological Chemistry*, *273*, 17680–17688.

27. Huang, B., Wu, P., Bowker–Kinley, M. M., & Harris, R. A. (2002). Regulation of pyruvate dehydrogenase kinase expression by peroxisome proliferator–activated receptor–alpha ligands, glucocorticoids, and insulin. *Diabetes*, *51*, 276–283.

28. Huang, B., Wu, P., Popov, K. M., & Harris, R. A. (2003). Starvation and diabetes reduce the amount of pyruvate dehydrogenase phosphatase in rat heart and kidney. *Diabetes*, *52*, 1371–1376.

29. Jackman, M. R., & Willis, W. T. (1996). Characteristics of mitochondria isolated from type I and type IIb skeletal muscle. *The American Journal of Physiology*, *270*, C673–C678.

30. Jilka, J. M., Rahmatullah, M., Kazemi, M., & Roche, T. E. (1986). Properties of a newly characterized protein of the bovine kidney pyruvate dehydrogenase complex. *The Journal of Biological Chemistry*, *261*, 1858–1867.

31. Kolobova, E., Tuganova, A., Boulatnikov, I., & Popov, K. M. (2001). Regulation of pyruvate dehydrogenase activity through phosphorylation at multiple sites. *The Biochemical Journal*, *358*, 69–77.

32. Lawson, J. E., Niu, X. D., Browning, K. S., Trong, H. L., Yan, J., & Reed, L. J. (1993). Molecular cloning and expression of the catalytic subunit of bovine pyruvate dehydrogenase phosphatase and sequence similarity with protein phosphatase 2C. *Biochemistry*, *32*, 8987–8993.

33. LeBlanc, P. J., Harris, R. A., & Peters, S. J. (2007). Skeletal muscle fiber type comparison of pyruvate dehydrogenase phosphatase activity and isoform

expression in fed and food–deprived rats. *American Journal of Physiology. Endocrinology and Metabolism*, *292*, E571–E576.

34. LeBlanc, P. J., Howarth, K. R., Gibala, M. J., & Heigenhauser, G. J. F. (2004a). Effects of 7 wk of endurance training on human skeletal muscle metabolism during submaximal exercise. *Journal of Applied Physiology*, *97*, 2148–2153.
35. LeBlanc, P. J., Mulligan, M., Antolic, A., MacPherson, L., Inglis, J. G., Martin, D., Roy, B. D., & Peters, S. J. (2008). Skeletal muscle type comparison of pyruvate dehydrogenase phosphatase activity and isoform expression: effects of obesity and endurance training. *American Journal of Physiology. Regulatory, Integrative and Comparative Physiology*, *295*, R1224–R1230.
36. LeBlanc, P. J., Peters, S. J., Tunstall, R. J., Cameron–Smith, D., & Heigenhauser G. J. F. (2004b). Effects of aerobic training on pyruvate dehydrogenase and pyruvate dehydrogenase kinase in human skeletal muscle. *The Journal of Physiology*, *557*, 559–570.
37. Linn, T. C., Pettit, F. H., & Reed, L. J. (1969). Alpha–keto acid dehydrogenase complexes. X. Regulation of the activity of the pyruvate dehydrogenase complex from beef kidney mitochondria by phosphorylation and dephosphorylation. *Proceedings of the National Academy of Sciences of the United States of America*, *62*, 234–241.
38. Love, L. K., LeBlanc, P. J., Inglis, J. G., Bradley, N. S., Choptiany, J., Heigenhauser, G. J. F., & Peters, S. J. (2011). The relationship between

human skeletal muscle pyruvate dehydrogenase phosphatase activity and muscle aerobic capacity. *Journal of Applied Physiology*, *111*, 427–434.

39. Maj, M. C., Cameron, J. M., & Robinson, B. H. (2006). Pyruvate dehydrogenase Phosphatase deficiency: Orphan disease or an under–diagnosed condition? *Molecular and Cellular Endocrinology*, *249*, 1–9.

40. Makinen, M. W., & Lee, C. P. (1968). Biochemical studies of skeletal muscle mitochondria. I. Microanalysis of cytochrome content, oxidative and phosphorylase activities of mammalian skeletal muscle mitochondria. *Archives of Biochemistry and Biophysics*, *126*, 75–82.

41. Margineantu, D. H., Brown, R. M., Brown, G. K., Marcus, A. H., & Capaldi, R. A. (2002). Heterogeneous distribution of pyruvate dehydrogenase in the matrix of mitochondria. *Mitochondrion*, *1*, 327–338.

42. Maury, J., Kerbey, A. L., Priestman, D. A., Patel, M. S., Girard, J., & Ferre, P. (1995). Pretranslational regulation of pyruvate dehydrogenase complex subunits in white adipose tissue during the suckling–weaning transition in the rat. *The Biochemical Journal*, *311*, 531–535.

43. Morgan, J. F., Campbell, M. E., & Morton, H. J. (1955). The nutrition of animal tissues cultivated in vitro. I. A survey of natural materials as supplements to synthetic medium 199. *Journal of the National Cancer Institute*, *16*, 557–567.

44. Morgan, J. F., Morton, H. J., & Parker, R. C. (1950). Nutrition of animal cells in tissue culture; initial studies on a synthetic medium. *Proceedings of the Society for Experimental Biology and Medicine*, *73*, 1–8.

45. Patel, M. S., & Roche, T. E. (1990). Molecular biology and biochemistry of pyruvate dehydrogenase complexes. *FASEB Journal*, *4*, 3224–3233.

46. Pehleman, T. L., Peters, S. J., Heigenhauser, G. J. F., & Spriet, L. L. (2005). Enzymatic regulation of glucose disposal in human skeletal muscle after a high–fat, low–carbohydrate diet. *Journal of Applied Physiology*, *98*, 100–107.

47. Peters, S. J. (2003). Regulation of PDH activity and isoform expression: diet and exercise. *Biochemical Society Transactions*, *31*, 1274–1280.

48. Peters, S. J., Harris, R. A., Wu, P., Pehleman, T. L., Heigenhauser, G. J., & Spriet, L. L. (2001). Human skeletal muscle PDH kinase activity and isoform expression during a 3–day high–fat/low–carbohydrate diet. *American Journal of Physiology. Endocrinology and Metabolism*, *281*, E1151–E1158.

49. Peters, S. J., St. Amand, T. A., Howlett, R. A., Heigenhauser, G. J., & Spriet, L. L. (1998). Human skeletal muscle pyruvate dehydrogenase kinase activity increases after a low–carbohydrate diet. *The American Journal of Physiology*, *275*, E980–E986.

50. Pirola, L., Johnston, A. M., & Van Obberghen, E. (2004). Modulation of insulin action. *Diabetologia*, *47*, 170–184.

51. Popp, D. A., Klechle, F. L., Kotagal, N., & Jarett, L. (1980). Insulin stimulation of pyruvate dehydrogenase in an isolated plasma membrane–mitochondrial mixture occurs by activation of pyruvate dehydrogenase phosphatase. *The Journal of Biological Chemistry*, *255*,7540–7543.

52. Proctor, D. N., O'Brien, P. C., Atkinson, E. J., & Nair, K. S. (1999). Comparison of techniques to estimate total body skeletal muscle mass in people of different age groups. *The American Journal of Physiology*, *277*, E489–E495.

53. Putman, C. T., Spriet, L. L., Hultman, E., Lindinger, M. I., Lands, L. C., McKelvie, R. S., … Heigenhauser, G. J. F. (1993). Pyruvate dehydrogenase activity and acetyl group accumulation during exercise after different diets. *The American Journal of Physiology*, *265*, E752–E7560.

54. Robinson, B. H., & Chun, K. (1993). The relationships between transketolase, yeast pyruvate decarboxylase and pyruvate dehydrogenase of the pyruvate dehydrogenase complex. *FEBS Letters*, *328*, 99–102.

55. Schnaitman, C., & Greenawalt, J. W. (1968). Enzymatic properties of the inner and outer membranes of rat liver mitochondria. *The Journal of Cell Biology*, *38*, 158–175.

56. Segal, S. S., & Faulkner, J. A. (1985). Temperature–dependent physiological stability of rat skeletal muscle in vitro. *The American Journal of Physiology*, *248*, C265–C270.

57. Smith, A. C., Bruce, C. R., & Dyck, D. J. (2005). AMP kinase activation with AICAR simultaneously increases fatty acid and glucose oxidation in resting rat soleus muscle. *The Journal of Physiology*, *565*, 537–546.

58. Smith, A. C., Mullen, K. L., Junkin, K. A., Nickerson, J., Chabowski, A., Bonen, A., & Dyck, D. J. (2007). Metformin and exercise reduce muscle

FAT/CD36 and lipid accumulation and blunt the progression of high–fat diet–induced hyperglycemia. *American Journal of Physiology. Endocrinology and Metabolism*, *293*, E172–E181.

59. Smolle, M., & Lindsay, J. G. (2006). Molecular architecture of the pyruvate dehydrogenase complex: bridging the gap. *Biochemical Society Transactions*, *34*, 815–818.

60. Spriet, L. L., & Heigenhauser, G. J. F. (2002). Regulation of pyruvate dehydrogenase (PDH) activity in human skeletal muscle during exercise. *Exercise and Sport Sciences Reviews*, *30*, 91–95.

61. Srere, P. A. (1969). Citrate Synthase: [EC 4.1.3.7. Citrate oxaloacetate lyase (CoA – acetylating)]. *Methods in Enzymology*, *13*, 3–11.

62. Stefanyk, L. E., Gulli, R. A., Ritchie, I. R., Chabowski, A., Snook, L. A., Bonen, A., & Dyck, D. J. (2011). Recovered insulin response by 2 weeks of leptin administration in high–fat fed rats is associated with restored AS160 activation and decreased reactive lipid accumulation. *American Journal of Physiology. Regulatory, Integrative and Comparative Physiology*, *301*, R159–R171.

63. Stump, C. S., Henriksen, E. J., Wei, Y., & Sowers, J. R. (2006). The metabolic syndrome: role of skeletal muscle metabolism. *Annals of Medicine*, *38*, 389–402.

64. Sugden, M. C., & Holness, M. J. (2003). Recent advances in mechanisms regulating glucose oxidation at the level of the pyruvate dehydrogenase

complex by PDKs. *American Journal of Physiology. Endocrinology and Metabolism*, *284*, E855–E862.

65. Sugden, M. C., Howard, R. M., Munday, M. R., & Holness, M. J. (1993). Mechanisms involved in the coordinate regulation of strategic enzymes of glucose metabolism. *Advances in Enzyme Regulation*, *33*, 71–95.

66. Wera, S., & Hemmings, B. A. (1995). Serine/threonine protein phosphatases. *The Biochemical Journal*, *311*, 17–29.

67. Wu, P., Inskeep, K., Bowker–Kinley, M. M., Popov, K. M., & Harris, R. A. (1999). Mechanism responsible for inactivation of skeletal muscle pyruvate dehydrogenase complex in starvation and diabetes. *Diabetes*, *48*, 1593–1599.

68. Wu, P., Sato, J., Zhao, Y., Jaskiewicz, J., Popov, K. M., & Harris, R. A. (1998). Starvation and diabetes increase the amount of pyruvate dehydrogenase kinase 4 in rat heart. *The Biochemical Journal*, *329*, 197–201.

69. Yan, J., Lawson, J. E., & Reed, L. J. (1996). Role of the regulatory subunit of bovine pyruvate dehydrogenase phosphatase. *Proceedings of the National Academy of Sciences of the United States of America*, *93*, 4953–4956.

70. Yang, E. B., Zhao, Y. N., Zhang, K., & Mack, P. (1999). Daphnetin, one of coumarin derivatives, is a protein kinase inhibitor. *Biochemical and Biophysical Research Communications*, *260*, 682–685.

71. Yeaman, S. J. (1989). The 2–oxo acid dehydrogenase complexes: recent advances. *The Biochemical Journal*, *257*, 625–632.

72. Yeaman, S. J., Hutcheson, E. T., Roche, T. E., Pettit, F. H., Brown, J. R., Reed, L. J., Watson, D. C., & Dixon, G. H. (1978). Sites of phosphorylation on pyruvate dehydrogenase from bovine kidney and heart. *Biochemistry*, *17*, 2364–2370.

Appendix 1: Laboratory Procedures

Appendix 1a. Skeletal Muscle Tissue Surgical Extraction: Extensor Digitorum Longus

Materials & Apparatus

- Pentobarbital sodium
- Saline
- Absorbent gauze
- Absorbent surgery pad
- Non–absorbable surgical suture
- Surgical tools
  - 1 pair operating scissors
  - 1 pair tissue forceps
  - 1 pair straight thin tip forceps
  - 1 pair curved thin tip forceps
  - 1 scalpel handle
  - 1 surgical blade
- Tissue culture media (Medium 199)
  - Refer to Appendix 3: Components of Medium 199
- 1 mL syringe
- 27–gauge X 1¼ inch needle

Reagents

1. Saline Diluted Pentobarbital Sodium

   - 73% (v/v) Saline
   - 27% (v/v) Pentobarbital sodium
     - Store at room temperature in a locked cabinet

Protocol

Surgical Preparation

1. Lead the rat into a cylinder toy, and retrieve from its cage by the base of the tail.
2. Place the rat onto the surgery pad and gently position the animal for intraperitoneal injection.

   (Hint: the use of a cylinder toy as an anesthetic aid enables the surgeon to handle the rat in a comfortable manner. Through repeated observation, this technique significantly reduces the amount of stress placed upon the animal when moving from the rat's cage to the lab bench. This device enables easier location of the injection site, and the application of an accurate needle stick, without placing force directly upon the animal.)
3. Administer an introductory dose of anesthetic and return the rat to its cage.
4. Allow sufficient time for the animal to rest and fall under anesthesia.
5. Continually test palpebral and toe–pinch reflexes. Do not begin the surgical procedure until these reflexes are entirely withdrawn.
6. Top up the rat with additional injections if necessary in order to achieve the appropriate level of anesthesia.
7. Record the weight of the animal during this prepatory period.

Surgical Extraction

8. Begin surgery by cutting around the ankle joint with operating scissors, directly distal to the hindlimb fur line.

9. Using operating scissors, cut proximally along the medial line of the hindlimb.

   (Hint: this cut allows for gentle retraction of the hindlimb epidermis with minimal force, significantly reducing the amount of stress placed upon the hindlimb.)
10. Retract the epidermis in order to expose the entire hindlimb.
11. Perform blunt dissection on the epidermis of the anterior foot in order to expose tendons of the superficial distal anterior hindlimb musculature.
12. Locate and isolate the distal tibialis anterior (TA) tendon, and make small incisions on either side with a scalpel.
13. Using forceps (pattern 5), raise the distal TA tendon in order to fully isolate this tendon from other hindlimb musculature.
14. Cut the distal TA tendon.
15. Dissect through the medial fascia covering TA, cutting proximally towards the knee joint with direct pressure against the tibia.

    (Hint: ensure that this cut is superficial as the sole purpose is to penetrate the fascia; a deep incision will damage the extensor digitorum longus (EDL) muscle.)
16. Using forceps (pattern 7), pinch the distal belly of the TA muscle and retract until this tissue is solely anchored at the proximal attachment.
17. Grasp TA at the proximal attachment and remove this tissue.

    (Hint: a poor dissection can leave plenty of frayed muscle and connective tissue. In order to obtain a clean dissection, grasp TA as close to the proximal attachment as possible and slowly retract with force until the tissue separates naturally. This technique will result in a clean kneecap with a clear view of the EDL muscle.)
18. Using forceps (pattern 7), slide the curved tips of this tool underneath EDL.

19. Gently glide along the length of the muscle in order to dissect free from connective tissue, and to obtain a cleaner view of both tendons.
20. Remove as much connective tissue at the ankle joint as possible in order to fully expose the distal EDL tendon.
21. Fasten one suture with a double knot around the distal tendon.

    (Hint: it is crucial to tie the knots of this suture as close to the muscle as possible, in order to obtain ideal installation conditions within the incubation reservoir.)
22. Using a scalpel, perform fine dissection upon the lateral musculature above the knee joint in order to fully expose the proximal EDL tendon.

    (Hint: deep or careless dissection can damage the proximal EDL tendon. It is imperative to gently cut through the vastus musculature leaving this tendon intact.)
23. Using forceps (pattern 7), glide underneath EDL at the knee joint with force in order to detach the proximal tendon from the kneecap.
24. Fasten the second suture with a double knot around the proximal tendon.

    (Hint: the knots of this suture do not need to be tied against the tissue, as additional length to the second suture will allow for a quick and easy installation into the incubation reservoir.)
25. Cut both EDL tendons and proceed to suspension within the incubation reservoir.

References

1. Gittings, W. (2009). M.Sc. Thesis. Brock University, Ontario, Canada.

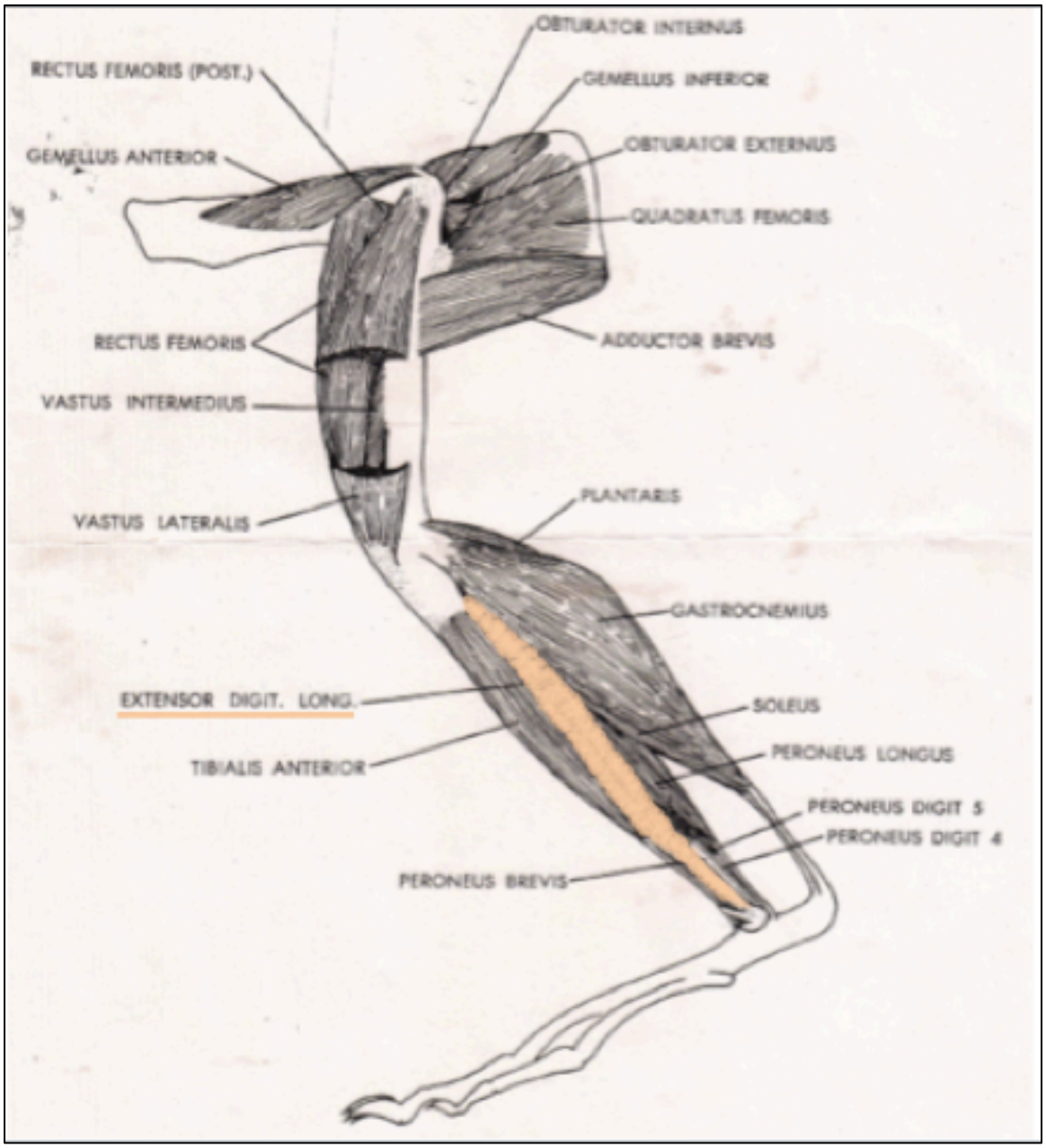

Figure A1.1. Extensor Digitorum Longus amongst the rat hindlimb musculature.

Appendix 1b. Isolation of Skeletal Muscle Tissue Subsarcolemmal Mitochondria

Materials & Apparatus

- Adenosine triphosphate (ATP)
- Bovine serum albumin (BSA)
- Disodium ethylenediaminetetraacetic acid (Na_2EDTA)
- Kinase inhibitor (7,8–dihydroxycoumarin)
- Magnesium Sulfate ($MgSO_4$)
- Mannitol
- Phosphatase inhibitor cocktail
- Potassium chloride (KCl)
- Sucrose
- Tris base
- Tris hydrochloride (Tris HCl)
- Glass tissue grinders
- Mincing scissors
- Petri dish

Reagents

1. Chappell–Perry Solution 1 – pH 7.4
    - 100 mM KCl
    - 40 mM Tris HCl
    - 10 mM Tris base
    - 5 mM $MgSO_4$
    - 5 mM Na_2EDTA
    - 1 mM ATP
    - ddH_2O (500 mL final volume)
        - Store at 4° C
2. Chappell–Perry Solution 2 – pH 7.4
    - 100 mM KCl
    - 40 mM Tris HCl
    - 5 mM Tris base
    - 1 mM $MgSO_4$
    - 100 μM Na_2EDTA
    - 250 μM ATP
    - 1% BSA
    - ddH_2O (500 mL final volume)
        - Store at 4° C

3. Chappell–Perry Solution 3 – pH 7.4

    - 100 mM KCl
    - 40 mM Tris HCl
    - 5 mM Tris base
    - 1 mM $MgSO_4$
    - 100 µM Na_2EDTA
    - 250 µM ATP
    - ddH_2O (500 mL final volume)
        - Store at 4° C

4. Sucrose & Mannitol – pH 7.4

    - 220 mM Sucrose
    - 70 mM Mannitol
    - 10 mM Tris HCl
    - 100 µM Na_2EDTA
    - ddH_2O (500 mL final volume)
        - Store at 4° C

- Per 10 mL of Solutions 1, 2, 3, and Sucrose & Mannitol

    - 200 µM 7,8–dihydroxycoumarin
    - 1 PhosSTOP tablet

Protocol

Tissue Preparation

1. Prior to any handling of fresh tissue, gather the following materials and immediately place them on ice: one petri dish, glass tissue grinders, one eppendorf tube, one glass culture tube, and a working volume of solution 1.
   (Hint: label the eppendorf and culture tubes for the sample to be processed. Ensure that the homogenizing plunger is placed within the homogenizing potter to avoid any water contamination. Place the petri dish upside down, and depress it to ensure that the underside is in direct contact with ice.)
2. Add a base volume of solution 1 to the labeled eppendorf tube (Example: 500 µL).
3. Place freshly collected EDL tissue onto the petri dish and roughly mince.
   (Hint: ensure that any fresh tissue is on ice at all times in order to maintain tissue viability.)
4. Isolate a small chunk (~5–10 mg) of minced tissue and immediately snap–freeze it in liquid nitrogen.
5. Transfer the chunk to a labeled eppendorf tube. Keep this tissue in liquid nitrogen until it can be transferred to –80° C storage.
   (Hint: this chunk will be reserved for use in the citrate synthase assay for the measurement of mitochondrial recovery).
6. Working as quickly as possible, transfer the remaining minced tissue to a weigh scale and record its weight in milligrams (Example: 40 mg).
   (Hint: this step must be done as quickly as possible as the tissue sample will be taken off ice, and tissue viability could potentially be compromised).

7. Once the tissue has been weighed, immediately transfer it to the labeled eppendorf containing solution 1. Keep this eppendorf tube on ice.
8. Continue to mince the tissue in the eppendorf until only tiny chunks remain suspended.
9. Calculate the remaining volume of solution 1 required in order to produce a 20–fold dilute homogenate (Example: 40 mg of tissue within 800 µL of solution 1).
10. Cut off the end of a 1 mL pipette tip and transfer the minced tissue into the homogenizing potter.

    (Hint: when pipetting the minced tissue into the homogenizing potter, pre–cutting the tip will decrease the likelihood that any tissue will remain left behind in the pipette tip).
11. Once the tissue has been transferred, place the potter back on ice and add the remaining volume of solution 1 (Example: 300 µL).
12. Gently homogenize the tissue on ice at all times for a minimum of 30 plunges, or until a pink opaque homogenate is produced.

    (Hint: homogenizations for mitochondrial isolation must be performed as gently and patiently as possible in order to preserve intact mitochondria).
13. Once fully homogenized, rinse the inner walls of the potter with the homogenized tissue to collect any mitochondria that may have clung to the sides of the potter.
14. Transfer the homogenate to the labeled culture tube.

Mitochondrial Isolation

15. Spin #1: swinging bucket rotor, 4° C, 10 minutes, 700 x *g*.

    (Hint: the purpose of spin #1 is to pellet out all bulky cellular debris).

16. Retain the supernatant, which contains the mitochondria, and discard the pellet.
17. Transfer the supernatant to a clean and labeled eppendorf tube.
18. Spin #2: small rotor, 4° C, 10 minutes, 14,000 rpm.
19. Retain the pellet, which contains the mitochondria, and discard the supernatant.
20. Resuspend the mitochondrial pellet in 10 volumes of solution 2 (Example: 400 µL).
21. Spin #3: small rotor, 4° C, 10 minutes, 7,000 rpm.

    (Hint: the purpose of spin #3 is the first cleaning step. Solution 2 contains BSA, which will bind all free fatty acids within the sample.)

22. Retain the mitochondrial pellet and discard the supernatant.
23. Resuspend the mitochondrial pellet in 10 volumes of solution 3.
24. Spin #4: small rotor, 4° C, 10 minutes, 7,000 rpm.

    (Hint: the purpose of spin #4 is the second cleaning step. Solution 3 is very similar in contents to solution 1, and will wash the resuspended mitochondria).

25. Retain the clean mitochondrial pellet and discard the supernatant.
26. Resuspend the mitochondrial pellet in sucrose & mannitol at a 1:1 w/v ratio (Example: 40 µL).
27. Transfer 5 µL of the mitochondrial extract into a labeled eppendorf containing 95 µL of sucrose & mannitol to produce a 20–fold dilute total mitochondrial suspension.

(Hint: this suspension will be reserved for use in the citrate synthase assay for the measurement of mitochondrial recovery).

28. Immediately snap–freeze the mitochondrial extract and total suspension in liquid nitrogen.
29. The subsarcolemmal mitochondrial isolation is now complete. Three subsamples should result for every fresh tissue sample that is processed: 1) whole muscle tissue chunk; 2) mitochondrial extract; and 3) total mitochondrial suspension. Store all samples at –80° C for future use.

References

1. Jackman, M. R., & Willis, W. T. (1996). Characteristics of mitochondria isolated from type I and type IIb skeletal muscle. *The American Journal of Physiology*, *270*, C673–C678.
2. Makinen, M. W., & Lee, C. P. (1968). Biochemical studies of skeletal muscle mitochondria. I. Microanalysis of cytochrome content, oxidative and phosphorylase activities of mammalian skeletal muscle mitochondria. *Archives of Biochemistry and Biophysics*, *126*, 75–82.

Appendix 1c. Homogenization of Whole Skeletal Muscle Tissue

Materials & Apparatus

- Ethylene glycol tetraacetic acid (EGTA)
- Kinase inhibitor (7,8–dihydroxycoumarin)
- Phosphatase inhibitor cocktail
- Protease inhibitor cocktail
- Sodium chloride (NaCl)
- Tris–hydrochloride (Tris HCl)
- Glass tissue grinders

Reagents

1. Lysis Buffer – pH 6.8
    - 150 mM NaCl
    - 50 mM Tris HCl
    - 1 mM EGTA
    - ddH_2O (1 L final volume)
        - Store at 4° C

- Per 10 mL Lysis Buffer
    - 200 μM 7,8–dihydroxycoumarin
    - 1 cOmplete ULTRA EDTA–free tablet
    - 1 PhosSTOP tablet
        - Make fresh before use

Protocol

1. Gather tissue grinders and lysis buffer from storage and place these materials on ice. Allow sufficient time for cooling before processing any tissue samples.
   (Hint: keep the homogenizing pestle inside the potter to avoid water contamination within the homogenization apparatus.)
2. Retrieve EDL tissue samples from –80° C storage and immediately place in liquid nitrogen prior to handling.
3. Using a foam stand for support, place a base volume of lysis buffer into the homogenizing potter (Example: 200 μL).
4. Place the potter onto a weigh scale and tare the scale.
5. Using tweezers, drop the frozen wet tissue into the potter. Allow for the scale to settle and record the weight of the tissue.
   (Hint: frozen tissue should be placed in cold buffer upon removal from liquid nitrogen in order to maintain tissue viability.)
6. Calculate the remaining volume of lysis buffer required in order to produce a 25–fold dilute homogenate (Example: 40 mg of skeletal muscle tissue within 1 mL of lysis buffer).
7. Place the potter on ice, and add the remaining lysis buffer (Example: 800 μL).
8. Homogenize the tissue on ice at all times for a minimum of 30 plunges, or until a pink opaque homogenate is produced.
   (Hint: when held up to light, with the pestle fully depressed into the potter, large connective debris should be the only visible material left unprocessed.)
9. Store whole homogenate in a labeled eppendorf tube at –80° C.

References

1. Yang, E. B., Zhao, Y. N., Zhang, K., & Mack, P. (1999). Daphnetin, one of coumarin derivatives, is a protein kinase inhibitor. *Biochemical and Biophysical Research Communications*, *260*, 682–685.

Appendix 1d. Quantitative Determination of Proteins: The Bradford Method

Materials & Apparatus

- Bovine serum albumin (BSA)
- Protein assay dye reagent concentrate
- Microplate reader
- Skirted microtiter 96–well plate

Reagents

1. Stock BSA Solution (1 mg/mL)
    - 100 g bovine serum albumin
    - ddH_2O (100 mL final volume)
        - Aliquot into eppendorf tubes for individual trials
        - Store aliquots at –20° C and thaw before use
2. Stock Protein Assay Dye Reagent (1:4 dilution)
    - 20% (v/v) concentrated colorimetric assay dye
    - 80% (v/v) ddH_2O
        - Store at 4° C

Protocol

Standard Curve Preparation

1. Retrieve all tissue samples from –80° C storage and place on ice.
2. Remove one aliquot of 1 mg/mL stock BSA solution from storage. Let thaw and immediately place on ice.
3. Prepare all BSA standard solutions and store in labeled eppendorf tubes on ice.

Table A1.1. *Volumes of Stock BSA and ddH_2O required for the preparation of the Bradford protein assay standard solutions.*

Protein Concentration (mg/mL)	**Stock BSA Solution (µL)**	**ddH_2O (µL)**
1	1000	0
0.5	500 (from 1 mg/mL)	500
0.25	500 (from 0.5 mg/mL)	500
0.125	500 (from 0.25 mg/mL)	500
0.05	100 (from 0.5 mg/mL)	900
0	0	1000

Sample Preparation

4. Prepare labeled eppendorf tubes for all samples to be analyzed for protein quantification.
5. Prepare 10–fold dilutions for all samples by loading individual eppendorf tubes with 10 µL of whole homogenate and 90 µL of ddH_2O.
   (Hint: when working with mitochondrial samples, 20–fold dilutions are required).
6. Return whole homogenates to –80° C storage, and keep diluted samples on ice.

Bradford Protein Assay

7. Retrieve a clean 96–well plate. If using an old plate, wash it thoroughly in order to ensure that the plate is free of any remnants from previous use.
   (Hint: the Bradford method is a sensitive spectrophotometric procedure that is fully dependent upon samples' color development and subsequent light absorption.

Colour presents as a result of a reaction between the protein assay dye reagent and the positively charged amine groups of proteins within a sample. Consequently, any debris on the well plate could interfere with absorption readings.)

8. Pipette 10 μL of each prepared standard solution and diluted sample into the 96–well plate in triplicate.
9. Pipette 200 μL of stock protein assay dye reagent into each well.
   (Hint: use of a multi–channel pipette will save time at this step. However, individually loading each well with a single channel pipette will lead to greater consistency, accuracy and superior results.)
10. Allow a minimum of 2 minutes to pass for proper colour development to occur (**Figure A1.2**).
11. Insert the well plate into the microplate reader to generate absorbance readings.
12. Open KC4™ data analysis software, and ensure that the reading parameters are set to absorbance.
13. Define the reading parameters by the following details: absorbance wavelength of 595 nanometers, shaking intensity level of 3 and shaking duration of 5 seconds (**Figure A1.3**).
14. Proceed to read the absorbance of each standard and sample (**Figure A1.4**).
15. Copy the absorbance readings into a Microsoft® Excel spreadsheet, and generate a standard curve by plotting known protein concentrations (BSA standard solutions) against their average absorbance readings.

16. Outfit the standard curve with a polynomial trendline, and display the quadratic equation derived from this curve (**Figure A1.5**).

    (Hint: set BSA standards along the Y–axis and mean absorbance readings along the X–axis. With this setup, one can apply the absorbance readings as the unknown 'X' and solve for 'Y' (sample protein concentration) using this quadratic equation.)

17. Subtract the average absorbance reading of water for every sample, and calculate the unknown protein concentrations for all samples using the quadratic equation.

    (Hint: ensure that all protein concentrations are multiplied by their dilution factor in order to obtain true quantifications, as sample homogenates were diluted 10–fold with ddH_2O.)

References

1. Bradford, M. M. (1976). A rapid and sensitive method for the quantification of microgram quantities of protein utilizing the principle of protein–dye binding. *Analytical Biochemistry*, *72*, 248–254.

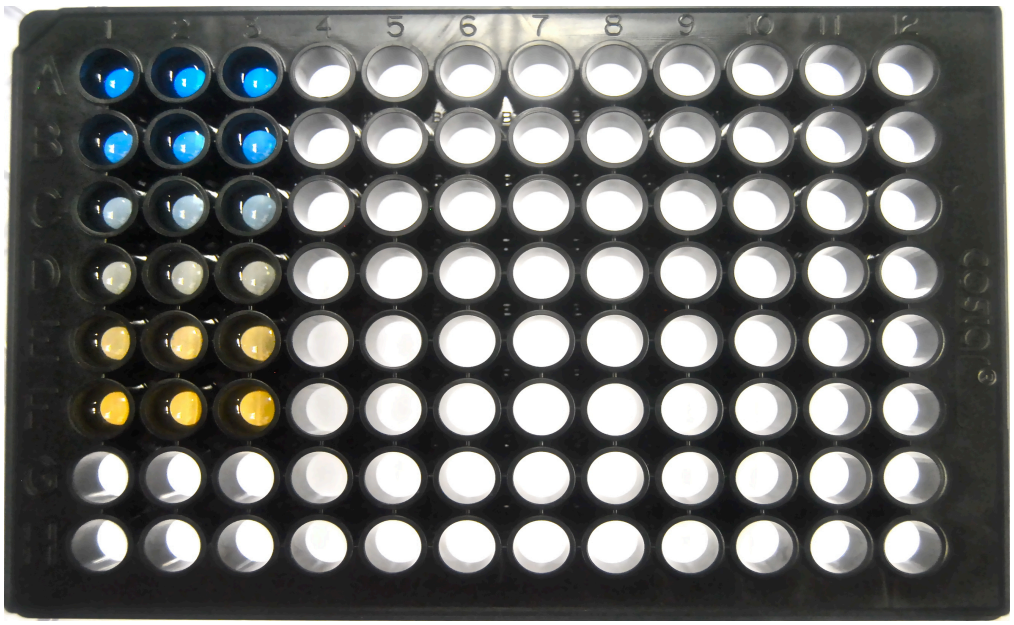

Figure A1.2. 96–well plate with BSA standards loaded in triplicate.

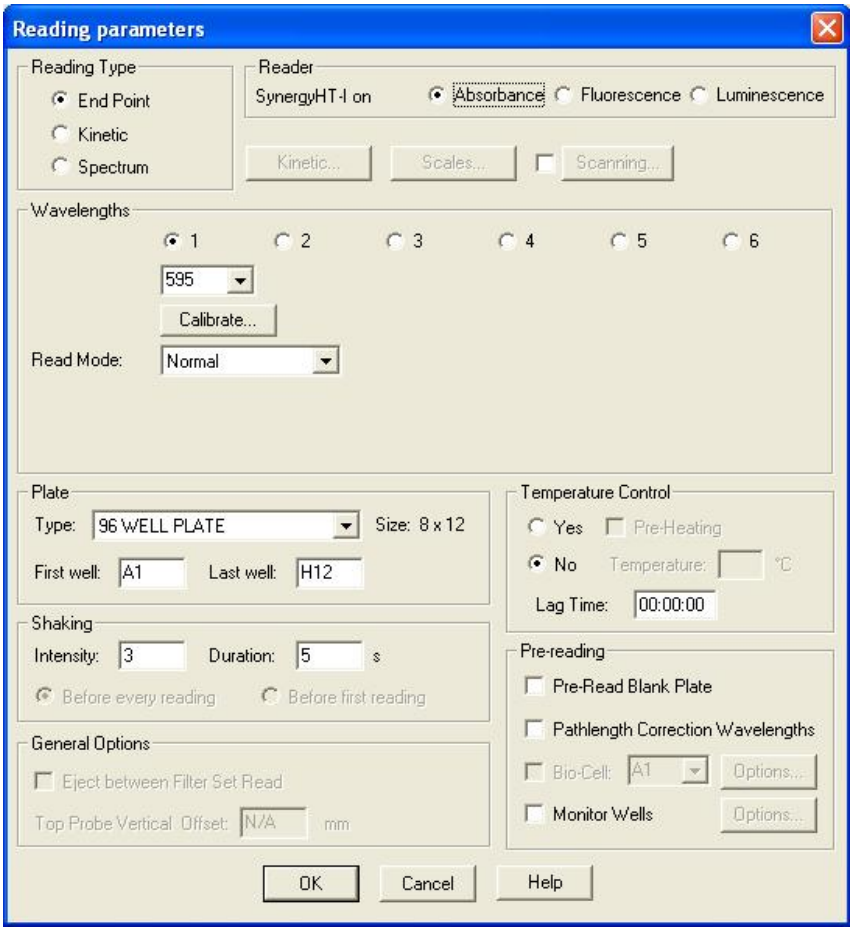

Figure A1.3. Reading parameters in preparation for absorbance quantification.

RESULTS

Data: M 595

	1	2	3	4	5	6	7	8	9	10	11	12
A	1.198	1.193	1.184	0.048	0.053	0.052	0.052	0.048	0.050	0.048	0.048	0.047
B	0.920	0.910	0.940	0.048	0.051	0.051	0.051	0.050	0.050	0.048	0.047	0.048
C	0.618	0.627	0.632	0.050	0.053	0.051	0.054	0.049	0.049	0.048	0.048	0.048
D	0.471	0.470	0.471	0.050	0.059	0.053	0.062	0.047	0.051	0.048	0.048	0.047
E	0.346	0.346	0.346	0.048	0.048	0.048	0.047	0.050	0.049	0.049	0.048	0.050
F	0.273	0.265	0.264	0.048	0.049	0.051	0.050	0.052	0.048	0.048	0.049	0.048
G	0.047	0.047	0.048	0.047	0.047	0.048	0.048	0.046	0.047	0.047	0.049	0.046
H	0.047	0.047	0.047	0.046	0.045	0.046	0.045	0.046	0.045	0.046	0.047	0.047

Change Mask Statistics... Help

Figure A1.4. Absorbance readings for 96 wells with standard values highlighted.

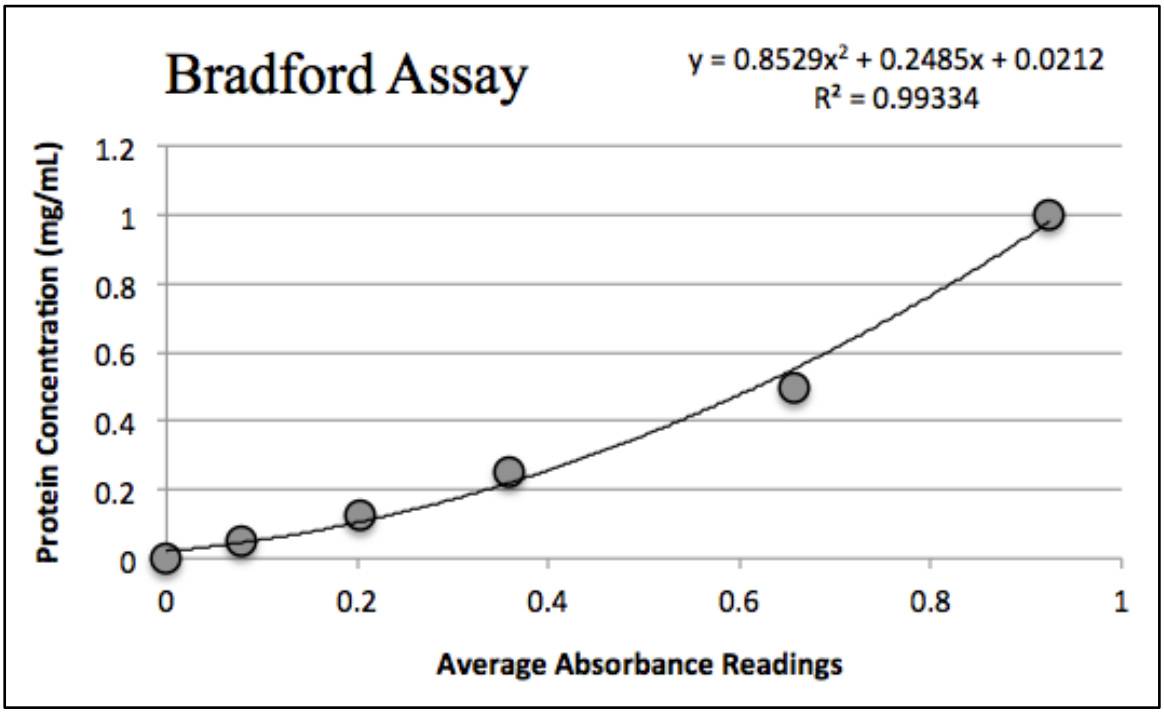

Figure A1.5. Scatterplot displaying known protein concentrations the against mean absorbance readings.

Appendix 1e. Immunoprecipitation of Serine–Phosphorylated Proteins

Materials & Apparatus

- Anti–phosphoserine primary antibody
- Bromophenol blue
- Disodium hydrogen phosphate (Na_2HPO_4)
- Glycerol
- 2–mercaptoethanol
- Potassium chloride (KCl)
- Potassium dihydrogen phosphate (KH_2PO_4)
- Protein G PLUS–Agarose conjugate bead suspension
- Sodium chloride (NaCl)
- Sodium dodecyl sulfate (SDS)
- Tris base
- 1 mL syringe

Reagents

1. 10x Stock Phosphate Buffered Saline (PBS) – pH 7.4
    - 1.37 M NaCl
    - 30 mM KCl
    - 80 mM Na_2HPO_4
    - 30 mM KH_2PO_4
    - ddH_2O (100 mL final volume)
        - Store at 4° C
        - Dilute to 1x PBS as needed
2. 2x Sample Buffer – pH 6.8
    - 25% (v/v) 1 M Tris base
    - 10% (v/v) glycerol
    - 20% (v/v) 10% SDS
    - 5% (v/v) 2–mercaptoethanol
    - 0.01% (w/v) bromophenol blue
    - ddH_2O (10 mL final volume)
        - Store at 4° C

Protocol

Sample Preparation

1. Retrieve all tissue homogenates from –80° C storage, and immediately place in liquid nitrogen before handling. Let thaw and immediately place on ice.
2. Based upon previously collected protein quantification results, aliquot 500 µg of protein per sample into individual eppendorf tubes.
    - Refer to Appendix 1d: Bradford Method.

   (Hint: vortex all samples thoroughly in order to ensure that a homogeneous mixture of whole tissue extract is drawn for immunoprecipitation.)
3. Load all 500 µg samples with 40 µL of anti–phosphoserine primary antibody.
    - Refer to Appendix 2: Calculations.
4. Fill the remaining volume of each eppendorf tube with additional lysis buffer.
    - Refer to Appendix 1c: Homogenization of Whole Tissue, for the preparation of lysis buffer.

   (Hint: previous trials excluding step #4 have led to the accumulation of sample debris along the inner walls of eppendorf tubes. With prolonged agitation, some contents of the immunoprecipitation samples are being shaken out of solution. This debris, the contents of which are unspecified, clings to the walls of the eppendorf and does not reach the pellet with centrifugation. Filling the dead space within each eppendorf tube with lysis buffer prevents this accumulation without a) altering protein concentrations within the sample, and b) disturbing any interactions between proteins of interest, primary antibody and agarose beads. As a result of this adjustment, it can be stated with increased confidence that all

proteins of interest are reaching the immunoprecipitated pellet post–centrifugation.)

5. Incubate all samples for 24 hours at 4° C with gentle agitation.
6. Upon recommencement, load all samples with 20 µL of agarose bead suspension.
7. Incubate all samples for 24 hours at 4° C with gentle agitation.

Sample Cleaning

8. Centrifuge all samples at 4° C at 13,000 rpm for 5 minutes.
9. Using a syringe and needle, aspirate and discard all supernatants.

   (Hint: depending on the application of the immunoprecipitation method, the supernatant may need to be retained and analyzed in order to ensure that all protein of interest has been collected in the pellet. The use of this method in the current study aims to collect all phosphorylated pyruvate dehydrogenase phosphatase (PDP) proteins. Dephosphorylated PDP will be present in the supernatant and is not of interest for subsequent analysis. Therefore, in this instance, the supernatant can be discarded.
10. Load all samples with 200 µL of 1x PBS. Gently resuspend pellets.
11. Repeat steps 8–10 twice more, for a total of three 1x PBS washes.
12. Once supernatants have been aspirated after the final wash, load all samples with 80 µL of 2x sample buffer.
13. Samples are now prepared for gel electrophoresis. Keep samples on ice for immediate use, however samples can be frozen at –80° C for next day use.

References

1. Elion, E. A. (2006). Detection of protein–protein interactions by coprecipitation. *Current Protocols in Neuroscience*, *35*, 5.25.1–5.25.10.

Appendix 1f. Western Blotting: Polyacrylamide Gel Electrophoresis

Materials & Apparatus

- Chemicals
  - 30% Acrylamide/bis–acrylamide solution
  - Ammonium persulfate (APS)
  - Glycine
  - Hydrochloric acid (HCl)
  - Methanol
  - Resolving gel buffer
  - Sodium chloride (NaCl)
  - Sodium dodecyl sulfate (SDS)
  - Sodium hydroxide (NaOH)
  - Stacking gel buffer
  - Tetramethylethylenediamine (TEMED)
  - Tris base
  - Tween 20
- Mini–PROTEAN Tetra Cell electrophoresis kit
  - Casting frame
  - Casting stand
  - Electrode assembly
  - Mini tank & lid
  - PowerPac power supply
  - Rubber gasket
  - Short plate
  - Spacer plate
  - 10–lane gel combs
- Western blot development materials
  - Horseradish peroxidase chemiluminescent substrate
  - ImageJ imaging software
  - Polyvinylidene fluoride (PVDF) membrane
  - Ponceau S Stain Solution
  - Primary antibody (specific against protein of interest)
  - Secondary antibody (horseradish peroxidase conjugated)
  - Western blot imaging system
- Other
  - Disposable square petri dishes
  - Kaleidoscope protein standard
  - Non–fat dry skim milk
  - Protein transfer filters (pads & paper)
  - Rocking platform

Reagents

1. 10% Ammonium Persulfate

    - 40 mg APS
    - ddH_2O (400 µL final volume)
        - Make fresh before use
        - Measures sufficient volume for 2 gels

2. 5% Blocking Solution

    - 5% (w/v) non–fat dry skim milk
    - 95% (v/v) TBST (100 mL final volume)
        - Make fresh before use
        - Measures sufficient to perform one experiment with 2 gels

3. 10x Stock Electrode (Running) Buffer – pH 8.3

    - 250 mM tris base
    - 1.92 M glycine
    - 1% (w/v) SDS
    - ddH_2O (1 L final volume)
        - Store at 4° C

4. 1 M Hydrochloric Acid

    - 31.16 mL stock HCl (32.09 M)
    - 968.84 mL ddH_2O
        - Store at room temperature with other acids

5. 10% Sodium Dodecyl Sulfate

    - 50 g SDS
    - ddH_2O (500 mL final volume)
        - Store at room temperature

6. Sodium Hydroxide

    - 0.1 M NaOH
    - ddH_2O (1 L final volume)
        - Store at room temperature

7. Transfer Buffer – pH 8.3

    - 31.25 mM tris base
    - 240 mM glycine
    - 10 mL 10% SDS
    - ddH_2O (800 mL final volume)
    - 200 mL methanol
        - Make fresh before use

8. 10x Stock Tris–Buffered Saline – pH 7.5

    - 200 mM tris base
    - 1.37 M NaCl
    - 38 mL 1M hydrochloric acid
    - ddH_2O (1 L final volume)
        - Store at 4° C

9. Tris–Buffered Saline with Tween (TBST)

    - 100 mL 10x TBS
    - 4 mL 25% Tween 20
    - ddH_2O (1 L final volume)
        - Store at 4° C

10. 25% Tween 20

    - 10 mL Tween 20
    - ddH_2O (40 mL final volume)
        - Store at room temperature

Protocol

Polyacrylamide Gel Preparation

1. Retrieve spacer plates, short plates, casting frames and a casting stand in order to assemble glass cassette sandwiches to contain polyacrylamide gels.
2. Line the protruding left and right edges of the spacer plate with ddH_2O before introducing the short plate in order to obtain a tight seal between the glassware.
3. Align both plates flush on a flat surface during assembly into the casting frame, ensuring that the borders of both glass plates are uniform.
4. Engage both pressure cams of the casting frame, and place the frame into the casting stand with rubber gaskets in place at the floor of the stand.

   (Hint: Sliding 1 mL pipette tips behind the spring–loaded levers of the casting stand will provide added pressure and a tighter seal between glass plates and the rubber gasket. This addition, along with steps 3 & 4, will eliminate any risk of leakage while gel solutions are polymerizing in the casting stand.)
5. Prepare separating and stacking polyacrylamide gels by mixing all ingredients, except for 10% APS and TEMED in 50 mL falcon tubes.

Table A1.2. *Volumes of all reagents required for the preparation of polyacrylamide gels in Western blotting.*

Gel Component	10% Separating Gel	6% Stacking Gel
30% Acrylamide Solution	6.66 mL	2 mL
Resolving Gel Buffer	5 mL	---
Stacking Gel Buffer	---	2.5 mL
ddH_2O	7.92 mL	5.4 mL
10% APS	200 µL	100 µL
TEMED	20 µL	20 µL

*Volumes listed are sufficient for 2 gels

6. Insert a 10–lane comb between spacer and short plates, and mark a guideline 1 cm below the comb teeth. This will be the height to which separating gel is poured.

7. Immediately prior to pouring 10% separating solution into the cassette sandwich, add 10% APS and TEMED in order to initiate the gel polymerization reaction.
8. Mix 10% separating solution rapidly with a transfer pipette, and proceed to pipette the solution into the sandwich up to the marked guideline.
9. Overlay the separating solution with methanol in order to flatten the separating gel, and to eliminate bubbles remaining along the top surface of the solution. (Hint: eliminating any bubbles is crucial, as their presence can negatively affect sample loading and protein migration. Adhering to this tip is a good first step towards obtaining clean blots for protein quantification.)
10. Once the separating gel has polymerized (~30 minutes), drain all methanol from the cassette. Proceed to rinse the gel surface with ddH_2O.
11. Repeat the same preparation for the 6% stacking solution with 10% APS and TEMED. Pipette this solution into the frame in order to fill the remaining volume. (Hint: pipette the stacking solution until it overflows out of the glass cassette. Doing so will force bubbles away from the top surface of the gel, as trapping bubbles within the stacking gel and sample wells is undesirable for clean blots.
12. Insert a 10–lane comb into the cassette, and let the 6% stacking gel polymerize.

Sample Processing – Protein Migration

13. Retrieve previously prepared samples from storage and let thaw. Once thawed, keep samples on ice.
14. Boil samples for 5 minutes, and store them on ice for 5 minutes before loading into gels.

15. Retrieve the electrode assembly for protein migration, and rest it on a clean flat surface with the clamping arms open.
16. Retrieve glass cassettes containing polymerized gels from the casting stand, and insert them into the electrode assembly with short plates facing inward.
    (Hint: when working with an odd number of gels, a buffer dam must be used.)
17. Close the clamping arms of the electrode assembly to produce a functional assembly. Apply firm pressure to the tops and sides of both cassettes during this process, in order to ensure that a leak–proof seal is achieved.
18. Place the electrode assembly into the tank, and fill the inner chamber (space between both cassettes) with 1x running buffer until short plates are submerged.
19. Remove lane combs and choose one well to load a kaleidoscope protein standard.
20. Load samples into remaining wells with gel loading pipette tips.
    - For immunoprecipitated samples, pipette from the top suspension containing proteins of interest from the rest of the sample. After boiling, a clear separation within the sample can be seen with the lower fraction containing agarose beads and primary antibody, which must be avoided (**Figure A1.6**).
    - For whole tissue samples, vortex boiled samples thoroughly in order to obtain a homogenous mixture of whole homogenate, sample buffer and ddH_2O.
21. Fill the outer chamber of the tank with 550 mL of 1x running buffer.
22. Place the lid onto the electrophoresis tank with the proper colour coding aligned, and insert the electrical leads into the power supply.

23. Run electrophoresis for 100 minutes with a 120–volt constant.

Membrane Processing – Protein Transfer

24. Retrieve the electrode assembly for protein transfer as well as a fresh tank.
25. Cut PVDF membrane to the dimensions of the gel and rinse with methanol.
26. Soak all transfer materials in freshly prepared transfer buffer to equilibrate before electrophoresis.
27. Prepare the gel cassette sandwich in a shallow container filled with transfer buffer in the following order:
    - Clear side of the plastic cassette lying flat in the container
    - 1 pre–soaked foam pad
    - 1 pre–soaked filter pad (roll out bubbles with glass culture tube)
    - 2 pre–soaked filter papers (roll out bubbles with glass culture tube)
    - PVDF membrane
    - Equilibrated gel
    - 2 pre–soaked filter papers (roll out bubbles with glass culture tube)
    - 1 pre–soaked filter pad (roll out bubbles with glass culture tube)
    - 1 pre–soaked foam pad
    - Fold black side of the cassette over and lock sandwich in place
28. Insert the gel cassette sandwich into the electrode assembly, ensuring that the black side of the cassette is inserted against the black side of the assembly.
29. Place the electrode assembly into the tank, and fill the tank completely with transfer buffer.

30. Place the tank in a large enough container to surround it with ice. Add an ice pack into the electrophoresis tank in order to complete the cooling unit.
31. Place a stir bar into the tank in order to maintain even cooling throughout the transfer.
32. Place the lid onto the electrophoresis tank with the proper colour coding aligned, and insert the electrical leads into the power supply.
33. Run electrophoresis for 60 minutes with a 100–volt constant.

Membrane Processing – Protein Staining

34. Place the membrane in a disposable square petri dish with the proteins facing upward.
35. Add 10 mL of Ponceau S solution in order to stain protein bands.
36. Place the petri dish onto the rocking device, and periodically observe the membrane until stained bands are visualized clearly (~5 minutes).
37. Pour off Ponceau S solution. Rinse the membrane in 10 mL of TBST to wash off any excess staining solution. Repeat TBST wash twice more.
38. Pour off TBST. Immediately save a visual for a reference of total protein content in each lane using transparent film.

    (Hint: this step is crucial towards eliminating any error that may have occurred during sample loading. Protein of interest contents must be normalized to total protein contents in order to control for any error during sample loading.)
39. Proceed to reverse staining through the addition of 10 mL 0.1 M NaOH.
40. Pour off NaOH. Rinse the membrane in 10 mL ddH_2O for 5 minutes, and repeat this rinse another two times.

Membrane Processing – Blocking

41. Place the membrane in a clean square petri dish, and add 10 mL of freshly prepared 5% blocking solution. Cover the dish with Parafilm & lid.
42. Place the petri dish onto the rocking device, and proceed to block the membrane at room temperature for 1 hour.

    (Hint: blocking is essential towards eliminating non–specific protein interactions throughout blot development. The target and both antibodies are all proteins, and blocking assists in the assurance that proper binding occurs between these molecules. Diluted proteins in the skim milk attach to the membrane in all places where target proteins are not bound. Once antibody is introduced, all binding sites are filled except for those on the target protein of interest.)

Membrane Processing – Blot Development

43. Prepare primary antibody incubating solution, against the target protein of interest, in a clean square petri dish.
44. Remove the membrane from the blocking solution, and wash it with 10 mL of TBST for 5 minutes. Repeat TBST was twice more.
45. Place the membrane into the petri dish containing primary incubating solution.
46. Cover the square petri dish with Parafilm® & lid, and incubate overnight at 4° C with gentle agitation. This step concludes day one of the experiment.
47. Recommence experiment on day two. Pour off primary incubating solution, and wash the membrane with 10 mL TBST for 5 minutes. Repeat wash two times.
48. Prepare secondary antibody incubating solution, against the primary antibody, in a clean square petri dish.

49. Place the membrane into the dish containing secondary incubating solution. Cover the dish with Parafilm® & lid, and incubate for 1–2 hours at room temperature.
50. Pour off secondary incubating solution, and perform a 3 x 5 minute TBST wash. Dry the membrane as much as possible, without interfering or making any contact with the protein side of the membrane, before introducing chemiluminescent reagent.
51. After the third wash, pour off TBST and baste the membrane with 2 mL of chemiluminescent substrate for 3 minutes. Once again, dry the membrane as much as possible.
52. Place the membrane between two sheets of transparent film in preparation for development and protein visualization.
53. Place the protected membrane into the imaging station and develop the membrane according to pre–determined exposure settings.
54. Save a visual for a reference of protein content in each lane. Quantify protein of interest contents using ImageJ software.

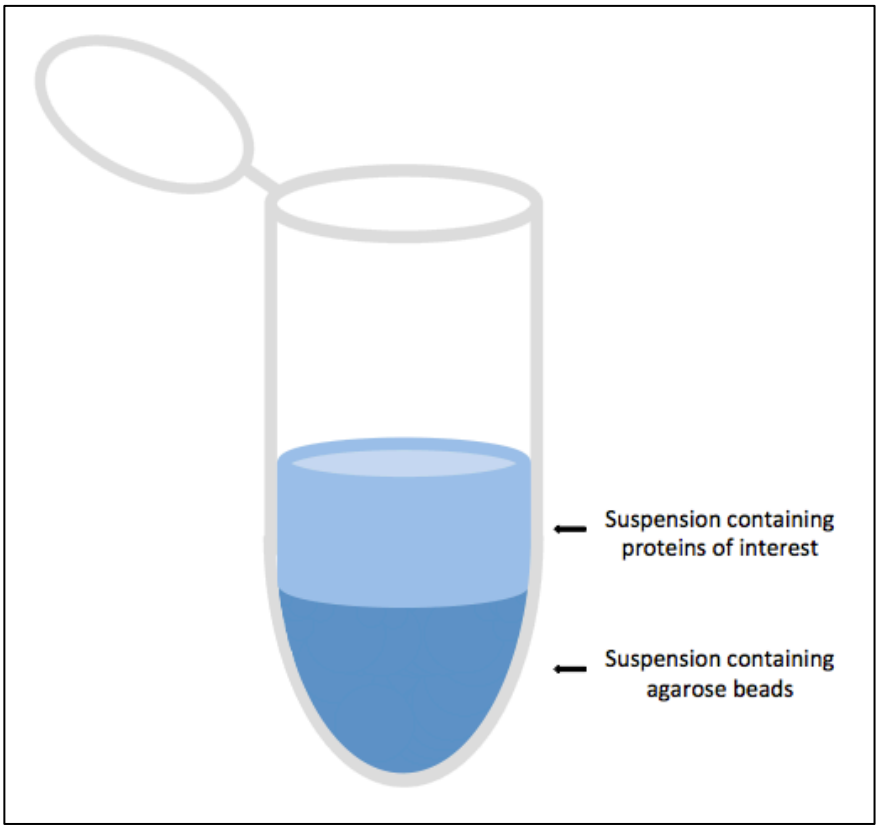

Figure A1.6. Separation within immunoprecipitated samples after boiling in preparation for Western blotting.

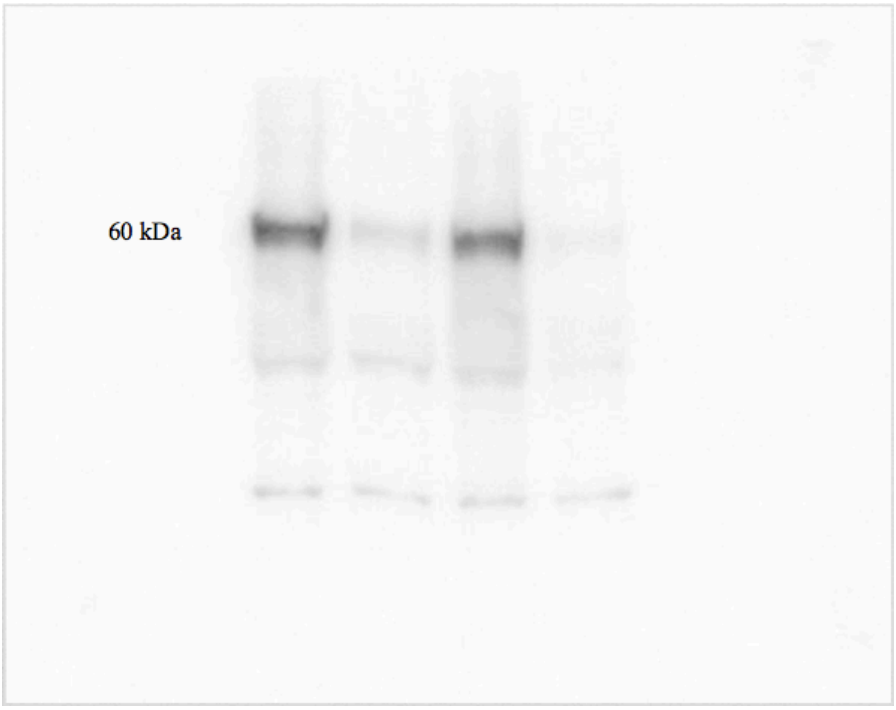

Figure A1.7. Full Western blot of phosphorylated Akt (pAkt, 60 kDa) protein in extensor digitorum longus skeletal muscle tissue.

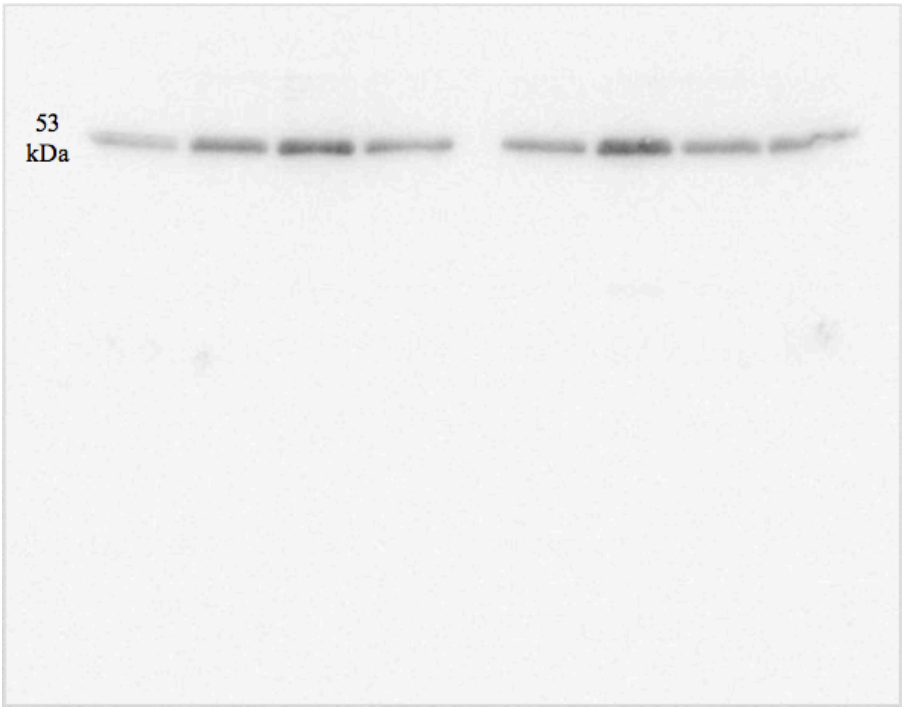

Figure A1.8. Full Western blot of immunoprecipitated serine–phosphorylated pyruvate dehydrogenase phosphatase 1 (pPDP1, 53 kDa) protein in extensor digitorum longus skeletal muscle tissue.

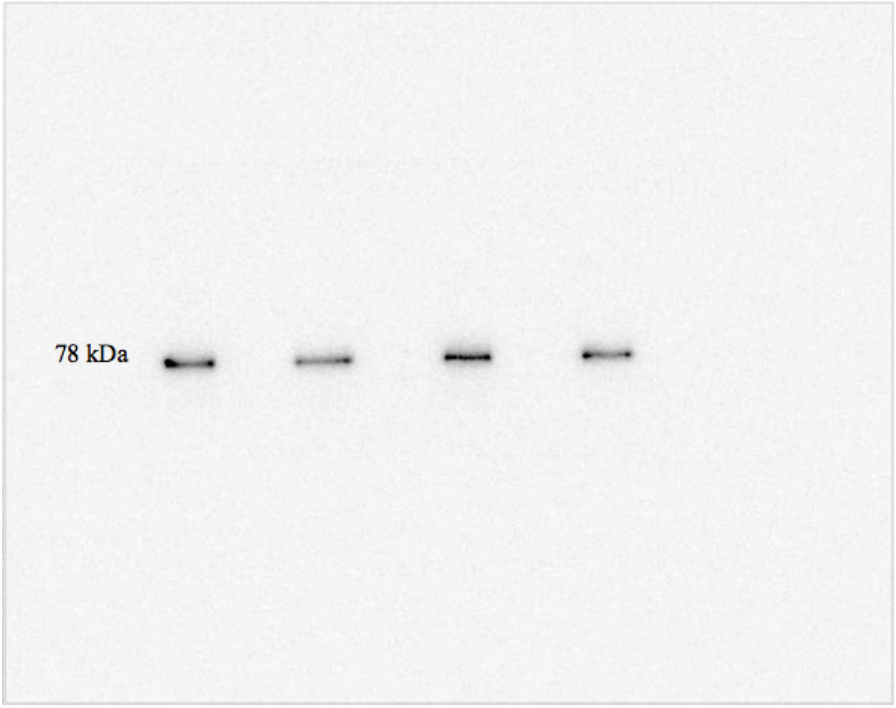

Figure A1.9. Full Western blot of protein kinase C–delta (PKCδ, 78 kDa) protein in mitochondrial subfractions from extensor digitorum longus skeletal muscle tissue.

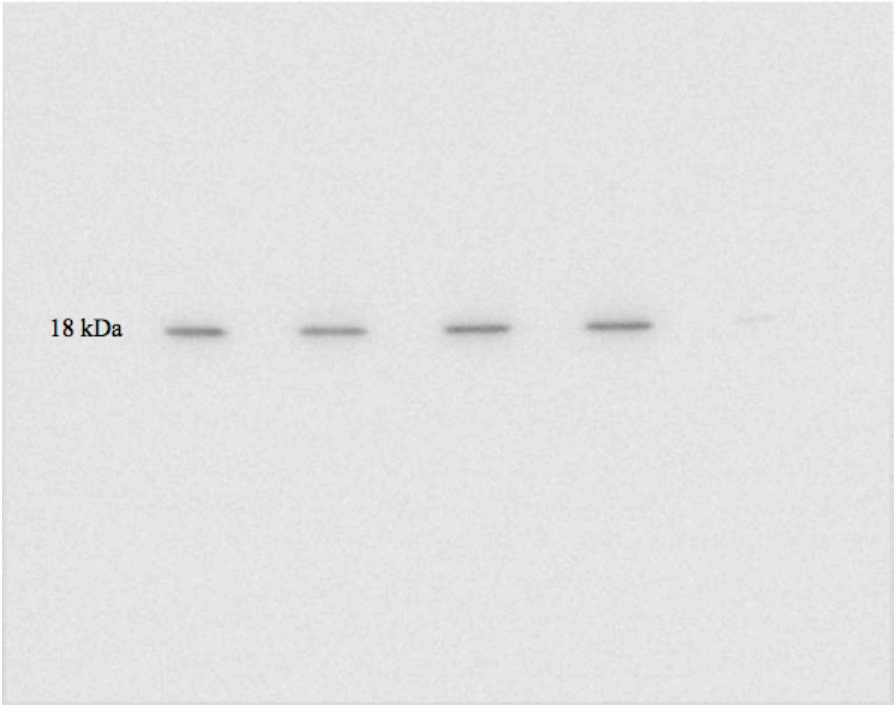

Figure A1.10. Full Western blot of cytochrome *c* oxidase subunit 4 (CoxIV, 18 kDa) protein in mitochondrial subfractions from extensor digitorum longus skeletal muscle tissue.

Appendix 1g. PDHa Activity Assay by Measurement of Acetyl–CoA Accumulation

Materials & Apparatus

- Coenzyme A (CoA)
- Dichloroacetic acid (DCA)
- Ethylenediaminetetraacetic acid (EDTA)
- Ethylene glycol tetraacetic acid (EGTA)
- Magnesium chloride ($MgCl_2$)
- Nicotinamide adenine dinucleotide (NAD^+)
- Perchloric acid (PCA)
- Potassium bicarbonate ($KHCO_3$)
- Potassium chloride (KCl)
- Pyruvate
- Sodium fluoride (NaF)
- Sucrose
- Thiamine pyrophosphate (TPP)
- Tris base
- Tris hydrochloride (Tris HCl)
- Triton X–100
- Block heater
- Glass tissue grinders
- Motor driven homogenizer
- 12 x 75 mm culture tubes

Reagents

1. Coenzyme A
    - 13 mM CoA
    - ddH_2O (2.5 mL final volume)
        - Make fresh before use

2. Nicotinamide Adenine Dinucleotide
    - 39 mM NAD^+
    - ddH_2O (2.5 mL final volume)
        - Make fresh before use

3. PDH*a* Assay Buffer – pH 7.8
    - 144.4 mM Tris base
    - 1.44 mM $MgCl_2$
    - 0.72 mM EDTA
    - ddH_2O (100 mL final volume)
        - Aliquot into 10 mL portions
        - Store aliquots at –20° C

4. PDH*a* Homogenizing Buffer – pH 7.8
    - 50 mM Tris HCl
    - 200 mM Sucrose
    - 50 mM KCl
    - 50 mM NaF
    - 5 mM DCA
    - 5 mM $MgCl_2$
    - 5 mM EGTA
    - 0.1% (v/v) Triton X–100
    - ddH_2O (100 mL final volume)
        - Aliquot into 1.5 mL portions
        - Store aliquots at –20° C

5. PDH*a* Incubating Solution
    - 8.33% (v/v) 39 mM NAD^+
    - 8.33% (v/v) 13 mM CoA
    - 8.33% (v/v) 13 mM TPP
    - 75% (v/v) PDH*a* assay buffer
        - Make fresh before use

6. 0.5 M Perchloric Acid

    - 1.45 mL Stock PCA (86.2 M)
    - ddH_2O (250 mL final volume)
        - Store at 4° C

7. Potassium Bicarbonate

    - 2.2 M $KHCO_3$
    - ddH_2O (40 mL final volume)
        - Store at 4° C

8. Pyruvate
    - 26 mM pyruvate
    - ddH_2O (1.25 mL final volume)
        - Make fresh before use

9. Thiamine Pyrophosphate
    - 13 mM TPP
    - ddH_2O (2.5 mL final volume)
        - Make fresh before use

Protocol

PDHa Homogenization Procedure

1. Retrieve all muscle samples from –80° C storage and place in liquid nitrogen.
2. Place a base volume of PDH*a* homogenizing buffer into a homogenizing potter (Example: 500 µL).
3. Using a foam stand for support, place the potter onto a weight scale and tare the scale.
4. Add a piece of wet frozen EDL muscle to the potter and record its weight in milligrams.

   (Hint: be sure to work quickly and ensure that the tissue sample does not thaw.)
5. Immediately begin homogenization of the sample, gently by hand with the potter on ice at all times.

   (Hint: it is imperative to introduce the tissue to kinase (DCA) and phosphatase (NaF) inhibitors as soon as possible, in order to lock the phosphorylation state of the sample.)
6. Keep the potter on ice, and calculate the remaining volume of homogenizing buffer required in order to produce a 30–fold dilute homogenate.

   (Example: 30 mg of skeletal muscle tissue within 900 µL of PDH*a* homogenizing buffer.)
7. Add the remaining buffer to achieve the desired dilution (Example: 400 µL).
8. Continue to homogenize the sample on ice with a motor driven glass pestle for 50 seconds at 400 rpm.

9. While using the motor driven homogenizer, periodically check the potter to ensure that the entire tissue sample is being processed.
10. Continue homogenizing until an opaque homogenate is produced.

    (Hint: when held up to light with the pestle fully depressed into the potter, large connective debris should be the only visible material left unprocessed.)
11. Place the homogenate in a labeled eppendorf tube and snap–freeze in liquid nitrogen as quickly as possible. The sample is now prepared for analysis of PDH*a* activity.

    (Hint: it is crucial to snap freeze the sample as soon as possible, as cellular contents will reform within solution at room temperature that contain the PDH complex. If this reformation occurs, resulting PDH*a* activities will be lower than expected.)

Assay Preparation

12. Pre–heat a block heater 37° C, and use a thermometer to ensure temperature maintenance throughout the assay.
13. Retrieve a sufficient volume of PDH*a* assay buffer from –20° C storage.
14. Prepare and combine all reagents included in the PDH*a* incubating solution.
    - 2.5 mL 13 mM CoA
    - 2.5 mL 39 mM NAD^+
    - 2.5 mL 13 mM TPP
    - 22.5 mL PDH*a* assay buffer
15. Prepare and pre–warm (37 °C) 1.25 mL 26 mM pyruvate in an eppendorf tube.

16. Label three glass culture tubes for every sample to be assayed.
    - Samples are run in duplicate (A & B), in addition to a blank (C).
17. Label nine eppendorf tubes for every sample to be assayed.
    - 1, 2 and 3 minute time points for muscle samples A, B and C.
18. Pre–load 40 µL of 0.5 M PCA into each of the labeled eppendorf tubes.
19. Pipette 720 µL of PDH*a* incubating solution into each culture tube of the first muscle sample to be processed. Pre–warm the culture tubes in the block heater.

PDHa Assay

20. Using a positive displacement pipette, add 30 µL of homogenate into the culture tubes. Gently vortex each tube.

    (Hint: thaw each homogenate on at a time immediately prior to analysis to prevent sample warming.)
21. Initiate the PDH reaction by adding 30 µL of 26 mM pyruvate, and gently vortex the culture tube after doing so. Return sample to the block heater and start a timer.

    (Hint: blank reactions are initiated with ddH_2O, replacing 26 mM pyruvate.)
22. After precisely 1 minute, withdraw 200 µL of the incubation mixture and pipette into the appropriately labeled eppendorf tube pre–loaded with 0.5 M PCA. Vortex the acidified aliquot, and store at one ice until the completion of the trial.
23. Repeat step #22 at 2 and 3–minute intervals to obtain three aliquots to be analyzed for the determination of the PDH*a* reaction rate.
24. Repeat steps #19 through 23 for all samples (duplicates and blanks).
25. Keep acidified samples on ice for a minimum of 5 minutes.

26. After 5 minutes, neutralize each sample through the addition of 10 μL of 1 M $KHCO_3$.
27. Allow all neutralized samples to sit for 5 minutes at room temperature.
28. Store all samples at –80 °C for future acetyl–CoA analysis.

References

1. Constantin–Teodosiu, D., Cederblad, G., & Hultman, E. (1991). A sensitive radioisotopic assay of pyruvate dehydrogenase complex in human muscle tissue. *Analytical Biochemistry*, *198*, 347–351.
2. Putman, C. T., Spriet, L. L., Hultman, E., Lindinger, M. I., Lands, L. C., McKelvie, R. S., … Heigenhauser, G. J. F. (1993). Pyruvate dehydrogenase activity and acetyl group accumulation during exercise after different diets. *The American Journal of Physiology*, *265*, E752–E7560.

Appendix 1h. Determination of Acetyl–CoA Accumulation

Materials & Apparatus

- Acetyl–CoA
- Alpha–ketoglutaric acid (α–KG)
- Aspartate transaminase (AST)
- Aspartate: ^{14}C radiochemical
- Citrate synthase (CS)
- Copper sulfate ($CuSO_4$)
- Dithiothreitol (DTT)
- Dowex cation exchange resin
- Ethylenediaminetetraacetic acid (EDTA)
- N–ethylmaleimide (NEM)
- N–[2–Hydroxyethyl]–piperazineethanesulfonic acid (HEPES)
- Perchloric acid (PCA)
- Potassium acetate (K–acetate)
- Potassium glutamate (K–glut)
- Potassium hydroxide (KOH)
- Scintillation cocktail fluid
- 12 x 75 mm culture tubes
- Scintillation counter

Reagents

1. Acetyl–CoA Assay Buffer
    - 9% (v/v) 0.1 M DTT
    - 34.125% (v/v) 1 mM $CuSO_4$
    - 34.125% (v/v) 400 mM potassium acetate
    - 22.75% (v/v) ddH_2O
        - Make fresh before use
2. Acetyl–CoA
    - 2 mM Acetyl–CoA
    - ddH_2O (10 mL final volume)
        - Dilute into 2 µM aliquots for individual trial use
        - Store aliquots at –20° C
3. α–Ketoglutaric Acid
    - 8 mM α–KG
    - ddH_2O (10 mL final volume)
        - Make fresh before use
4. 40 µM ^{14}C–Aspartate
    - 200 µL Stock ^{14}C–Aspartate
    - ddH_2O (1 mL final volume)
        - Store at 4° C
5. 1:10 Aspartate Transaminase
    - 9% (v/v) AST
    - 91% (v/v) ddH_2O
        - Aliquot into 200 µL portions
        - Store aliquots at –20° C
6. 1:10 Citrate Synthase
    - 9% (v/v) CS
    - 91% (v/v) ddH_2O
        - Aliquot into 500 µL portions
        - Store aliquots at –20° C

7. Copper Sulfate

    - 1 mM $CuSO_4$
    - ddH_2O (50 mL final volume)
        - Aliquot into 1 mL portions
        - Store aliquots at –20° C

8. Dithiothreitol

    - 100 mM DTT
    - ddH_2O (10 mL final volume)
        - Aliquot into 500 µL portions
        - Store aliquots at –20° C

9. Dowex Cation Resin

    - 37.5% (w/v) Dowex
    - 62.5% (v/v) ddH_2O
        - Store at room temperature

10. Ethylenediaminetetraacetic acid

    - 11 mM EDTA
    - ddH_2O (50 mL final volume)
        - Aliquot into 1 mL portions
        - Store aliquots at –20° C

11. Ethylenediaminetetraacetic acid

    - 60 mM EDTA
    - ddH_2O (50 mL final volume)
        - Aliquot into 1 mL portions
        - Store aliquots at –20° C

12. N–ethylmaleimide

    - 30 mM NEM
    - ddH_2O (50 mL final volume)
        - Aliquot into 1 mL portions
        - Store aliquots at –20° C

13. N–(2–Hydroxyethyl)–piperazine–N'–(2–ethanesulfonic acid) – pH 7.4

    - 500 mM HEPES
    - ddH_2O (100 mL final volume)
        - Store at 4° C

14. 1 M Perchloric Acid

    - 1.16 mL Stock PCA (86.2 M)
    - ddH_2O (100 mL final volume)
        - Store at 4° C

15. Potassium Acetate

    - 400 mM potassium acetate
    - ddH_2O (50 mL final volume)
        - Aliquot into 1 mL portions
        - Store aliquots at –20° C

16. Potassium Hydroxide

    - 600 mM KOH
    - ddH_2O (100 mL final volume)
        - Store at 4° C

17. Potassium Glutamate

    - 178 mM K–glut
    - ddH_2O (50 mL final volume)
        - Aliquot into 1 mL portions
        - Store aliquots at –20° C

Protocol

Assay Preparation

1. Thaw neutralized PDH*a* samples and place them on ice.
2. Label glass culture tubes for all samples to be assayed as well as acetyl–CoA standards.
3. Prepare acetyl–CoA standards in duplicate.

Table A1.3. *Volumes of Acetyl–CoA and ddH_2O required for the preparation of the Acetyl–CoA assay standard solutions.*

Concentration (mM)	2 µM Acetyl–CoA (µL)	ddH_2O (µL)	Total Volume (µL)
0	0	220	220
40	4	216	220
125	12.5	207.5	220
250	25	195	220
375	37.5	182.5	220
500	50	170	220

4. Load all culture tubes assigned to PDH*a* samples with 200 µL of ddH_2O.
5. Load 20 µL of neutralized PDH*a* samples into respective culture tubes.
6. Prepare acetyl–CoA assay buffer consisting of 0.1 M DTT, 1 mM $CuSO_4$, 400 mM K–acetate and ddH_2O.
    - Premix 1 mM $CuSO_4$, 400 mM K–acetate and ddH_2O in a 3:3:2 ratio.

Table A1.4. *Volume of Acetyl–CoA buffers required per number of samples processed.*

		Number of Culture Tubes				
Reagent	**µL/tube**	**30**	**40**	**60**	**80**	**100**
0.1 M DTT	2	60	80	120	160	200
$CuSO_4$–K–acetate–ddH_2O (3:3:2)	20	600	800	1200	1600	2000

Acetyl–CoA Assay

7. Add 20 µL of acetyl–CoA assay buffer to each culture tube. Vortex all samples, and incubate at room temperature for 30 minutes.
8. Prepare the radiolabeled ^{14}C–oxaloacetate reaction during this incubation. Refer to 'Preparation of Radiolabeled ^{14}C–oxaloacetate' (page 137).
9. Once the assay buffer incubation has concluded, add 20 µL of 60 mM EDTA to each culture tube. Vortex all samples, and incubate at room temperature for 5 minutes.
10. Following the 60 mM EDTA incubation, add 30 µL of 30 mM NEM to each culture tube. Vortex all samples, and incubate at room temperature for 5 minutes.
11. Following the 30 mM NEM incubation, add 20 µL of radiolabeled ^{14}C–oxaloacetate and 10 µL of 1:10 citrate synthase to each culture tube. Vortex all samples, and incubate at room temperature for 20 minutes.

Key Reaction #2

^{14}C–oxaloacetate + acetyl–CoA →→ CS →→ ^{14}C–citrate + CoA

(Significance: radiolabeled citrate is produced from ^{14}C–oxaloacetate and existing concentrations of acetyl–CoA within each sample. This reaction enables the eventual counting of radiolabeled citrate, which will reflect each sample's acetyl–CoA concentration.)

12. Prepare the transamination reagent during this incubation. Refer to 'Preparation of Transamination Reagent' (page 139).

13. Following the ^{14}C–oxaloacetate and citrate synthase incubation, add 30 µL of the transamination reagent to each culture tube. Vortex all samples, and incubate at room temperature for 20 minutes.

Key Reaction #3

^{14}C–oxaloacetate + glutamate →→ AST →→ ^{14}C–aspartate + α–ketoglutarate

(Significance: reversing reaction #1 with transamination reagent enables the isolation of negatively charged ^{14}C–citrate molecules. At this point in the assay, all samples contain radiolabeled citrate as well as any leftover radiolabeled oxaloacetate that was not processed in the citrate synthase reaction. Both ^{14}C–citrate and ^{14}C–oxaloacetate contain negatively charged ketone groups and if left alone in each sample, all labeled carbons would eventually be detected in scintillation counting, which would not be reflective of each sample's acetyl–CoA concentrations. Therefore, all remaining ^{14}C–oxaloacetate is reprocessed into ^{14}C–aspartate, which contains positively charged amine groups. All positively charge radiolabeled molecules will eventually be separated from the sample, leaving a purified extract containing negatively charged ^{14}C–citrate.

14. Prepare the Dowex cation exchange resin during this incubation.
15. Prepare one 20 mL scintillation vial for each sample with appropriate labeling during this incubation, and load 5 mL of scintillation cocktail fluid to each vial.
16. Following the transamination reagent incubation, add 1 mL of Dowex cation exchange resin to each culture tube. Cap every sample tightly and invert by hand for 2 minutes.

(Hint: the addition of ion exchange resin will separate all samples by charge, which will isolate positively and negatively charged radiolabeled molecules into separate fractions.)

17. Centrifuge all samples at 3,000 rpm for 2 minutes at room temperature.
18. Aspirate 500 μL of the supernatant from each sample, and deposit into respective scintillation vials. Tightly seal and shake all vials for thorough mixing.
    (Hint: the supernatant is the fraction of the sample that contains negatively charged ^{14}C–citrate, which reflects each sample's acetyl–CoA concentration.)
19. Count each sample in a liquid scintillation counter to quantify ionizing radiation from each sample.
20. Calculate PDH*a* activity for each sample (mmol/minute/kg wet weight tissue) based upon ionization counts per minute.
    - Refer to Appendix 2: Calculations.

Preparation of Radiolabeled ^{14}C–Oxaloacetate

1. Combine the following ingredients in an eppendorf tube. Appropriate volumes must be determined based upon the number of samples involved.

Table A1.5. *Volume of reagents required for radiolabel preparation per number of samples processed.*

		Number of Culture Tubes				
Reagent	**µL/Tube**	**30**	**40**	**60**	**80**	**100**
0.5 M HEPES	0.67	20.1	26.8	40.2	53.6	67
11 mM EDTA	1	30	40	60	80	100
(1:10) AST*	0.33	9.9	13.2	19.8	26.4	33
8 mM α–KG**	0.67	20.1	26.8	40.2	53.6	67
40 µM ^{14}C–Aspartate**	3.33	99.9	133.2	199.8	266.4	333

* Enzyme involved in key reaction #1
** Reactant involved in key reaction #1

2. Incubate reagents for 10 minutes at room temperature for reaction to proceed.

Key Reaction #1

^{14}C–aspartate + α–ketoglutarate →→ AST →→ ^{14}C–oxaloacetate + glutamate

(Significance: preparing radiolabeled oxaloacetate from ^{14}C–aspartate enables the assay to utilize existing concentrations of acetyl–CoA within each sample. The end goal of the assay is to count each sample's concentration of radiolabeled citrate, which is reflective of acetyl–CoA concentrations.)

Table A1.6. *Volume of PCA required for radiolabel preparation per number of samples processed.*

		Number of Culture Tubes				
Reagent	**µL/Tube**	**30**	**40**	**60**	**80**	**100**
1 M PCA	0.67	20.1	26.8	40.2	53.6	67

3. Incubate acidified reagents for 10 minutes on ice to halt the reaction.
4. Upon the completion of this second incubation, neutralize reagents through the addition of a base (600 mM KOH).

Table A1.9. *Volume of KOH and EDTA required for radiolabel preparation per number of samples processed*.

		Number of Culture Tubes				
Reagent	**µL/Tube**	**30**	**40**	**60**	**80**	**100**
6 00 mM KOH	1.33	39.9	53.2	79.8	106.4	133
11 mM EDTA	12	360	480	720	960	1200

5. Store this preparation on ice for a minimum of 5 minutes before integration into the acetyl–CoA assay.

Preparation of Transamination Reagent

1. Combine the following ingredients in an eppendorf tube. Appropriate volumes must be determined based upon the number of samples involved.

Table A1.8. *Volume of reagents required for transamination reagent preparation per number of samples to be assayed*.

		Number of Culture Tubes				
Reagent	**µL/Tube**	**30**	**40**	**60**	**80**	**100**
178 mM K–glut**	30	900	1200	1800	2400	3000
(1:10) AST*	3.33	99.9	133.2	199.8	266.4	333
ddH_2O	6.66	199.8	266.4	399.6	532.8	666

* Enzyme involved in key reaction #3
** Reactant involved in key reaction #3

2. Store this preparation on ice prior to integration into the acetyl–CoA assay.

References

1. Constantin–Teodosiu, D., Carlin, J. I., Cederblad, G., Harris, R. C., & Hultman, E. (1991). Acetyl group accumulation and pyruvate dehydrogenase activity in human muscle during incremental exercise. *Acta Physiologica Scandinavica*, *143*, 367–372.

Appendix 1i. Citrate Synthase Activity Assay

Materials & Apparatus

- Acetyl–CoA
- Bovine serum albumin (BSA)
- 5,5'–dithiobis[2–nitrobenzoic acid] (DTNB)
- Oxaloacetic acid
- Potassium phosphate (KH_2PO_4)
- Tris base
- Triton–X 100
- Blackened sidewall microcuvettes
- Glass tissue grinders
- Spectrophotometer

Reagents

1. Citrate Synthase Homogenizing Buffer – pH 7.3
    - 0.1 M KH_2PO_4
    - 0.05% (w/v) BSA
    - ddH_2O (100 mL final volume)
        - Store at 4° C
2. Tris Buffer – pH 8.3
    - 100 mM Tris base
    - ddH_2O (250 mL final volume)
        - Store at 4° C
3. 5,5'–dithiobis [2–nitrobenzoic acid]
    - 1 mM DTNB
    - Tris Buffer (10 mL final volume)
        - Store at 4° C
        - Must be stored in opaque container
        - Fresh reagent required every 1–2 weeks
4. Acetyl–CoA
    - 3 mM Acetyl–CoA
    - ddH_2O (5 mL final volume)
        - Aliquot into 200 µL portions
        - Freeze aliquots at –80° C

5. 10% Triton

    - 10% (v/v) Triton–X 100
    - 90% (v/v) ddH_2O (1 mL final volume)
        - Store at 4° C

6. Oxaloacetic Acid

    - 10 mM Oxaloacetic acid
    - Tris Buffer (1 mL final volume)
        - Prepare fresh daily
        - Store on ice throughout assay

Protocol

Tissue Homogenization

1. Gather tissue grinders and citrate synthase homogenizing buffer from storage and place these materials on ice. Allow sufficient time for cooling before processing any tissue samples.

   (Hint: keep the homogenizing pestle inside the potter to avoid water contamination within the homogenization apparatus.)
2. Retrieve EDL tissue chunks from –80° C storage and immediately place in liquid nitrogen prior to handling.
   - Refer to Appendix 1b: Mitochondrial isolations.
3. Using a foam stand for support, place a base volume of buffer into the homogenizing potter (Example: 500 μL).
4. Place the potter onto a weigh scale and tare the scale.
5. Drop the frozen chunk of EDL tissue into the potter. Allow for the scale to settle and record the weight of the tissue.
6. Calculate the remaining volume of homogenization buffer required in order to produce a 100–fold dilute homogenate (Example: 10 mg chunk within 1 mL of homogenizing buffer).
7. Place the potter back on ice, and add the remaining buffer (Example: 500 μL).
8. Rigorously homogenize the tissue on ice at all times until an opaque homogenate is produced.

   (Hint: some homogenization procedures require gentle tissue grinding, however

the citrate synthase assay requires mitochondrial contents to be suspended in solution. Therefore, rigorous tissue grinding is permissible in this instance.)

9. Snap–freeze samples in liquid nitrogen. Store citrate synthase whole homogenate in a labeled eppendorf at –80° C.

   (Hint: samples need to be frozen and thawed three times in order to release mitochondrial contents for enzyme activity analysis.)

Citrate Synthase Assay

10. Retrieve samples (citrate synthase whole homogenates or mitochondrial total suspensions) and acetyl–CoA from –80° C storage. Immediately place on ice once thawed.
11. Retrieve tris buffer, DTNB, and 10% triton from 4° C storage and immediately place on ice.
12. Prepare fresh oxaloacetic acid and immediately place on ice.
13. Prepare as many samples as desired with tris buffer, DTNB, acetyl–CoA and 10% triton.

    (Hint: spectrophotometer can run a maximum of 8 samples per trial.)

Table A1.9. *Volume of reagents required for the preparation of citrate synthase assay samples*.

		Number of samples to assay		
Reagent	**µL per cuvette**	**2**	**8**	**16**
Tris buffer	150	325 µL	1300 µL	2500 µL
DTNB	25	60 µL	225 µL	425 µL
Acetyl–CoA	40	80 µL	320 µL	640 µL
10% Triton	10	25 µL	100 µL	175 µL

14. Turn on the spectrophotometer and open the SwiftII software program.
15. Open the reaction kinetics function, and select the citrate synthase software procedure.

(Hint: the following steps of the assay must be performed diligently with haste. If inexperienced with the assay protocol, practice with a small number of samples before becoming accustomed to the required pace. Process more samples per trial once confident with the execution of the assay. It is crucial to have the assay software set up and one click away from running before continuing sample preparation.)

16. Working as quickly and accurately as possible, add 15 µL of oxaloacetic acid to each microcuvette. Mix the samples thoroughly with clean stir sticks.
17. Load all samples (maximum of 8) into the spectrophotometer and close the lid. (Hint: if using microcuvettes, the cuvette cannot be depressed all the way down into the sample chamber. This causes the transmission of light to pass over and miss the intended sample; consequently no change in absorbance will be recorded as the assay progresses. Only depress the cuvette so far that the top edge of the cuvette rests flush against the top edge of the sample chamber).
18. Run the citrate synthase assay. Ensure that the absorbance set to 412 nm.

References

1. Love, L. K., LeBlanc, P. J., Inglis, J. G., Bradley, N. S., Choptiany, J., Heigenhauser, G. J. F., & Peters, S. J. (2011). The relationship between human skeletal muscle pyruvate dehydrogenase phosphatase activity and muscle aerobic capacity. *Journal of Applied Physiology*, *111*, 427–434.
2. Srere, P. A. (1969). Citrate Synthase: [EC 4.1.3.7. Citrate oxaloacetate lyase (CoA – acetylating)]. *Methods in Enzymology*, *13*, 3–11.

Appendix 1j. Pyruvate Dehydrogenase Phosphatase Activity Assay

Materials & Apparatus

- Bovine serum albumin (BSA)
- Ethylenediaminetetraacetic acid (EDTA)
- Ethylene glycol tetraacetic acid (EGTA)
- Imidazole
- Magnesium chloride ($MgCl_2$)
- Mannitol
- 2–mercaptoethanol
- PDH E1α phosphopeptide
- Phosphatase inhibitor
- Serine/Threonine Phosphatase Assay System (Promega; Catalog # V2460)
  - Molybdate dye additive
  - Molybdate dye solution
  - Phosphate free water
  - Phosphate standard
  - Spin columns
- Sodium azide
- Sucrose
- Tris base
- Tris hydrochloride (Tris HCl)
- Centrifuge
- Skirted microtiter 96–well plate
- Spectrophotometer

Reagents

1. Sucrose & Mannitol (pH 7.4)
   - 220 mM Sucrose
   - 70 mM Mannitol
   - 10 mM Tris HCl
   - 0.1 mM EDTA
   - ddH_2O (100 mL final volume)
     - Store at 4° C

2. Column Storage Buffer
   - 10 mM Tris base (pH 7.5)
   - 1 mM EDTA
   - 0.02% (w/v) Sodium azide
   - ddH_2O (1 L final volume)
     - Store at 4° C

3. 5X PDP Assay Reaction Buffer

    - 250 mM Imidazole (pH 7.2)
    - 1 mM EGTA
    - 25 mM $MgCl_2$
    - 0.1% (v/v) 2–mercaptoethanol
    - 0.05% (w/v) BSA
    - ddH_2O (100 mL final volume)
        - Aliquot into 200 µL portions
        - Store aliquots at –80° C

4. Stock Phosphatase Assay Standard

    - 5% (v/v) Phosphate standard
    - 95% (v/v) Phosphate free water
        - Prepare fresh before use
        - Store on ice

5. PDH E1α Phosphopeptide

    - 1.5 mM Phosphopeptide
    - Phosphate free water (100 µL final volume)
        - Prepare fresh before use
        - Store on ice

6. Molybdate Dye Mixture

    - 1% (v/v) Molybdate dye additive
    - 99% (v/v) Molybdate dye solution
        - Prepare fresh before use
        - Store on ice

Protocol

Sample Preparation

1. Perform a Bradford Assay in order to determine the protein concentration of all mitochondrial extracts.
    - Refer to Appendix 1d: Bradford Method.
2. Dilute all samples with sucrose & mannitol to a final protein concentration of 2 µg/µL and a total volume of 30 µL.
3. Immediate snap–freeze 2 µg/µL samples in liquid nitrogen. Return leftover mitochondrial extracts to –80° C storage.
4. Freeze–thaw working samples in liquid nitrogen 3 times in order to lyse mitochondrial membranes.

   (Hint: samples need to be frozen and thawed in order to release mitochondrial contents for enzyme activity analysis.)
5. Spin samples at 21,000 x *g* for 1 hour at 4° C in order to pellet out bulky membrane proteins. Retain supernatants and transfer to clean eppendorfs for use in the PDP assay. Immediately store samples on ice.

Spin Column Preparation

6. Insert spin columns into spare 50 mL falcon tubes (collection reservoirs), and load spin columns with 10 mL of ddH_2O.

   (Hint: if ddH_2O does not filter through spin columns by gravity, remove columns from the falcon tubes and discard ddH_2O previously added to the spin column. Proceed to wet the underside of the glass filter using a 200 µL pipette and ~300 µL of ddH_2O. Once absorbed, reassemble the spin columns in falcon tubes and

reload 10 mL of ddH_2O into the columns. The spin columns should now begin draining by gravity. Gentle agitation or tapping may be required to start this process.)

7. Resuspend sephadex G–25 beads with a 5 mL pipette tip and load 10 mL into each spin column. Allow flow through to drain by gravity.
8. With the filtered sephadex now resting in the columns, load 10 mL of column storage buffer into each spin column. Allow flow through to drain by gravity.
9. Centrifuge spin columns at 600 x *g* for 5 minutes at 4° C in order to remove excess buffer that is coating Sephadex beads.
10. Place spin columns into fresh 50 mL falcon tubes. Load columns with diluted mitochondrial samples, and centrifuge at 600 x *g* for 5 minutes at 4° C in order to remove excess inorganic phosphate. Ensure that each falcon tube is appropriately labeled with each sample's details.
11. Retain samples and transfer into clean eppendorfs for application into the PDP assay.

PDP Assay

12. Prepare all assay reagents and store them on ice along with the purified mitochondrial samples.
13. Before preparing any samples, pre–heat the plate reader to 37° C.

    (Hint: turn on the plate reader and open the KC4™ software. In the settings function, adjust the pre–heating setting to 'on' and type in the desired temperature. Click OK and proceed to the control function. Select the 'pre–heat' tab and re–enter the desired temperature. Wait until the desired temperature has been reached,

which will only take a few minutes. The plate reader is now ready for the PDP assay.)

14. Retrieve a 96–well plate, and begin assay preparation by setting up the phosphate standard.
15. Dilute enough standard into phosphate–free water (1:19 ratio) to produce a large enough volume for the assay, which depends on the number of samples being processed. Furthermore, total volume is dependent upon whether the standard is to be run in singular, duplicate or triplicate wells.

Table A1.12. *Volume of stock phosphate standard and phosphate–free water required for the preparation of the PDP assay standard curve*.

Phosphate Standard Concentration (nM)	Stock Phosphate Standard (µL)	Phosphate–Free Water (µL)
2	40	10
1	20	30
0.5	10	40
0.2	4	46
0.1	2	48
0	0	50

*Total volume of Stock Standard (76 µL) and Phosphate–Free Water (224 µL) are sufficient to run the phosphate standard in singular wells.

16. Prepare sample and blank reaction mixtures directly into the 96–well plate. Like the phosphate standard, prepare enough materials to run as many wells as desired.
17. Prior to the addition of the peptide, insert the well plate into the plate reader and allow all reaction mixtures to equilibrate to 37° C for 10 minutes.

Table A1.13. *Volume of PDP assay components required for individual reactions*.

PDP Assay Component	Sample (µL)	Sample Blank (µL)	Phosphopeptide Blank (µL)
5X Reaction Buffer	10	10	10
Phosphatase Inhibitor	1	1	1
Phosphate–free Water	21	26	34
Mitochondrial Sample	5	0	5
Phosphopeptide	13	13	0

*Total volumes are sufficient to run samples in singular wells.

18. Once the equilibration phase has ended, remove the well plate from the plate reader and return to the lab bench. Add 13 µL of phosphopeptide to each well, aside from the peptide blanks, in order to initiate dephosphorylation reactions.
19. Incubate the 96–well plate for 30 minutes at 37° C to allow all reactions to proceed.
20. Once the incubation phase has ended, remove the well plate from the plate reader and return to the lab bench. Halt all reactions through the addition of 50 µL of molybdate dye mixture to each well.

    (Hint: ensure that the dye mixture is also added to the standard wells, as the change in absorbance within the standard curve is dependent on the interaction between the dye and the phosphate standard.)
21. Allow for 30 minutes of colour development at room temperature before measuring standard and sample absorbance. Cover the well plate with a kimwipe.
22. Measure absorbance in the plate reader at 600 nm.

References

1. LeBlanc, P. J., Mulligan, M., Antolic, A., MacPherson, L., Inglis, J. G., Martin, D., Roy, B. D., & Peters, S. J. (2008). Skeletal muscle type comparison of pyruvate dehydrogenase phosphatase activity and isoform expression: effects of obesity and endurance training. *American Journal of Physiology. Regulatory, Integrative and Comparative Physiology*, *295*, R1224–R1230.
2. LeBlanc, P. J., Harris, R. A., & Peters, S. J. (2007). Skeletal muscle fiber type comparison of pyruvate dehydrogenase phosphatase activity and isoform

expression in fed and food–deprived rats. *American Journal of Physiology. Endocrinology and Metabolism*, *292*, E571–E576.

3. Love, L. K., LeBlanc, P. J., Inglis, J. G., Bradley, N. S., Choptiany, J., Heigenhauser, G. J. F., & Peters, S. J. (2011). The relationship between human skeletal muscle pyruvate dehydrogenase phosphatase activity and muscle aerobic capacity. *Journal of Applied Physiology*, *111*, 427–434.

Appendix 2: Calculations

Appendix 2a. Dilution of Stock Insulin

- Laboratory Application: whole skeletal muscle tissue incubations.
- Details: incubations involve one experimental muscle (insulin + Medium 199) and one match–paired control from the same subject (Medium 199 only).
- Product Name: Humilin® R U–100
- Product Provider: local pharmacy
- Stock Concentration: 100 units/mL
- Desired Concentration: 10 milliunits/mL

Table A2.1. *Volume of stock insulin and Medium 199 required for application into whole skeletal muscle tissue incubations*.

Volume of Humilin–R (µL)	Volume of Medium 199 (µL)	Total Volume (mL)	Units of Insulin per mL	Milliunits of Insulin per mL
1000	0	1	100	100,000
100	900	1	10	10,000
10	990	1	1	1,000
1	999	1	0.1	100
0.1	999.9	1	0.01	10
1.5	14998.5	15*	0.01	10

*Tissue incubation reservoirs hold a total volume of 15 mL

Laboratory Preparation

Prior to insulin–stimulated incubations, experimental tissue samples underwent 30–minute equilibration incubations with Medium 199 only. For this equilibration period, experimental samples were incubated in 14 mL of Medium 199. During the equilibration period, a working solution was prepared containing 18 µL of Humilin–R and 11.982 mL of Medium 199 (1.5 µL Humilin–R per mL). This solution was prepared as an extension of the diluted insulin calculation presented in Table A2.1. Upon the conclusion of the equilibration period, 1 mL of the working solution was added to the incubation reservoir

in order to reach a final volume of 15 mL. Therefore, the incubating solution contained 1.5 µL of Humilin–R resulting in an insulin concentration of 10 milliunits per mL, thereby satisfying the desired insulin concentration for experimental samples.

References

1. Collier, C. A., Bruce, C. R., Smith, A. C., Lopaschuk, G., & Dyck, D. J. (2006). Metformin counters the insulin–induced suppression of fatty acid oxidation and stimulation of triacylglycerol storage in rodent skeletal muscle. *American Journal of Physiology. Endocrinology and Metabolism*, *291*, E182–E189.
2. Smith, A. C., Mullen, K. L., Junkin, K. A., Nickerson, J., Chabowski, A., Bonen, A., & Dyck, D. J. (2007). Metformin and exercise reduce muscle FAT/CD36 and lipid accumulation and blunt the progression of high–fat diet–induced hyperglycemia. *American Journal of Physiology. Endocrinology and Metabolism*, *293*, E172–E181.
3. Stefanyk, L. E., Gulli, R. A., Ritchie, I. R., Chabowski, A., Snook, L. A., Bonen, A., & Dyck, D. J. (2011). Recovered insulin response by 2 weeks of leptin administration in high–fat fed rats is associated with restored AS160 activation and decreased reactive lipid accumulation. *American Journal of Physiology. Regulatory, Integrative and Comparative Physiology*, *301*, R159–R171.

Appendix 2b. Dilution of Stock Kinase Inhibitor

- Laboratory Application: used as a component of Chappell–Perry solutions and sucrose & mannitol buffer for the isolation of subsarcolemmal mitochondria.
- Details: for the purpose of this study, it was deemed crucial to lock the phosphorylation state of all samples upon the conclusion of whole tissue incubations through the addition of kinase and phosphatase inhibitors.
- Product Name: 7,8–dihydroxycoumarin
- Product Provider: Sigma–Aldrich®
- Molecular Weight: 178.14 g/M
- Desired molarity: 200 μM

Table A2.2. *Molarity breakdown of stock kinase inhibitor required for application towards whole tissue homogenization procedures*.

Quantity of 7,8–dihydroxycoumarin (mg)	Final Volume of Working Solution (mL)	Molarity
178.14	1000	1 mM
35.63	1000	200 μM
3.56	100	200 μM
0.356	10	200 μM

Laboratory Preparation

The standard protocol for our lab when preparing working buffers for tissue homogenization procedures is to work with 10 mL aliquots from a larger stock solution. This is for practical reasons based upon the economical rationing of other products included in our homogenization buffers.

For the preparation of a 200 μM buffer with a final volume of 10 mL, only 0.356 milligrams of kinase inhibitor is required. This is a difficult and impractical quantity to work with, which led towards the need for alternative preparation. Stock kinase inhibitor

arrives in 5 milligram quantities, which led to the decision to resuspend the entire vial in methanol (preferential solubility). As a result, a pre–calculated volume of resuspended kinase inhibitor could now be included in each 10 mL aliquot of working buffer.

- 7,8–dihydroxycoumarin pack size: 5 mg
- Quantity required per 10 mL at 200 μM: 0.356 mg
- 5 ÷ 0.356 = 14.04

For every 5 milligram quantity of kinase inhibitor, the potential for 14 uses can be had when working at a concentration of 200 μM. Consequently, the entire vial was resuspended in 140.4 μL of methanol, which ensures a quantity of 0.356 milligrams per 10 μL of methanol suspension. This suspension was prepared based upon the required 200 μM concentration presented in Table A2.2. For every 10 mL aliquot of working homogenizing buffer, 10 μL of the 7,8–dihydroxycoumarin/methanol suspension was included in the final volume, thereby satisfying the required molarity to inhibit all kinase activity.

References

1. Yang, E. B., Zhao, Y. N., Zhang, K., & Mack, P. (1999). Daphnetin, one of coumarin derivatives, is a protein kinase inhibitor. *Biochemical and Biophysical Research Communications*, *260*, 682–685.

Appendix 2c. Determination of Anti–Phosphoserine Antibody Concentration

- Laboratory Application: immunoprecipitation of serine phosphorylated proteins.
- Details: through pilot testing it has been determined that both pyruvate dehydrogenase phosphatase isoforms are phosphorylated on serine residues within their polypeptide chains.
- Product Name: Anti–Phosphoserine Polyclonal Antibody
- Product Provider: Millipore™
- Stock Volume: 200 µL
- Stock Concentration: 0.25 µg/µL

Table A2.3. *Volume of anti–phosphoserine antibody required to immunoprecipitate all serine–phosphorylated protein within tissue extracts*.

Volume of Antibody Applied to Immunoprecipitation (µL)	Concentration of Antibody Applied to Immunoprecipitation (µg)	Quantity of Precipitated Tissue Extract Protein (µg)
200	50	2500
40	10	500
30	7.5	375
20	5	250
10	2.5	125

Laboratory Preparation

For the analysis of serine–phosphorylated PDP1 and PDP2 protein content between basal and insulin–stimulated samples, all muscles were snap–frozen in liquid nitrogen following whole tissue incubations. Samples would then be homogenized in lysis buffer, and whole homogenate protein concentrations (µg/µL) would be determined via Bradford assay. Anti–phosphoserine polyclonal antibody would then be added to the muscle homogenates in order to precipitate phosphorylated PDP1 and PDP2 for comparative analysis between conditions via Western blotting.

In order to properly demonstrate any change in phosphorylation between conditions, it was imperative to ensure that all phosphorylated proteins within a given sample were fully cleared. In other words, one would be unable to declare any change beyond a reasonable doubt if any phosphorylated PDP1 or PDP2 protein was not precipitated. Therefore, careful consideration was required to ensure that enough anti–phosphoserine antibody was applied in order to satisfy this condition.

According to product information provided by Millipore™, 10–20 μg of antibody is required in order to immunoprecipitate all serine–phosphorylated proteins per milligram of whole tissue protein. Based upon the protein concentration of the antibody (0.25 μg/μL), this equates to 40–80 μL. From an economic standpoint, allocating 80 μL of antibody to every sample was deemed impractical.

In order to compensate for this demanding calculation, this immunoprecipitation method was piloted using 20 μL of anti–phosphoserine antibody in order to precipitate all phosphorylated proteins within 250 μg of whole muscle homogenate. Unfortunately, this compensation resulted in immunoprecipitated pellets that were too small to analyze adequately via Western blotting. Through further pilot testing, it was determined that 40 μL of antibody and 500 μg of whole homogenate would suffice to execute this method successfully. Although this method was costly to execute, the final concentrations implemented in the PDP phosphorylation experiments were as cost–conscious as possible while still providing an opportunity for successful analysis.

Appendix 2d. Statistical Power

- Thesis Application: determination of the minimum sample size required to evaluate the null hypothesis.
- Details: studies conducted within the field of exercise physiology, and more specifically within our laboratory, typically involve 8 subjects per measure in order to evaluate research questions.

Summary of Literature

- Calculation of power is based upon the statistical test used to analyze a particular measurement
  - The only statistical tests used throughout the current study are T–tests, comparing the independent means of insulin–stimulated experimental groups and basal control groups
- Calculation of the minimum sample size is dependent upon 3 factors:
  - The expected magnitude or effect size (ES) of a particular phenomenon
  - The significance criterion (alpha "α" level) used in the statistical test
  - Acceptable statistical power

➢ Large effect sizes are typically expected within the field of exercise physiology
  - Large effect size for T–test analyses = **0.80**

➢ Traditional significance criteria are typically set at 0.01, 0.05, or 0.10
  - Criteria used throughout the current study = **0.05**

➢ Determination of appropriate sample size is based upon the default power setting
  - Acceptable statistical power = **0.80**

According to the criteria mentioned above (ES of 0.80, alpha of 0.05, and power of 0.80), the minimum sample size required to evaluate the null hypothesis is **26 subjects** per group.

Conclusion

Although the literature recommends a minimum sample size of 26 for the measures in the current study (Cohen, 1992), this guideline could not be met. The reasoning behind this shortcoming is based upon the need for ethical and practical execution of the study. Firstly, our laboratory works in full cooperation with Brock University's Animal Care and Use Committee. All animal work is performed with a commitment to study as few subjects as possible in order to conduct experiments. Under the guidance of my advisory committee, a sample size of 8 subjects per group, per measure has been deemed appropriate for the completion of my thesis. Secondly, all Master's theses are structured with a 2–year timeframe for completion in mind. Under these limitations, performing the necessary experiments with a sample size of 26 is unreasonable.

References

1. Cohen, J. (1992). A power primer. *Psychological Bulletin*, *112*, 155–159.

Appendix 2e. PDH Activity Calculations

- Laboratory Application: calculation of pyruvate dehydrogenase activity by the determination of acetyl–CoA concentration in whole muscle homogenates.
- Details: this calculation involves data produced from two separate assays. First, whole homogenates undergo the PDH*a* activity assay, where varying amounts of endogenous acetyl–CoA are produced on an individual sample basis. PDH*a* samples are then processed further in the acetyl–CoA through the use of radiolabeled tagging in order to label and isolate intramuscular concentrations of endogenous acetyl–CoA. Both assays involve dilution phases, which must be accounted for with calculations in order to determine whole muscle enzyme activity rates.

Dilution Factors

All dilution factors are recorded as the quotient obtained by dividing the total volume of a given solution by the sample volume contained within a given solution.

DF1: homogenization of samples for the PDH*a* Assay (30–fold dilution).

Total volume = 31 (30 µL of homogenizing buffer + 1 mg of tissue)

Sample volume = 1 (1 mg of wet weight skeletal muscle tissue)

DF1 = 31

DF2: incubation of homogenates and incubating solution for the PDH*a* Assay

Total volume = 750 (720 µL of PDH*a* incubation solution + 30 µL of whole homogenate)

Sample volume = 30

DF2 = 26

DF3: acidification and neutralization of samples following the PDH*a* Assay

Total volume = 250 (200 µL of sample + 40 µL of acid + 10 µL of base)

Sample volume = 200 (200 µL taken at 1, 2, and 3 minute intervals)

DF3 = 1.25

DF4: incubation of PDH*a* samples and ddH_2O for the Acetyl–CoA Assay

Total volume = 220 (200 µL of ddH_2O + 20 µL of neutralized PDH*a* sample)

Sample volume = 20

DF4 = 11

PDH*a* Activity Calculation

$$\text{PDH}a \text{ Activity (mmol acetyl–CoA} \bullet \text{min}^{-1} \bullet \text{kg}^{-1}) = \frac{(\text{Slope} \bullet \text{DF1} \bullet \text{DF2} \bullet \text{DF3} \bullet \text{DF4})}{1000}$$

*Slope refers to the linear expression of acetyl–CoA measurements taken at 1, 2, and 3–minute intervals as part of the PDH*a* Assay. The slope, which represents the rate of the PDH reaction (rate of acetyl–CoA production), is calculated based upon each sample's results from the acetyl–CoA assay. Please refer to the following appendices for additional information.

- Appendix 1g: PDH*a* Activity Assay
- Appendix 1h: Determination of Acetyl – CoA Accumulation

Appendix 2f. Citrate Synthase Calculations

- Laboratory Application: calculation of maximal citrate synthase activity in whole muscle homogenates and mitochondrial suspensions.
- Details: the determination of citrate synthase activity is performed in order to measure the mitochondrial recovery percentage following mitochondrial isolation procedures. Mitochondrial recovery values are then applied to experiments conducted using mitochondrial extracts as a normalizing control value.

Calculation of Citrate Synthase

1. $\frac{\Delta \text{ absorbance per minute} \bullet \text{total reaction volume}}{\text{sample volume} \bullet \text{molar extinction coefficient}}$
2. CS Activity (μmol/min/g) = quotient of equation #1 • tissue dilution factor

Reaction Components

- Δ absorbance per minute: determined by spectrophotometer following reaction
- Total reaction volume: 250 μL (sample volume + reagent volumes)
- Sample volume: 10 μL (regardless of sample specificity)
- Molar extinction coefficient: 13,600 (specific for DTNB at 412 nm wavelength)
- Tissue dilution factor: dependent upon specificity of sample
  - Whole homogenate (WH): 101
  - Total mitochondrial suspension (TS): 20

Dilution Factor Calculations

$$\text{Dilution Factor} = \frac{\text{total volume of solution}}{\text{sample volume}}$$

$$\text{Dilution Factor (WH)*} = \frac{101}{1} \qquad \text{Dilution Factor (TS)**} = \frac{100}{5}$$

*Citrate Synthase homogenization calls for 100–fold dilution (1 mg/100 μL)
**Total suspension = 5 μL mitochondrial extract + 95 μL sucrose & mannitol

References

1. Srere, P. A. (1969). Citrate Synthase: [EC 4.1.3.7. Citrate oxaloacetate lyase (CoA – acetylating)]. *Methods in Enzymology*, *13*, 3–11.

Appendix 3: Citrate Synthase Activity Assay Raw Data

Table A3. *Citrate synthase activity assay raw data for basal and insulin–stimulated samples*.

Sample	CS_{WH} Activity (µmol/minute/g wet weight tissue)	CS_{TS} Activity (µmol/minute/g wet weight tissue)	% Mitochondrial Recovery
Basal 1	36.37	1.96	5.39
Basal 2	21.20	2.52	11.89
Basal 3	20.46	2.84	13.88
Basal 4	33.38	3.85	11.53
Basal 5	28.98	3.83	13.22
Basal 6	31.62	2.64	8.35
Basal 7	36.35	3.99	10.98
Basal 8	26.40	2.72	10.30
Basal 9	28.63	3.44	12.02
Basal 10	29.50	3.35	11.36
Insulin 1	27.00	2.14	7.93
Insulin 2	30.93	2.82	9.12
Insulin 3	25.27	3.28	12.98
Insulin 4	31.90	3.94	12.35
Insulin 5	30.11	1.38	4.58
Insulin 6	24.95	3.81	15.27
Insulin 7	30.82	4.55	14.76
Insulin 8	28.42	3.74	13.16
Insulin 9	31.54	3.52	11.16
Insulin 10	31.17	2.93	9.40
Mean	29.25	3.16	10.98
Standard Error	0.94	0.18	0.64

Appendix 4: Components of Medium199

Product Name: Medium199 – with Earle's salts, L–glutamine, and sodium bicarbonate

- Form: liquid
- Impurities: endotoxin
- Sterility: sterile–filtered
- Suitability: cell culture
- Storage temperature: 2–8° C

Product Provider: Sigma–Aldrich®

Product Code: M4530–500ML

Components: M4530 [1X]	grams per Litre
Inorganic Salts	
o Calcium chloride dihydrate	0.2
o Iron(III) nitrate nonahydrate	0.00072
o Magnesium sulfate (anhydrous)	0.09767
o Potassium chloride	0.4
o Sodium acetate (anhydrous)	0.05
o Sodium bicarbonate	2.2
o Sodium chloride	6.8
o Monosodium phosphate (anhydrous)	0.122
Amino Acids	
o L–alanine	0.025
o L–arginine hydrochloride	0.07
o L–aspartic acid	0.03
o L–cystine hydrochloride monohydrate	0.00011
o L–cysteine dihydrochloride	0.026
o L–glutamic acid	0.0668
o L–glutamine	0.1
o Glycine	0.05
o L–histidine hydrochloride monohydrate	0.02188
o Hydroxy–L–proline	0.01
o L–isoleucine	0.02
o L–leucine	0.06
o L–lysine hydrochloride	0.07
o L–methionine	0.015
o L–phenylalanine	0.025
o L–proline	0.04

Amino Acids continued…	g/L
o L–serine	0.025
o L–threonine	0.03
o L–tryptophan	0.01
o L–tyrosine disodium dihydrate	0.05766
o L–valine	0.025

Vitamins

o Sodium ascorbic acid	0.0000566
o D–biotin	0.00001
o Calciferol	0.0001
o Choline chloride	0.0005
o Folic acid	0.00001
o Menadione (sodium bisulfite)	0.000016
o *Myo*–inositol	0.00005
o Niacinamide	0.000025
o Nicotinic acid	0.000025
o *P*–amino benzoic acid	0.00005
o D–pantothenic acid hemicalcium	0.00001
o Pyridoxal hydrochloride	0.000025
o Pyridoxine hydrochloride	0.000025
o Retinol acetate	0.00014
o Riboflavin	0.00001
o DL–α–tocopherol phosphate sodium	0.00001
o Thiamine hydrochloride	0.00001

Other

o Adenine sulfate	0.01
o Adenosine triphosphate disodium	0.001
o Adenosine monophosphate sodium	0.0002385
o Cholesterol	0.0002
o Deoxyribose	0.0005
o Glucose	1.0
o Glutathione (reduced)	0.00005
o Guanine hydrochloride	0.0003
o Hypoxanthine	0.0003
o Phenol red sodium	0.0213
o Tween 80	0.02
o Ribose	0.0005
o Thymine	0.0003
o Uracil	0.0003
o Xanthine sodium	0.000344

References

1. Morgan, J. F., Campbell, M. E., & Morton, H. J. (1955). The nutrition of animal tissues cultivated in vitro. I. A survey of natural materials as supplements to synthetic medium 199. *Journal of the National Cancer Institute*, *16*, 557–567.
2. Morgan, J. F., Morton, H. J., & Parker, R. C. (1950). Nutrition of animal cells in tissue culture; initial studies on a synthetic medium. *Proceedings of the Society for Experimental Biology and Medicine*, *73*, 1–8.